uOttawa

L'Université canadienne
Canada's university

FACULTÉ DES ÉTUDES SUPÉRIEURES ET POSTOCTORALES

uOttawa

L'Université canadienne
Canada's university

FACULTY OF GRADUATE AND POSDOCTORAL STUDIES

Lysanna Melanson-Drapeau
AUTEUR DE LA THÈSE / AUTHOR OF THESIS

Ph.D. (Biochemistry)
GRADE / DEGREE

Department of Biochemistry, Microbiology, and Immunology
FACULTÉ, ÉCOLE, DÉPARTEMENT / FACULTY, SCHOOL, DEPARTMENT

Connexin32-Mediated Control of Progenitor Cell Fate in Injured and Uninjured Adult Mouse Brain

TITRE DE LA THÈSE / TITLE OF THESIS

Steffany Bennett
DIRECTEUR (DIRECTRICE) DE LA THÈSE / THESIS SUPERVISOR

CO-DIRECTEUR (CO-DIRECTRICE) DE LA THÈSE / THESIS CO-SUPERVISOR

EXAMINATEURS (EXAMINATRICES) DE LA THÈSE / THESIS EXAMINERS

Rosalind Labow (absent)

Danica Stanimirovic

Dale Laird

Ian Lorimer

Gary W. Slater
Le Doyen de la Faculté des études supérieures et postdoctorales / Dean of the Faculty of Graduate and Postdoctoral Studies

CONNEXIN32-MEDIATED CONTROL OF PROGENITOR CELL FATE IN INJURED AND UNINJURED ADULT MOUSE BRAIN

Lysanne Melanson-Drapeau

Thesis submitted to the Faculty of Graduate and Postdoctoral Studies
in partial fulfillment of the requirements for the degree of
Doctor of Philosophy

Department of Biochemistry, Microbiology, and Immunology
Faculty of Medicine
University of Ottawa

Your file Votre référence
ISBN: 978-0-494-18598-8
Our file Notre référence
ISBN: 978-0-494-18598-8

Abstract

Gap junction protein expression has been implicated in progenitor cell proliferation, survival, and specification during development. The present study was undertaken to establish the role of the gap junction protein connexin32 in dictating progenitor cell fate in adult mouse brain. In the dentate gyrus of the hippocampus, I localized the connexin32 protein to a subset of $NG2^+$ early oligodendrocyte progenitors. In connexin32-null mutant mice, I found an increase in the total number of proliferating early oligodendrocyte progenitors and demonstrated that the turnover of these cells is constitutively enhanced (Chapter 2). Furthermore, behavioural testing in a learning and memory task revealed that connexin32-deficient mice exhibit impaired reference memory, indicating that progenitor cells may play a role in hippocampal associated cognitive function (Chapter 3). *In vitro* analysis further demonstrated that these progenitors are able to differentiate into neurons upon a neurogenic stimulus. In Chapter 4, I assessed the ability of hippocampal progenitors to activate and regenerate brain tissue *in vivo*, following kainic acid-induced epileptiform seizures, in the presence or absence of connexin32. I show that connexin32-null mutation promotes more effective neurogenesis from $NG2^+$ progenitor cells activated in the CA3a/b pyramidal zone, following excitotoxic injury. To confirm the role of connexin32 in determining progenitor cell fate, I performed a series of gain of function studies by inducing ectopic connexin32 expression in neurosphere progenitor cultures (Chapter 5). I show that connexin32 promotes oligodendrogenesis *in vitro*, at the expense of neurogenesis. These experiments provide insight into connexin-mediated control of neural progenitor specification and begin to identify connexins as possible therapeutic targets following brain injury.

General Acknowledgements

I would like to thank my supervisor, Dr Steffany A. L. Bennett, for giving me the opportunity to conduct my graduate studies in her laboratory. Her sustained patience, optimism, and guidance throughout the years were truly appreciated. I also wish to thank the members of my thesis advisory committee, Dr Michael Rudnicki, Dr Earl Brown, Dr Mary-Ellen Harper, and Dr Jenny Phipps, for their constructive comments and suggestions. I would further like to thank Dr Klaus Willecke and Dr David Paul for providing the connexin32 knockout mouse breeding pairs, as well as Dr Sheng Hou for generously donating the pAdTrack-GFP adenovirus. In addition, I wish to extend my sincere gratitude to all the past and present members of the Bennett laboratory as well as to my friends and family for their constant support and encouragements. I would further like to acknowledge Jim Bennett and Shawn Whitehead for their constructive advice concerning thesis revisions. This research was supported by grants from NSERC and CIHR to S.A.L. Bennett and a CGS studentship to LMD.

Table of Contents

List of abbreviations

aCSF: Artificial cerebrospinal fluid
ADP: Adenosine diphosphate
AMPA: Alpha-amino-3-hydroxy-5-methyl-4-isoxazolepropionic acid
ANOVA: One-way analysis of variance
ATP: Adenosine triphosphate
BDNF: Brain derived neurotrophic factor
bFGF: Basic fibroblast growth factor
BrDU: Bromodeoxyuridine
CA1, 2, 3, 3c, Py: Pyramidal cell fields of the hippocampus (*Cornu ammonis*)
cAMP: Cyclic adenosine monophosphate
CMTX: X-linked Charcot-Marie-Tooth disease
CNPase: 2' 3'-cyclic-nucleotide 3'-phosphodiesterase
CNS: Central nervous system
Cx: Connexin
Cx32KO: Connexin32 knockout
Cy3: Cyanine-3
DG: Dentate gyrus
DMEM/F12: Dulbecco's modified Eagle's medium F-12
DNA: Deoxyribonucleic acid
dNTP: Deoxynucleoside triphosphate
dUTP: Deoxy-uridine triphosphate
EDTA: Ethylenediaminetetraacetic acid
FITC: Fluorescein isothiocyanate
GABA: Gamma-aminobutyric acid
GalC: Galactocerebroside C
GCL: Granule cell layer
GFAP: Glial fibrillary acidic protein
GFP: Green fluorescent protein
GrDG: Granule cell layer of the dentate gyrus
H&E: Hematoxylin and eosin
hEGF: Human epidermal growth factor
IP_3: Inositol 1,4,5-trisphosphate
KA: Kainic acid
L.Mol: Lacunosum moleculaire
MANOVA: Multiple analysis of variance
MGPY: Methyl green pyronine Y
MOI: Multiplicity of infection
Mol: Molecular layer of the dentate gyrus
NAD^+: Nicotinamide adenine dinucleotide
NMDA: N-methyl-D-aspartate
NT2: Human teratocarcinoma-derived neural precursors
NT3, 4: Neurotrophin-3, -4
P3: Postnatal day 3
PBS: Phosphate buffered saline

PC12: Rat pheochromocytoma cells
PCR: Polymerase chain reaction
PDGFαR: Platelet-derived growth factor receptor alpha
PLP: Proteolipid protein
PoDG: Polymorphonuclear layer of the dentate gyrus
RNA: Ribonucleic acid
RT-PCR: Reverse transcription-polymerase chain reaction
SDS-PAGE: Sodium dodecyl sulfate – polyacrylamide gel electrophoresis
SEM: Standard error of the mean
SGZ: Subgranular zone
SH2, 3: Src homology 2, 3
S.Lu: Stratum lucidum
S.O: Stratum oriens
S.Rad: Stratum radiatum
SVZ: Subventricular zone
TdT: Terminal deoxynucleotidyl transferase
TUNEL: TdT-mediated dUTP nick end labelling
v-SRC: Rous sarcoma virus transforming protein
WT: Wildtype
ZO-1, -2: Zona occludens-1, -2

List of Figures and Tables

Chapter 1: General introduction

1.1 Neurodegenerative diseases

Given our aging population, the prevalence of neurodegenerative disorders such as amylolateral sclerosis, Alzheimer's and Parkinson's disease is increasing, and yet treatment options continue to be severely limited. These progressive degenerative conditions are characterized by an insidious decline in mental and physical functions that dramatically reduces quality of life as well as life expectancy. Until recently, neuronal loss characteristic of most neurodegenerative disorders was deemed permanent and irreversible. Conventional medical treatments have focused on reducing the rate of neuronal death and ameliorating negative symptoms. Nonetheless, most degenerative disorders of the brain and spinal cord remain incurable (Ayetey, 2002).

Current therapy following acute brain injury such as cerebral ischemia is aimed at preventing cell death (reviewed in Komjati et al., 2005; Mergenthaler et al., 2004). However, these treatments are most effective when administered before or coincident with cerebral insult. Little can be done to replace lost neurons in the weeks that follow a stroke or to reverse the progressive reduction in neuronal number over the course of a neurodegenerative disorder such as Parkinson's disease. In the case of Alzheimer's disease, the loss of cognitive and memory functions has been attributed to multiple pathophysiological mechanisms. Structural damage includes inflammatory processes, tau-rich neurofibrillary tangles, and amyloid plaques, while cortical cholinergic deficits are represented by the loss of cholinergic neurons, a decrease in choline acetyltransferase activity, and severe losses of nicotinic binding sites (Burghaus et al., 2003; Lopez and Becker, 2002). The primary long-term treatment is the administration of

acetylcholinesterase inhibitors designed to increase cholinergic activity, although this therapy is only partially effective at boosting existing neuronal capacity and does not prevent the inevitable loss of memory function (Newhouse et al., 2001). In addition to promoting residual neuronal function, research has also centred on developing strategies to moderate the development of tangles and neuritic plaques and on the use of antioxidants in order to reduce or block the rate of neuronal loss (Di Matteo and Esposito, 2003; Suh and Checler, 2002), but the search for alternative strategies to prevent neurodegenerative decline remains vital.

There is now clear evidence suggesting that the adult mammalian brain contains neural stem and progenitor cells with the capacity for self-renewal and the ability to differentiate into functional neurons and glia (Gage, 2000). Recent progress using experimental models of brain injury indicate that the regenerative capacity of resident neural precursors can be enhanced even in the adult brain. Moreover, transplants of exogenous neural progenitors have been successful in partially reconfiguring damaged neuronal circuitry (Chiba et al., 2003; Magavi et al., 2000; McBride et al., 2004; Englund, 2002; Taguchi et al., 2004). Early clinical trials confirmed that cell transplantation has the potential to improve neurological function in the diseased brain (Kondziolka et al., 2000; Meltzer et al., 2001; Nelson et al., 2002). Mobilizing or introducing neural progenitor cells following injury represents a novel, potentially transformative approach to brain repair, yet this promise is far from validated.

In this thesis, I argue that a comprehensive understanding of the molecular mechanisms regulating progenitor fate is required if we are to explore the potential of cell replacement strategies. Validating the utility of neuroregenerative therapy requires a more

detailed understanding of how progenitors respond to environmental changes if their latent regenerative potential is to be harnessed or functional integration of transplanted populations is to be achieved safely. This insight is essential given recent reports that some brain tumors may, in fact, originate from the transformation of neural progenitors in both adult and childhood cancers (Singh et al., 2004a; Singh et al., 2003; Singh et al., 2004b). One of the goals of our laboratory is therefore to understand the cellular mechanisms underlying the proliferation, survival, and differentiation of progenitor cells in the adult central nervous system (CNS). Specifically, in this thesis, I focus on elucidating how connexin-mediated communication controls progenitor cell fate in injured and uninjured rodent brain, centering on the role of Cx32 in regulating progenitor number, survival, and specification.

1.2 Stem and progenitor cells in the adult mammalian brain

A stem cell is defined by three characteristics: 1) its ability to self-renew for an infinite number of divisions, 2) its capacity to divide asymmetrically in order to give rise to various cell types, and 3) the long-term maintenance of those two previous features (reviewed in Garry et al., 2003; Seaberg and van der Kooy, 2003). While asymmetrical division is also characteristic of progenitor cells, the latter are more restricted in that they can only self-renew for a limited number of times (Maric and Barker, 2004). The term 'precursor cell' is often used to encompass both pools of cells (stem and progenitor cells) when the capacity for self-renewal has not been empirically established. Totipotent stem cells have the capacity to form any cell type of the body. Early embryonic totipotent stem cells give rise to extra-embryonic tissues as well as to all germinal and somatic cells found in post-embryonic tissues and organs. Pluripotent stem cells retain the capacity to specify to

any cell type from all three germ layers, endoderm, mesoderm, and ectoderm, while multipotent stem or progenitor cells have the capacity to differentiate into a more restricted number of cell types, usually but not necessarily all cells within a given organ. The term "neural precursor cell" defines a stem or progenitor cell isolated from neural tissue with the capacity to differentiate into one or more of the three main cell types of the brain: astrocytes, oligodendrocytes, and neurons (Figure 1.1).

Once thought to be completely post-mitotic, the adult mammalian brain is now known to be composed of several neurogenic regions containing pools of stem and/or progenitor cells (Gage, 2000). Using [^{3}H]-thymidine as a mitotic label, Joseph Altman was the first to detect cell division in the adult mammalian brain, more precisely in the hippocampus and in the olfactory bulb (Altman, 1969; Altman and Das, 1965). In 1992, the concept of neurogenesis was strengthened by Reynolds and Weiss, who showed that precursor cells isolated from the forebrain could be differentiated into neurons *in vitro* (Reynolds and Weiss, 1992). Neurogenesis was later shown to occur in the hippocampal formation, more precisely in the dentate gyrus (Gage et al., 1998). The subventricular zone (SVZ) of the lateral ventricle and the subgranular zone (SGZ) of the dentate gyrus have since been identified as the two sites of the adult cerebrum containing the largest populations of neural precursors, capable of gliogenesis as well as neurogenesis (Gage, 2000). Other sites where adult multipotent precursors have been successfully cultured, albeit at a much lower frequency, include the septum, striatum, optic nerve, spinal cord, retina, and cerebellum (reviewed in Magavi and Macklis, 2002).

Postnatal neural progenitors are a heterogeneous population of cells with varying capacities for proliferation and specification to neurons, astrocytes, and oligodendrocytes (Gage, 2000). In the SVZ, commitment to a neuronal lineage involves at least three

Figure 1.1. Neural progenitor specification. Diagram representing the possible cellular phenotypes originating from a single neural progenitor cell. Neural progenitors give rise to neuronal and glial progenitors. The latter can specify to mature astrocytes as well as to early oligodendrocyte progenitors, which in turn differentiate to late oligodendrocyte progenitors before becoming mature oligodendroytes. Neuronal progenitors specify to an intermediate neuronal phenotype before differentiating to mature neurons. Dotted line shows recent observation that $NG2^+$ progenitors can give rise to mature neurons *in vitro*, in the presence of a neurogenic stimulus. Specific proteins expressed at various stages of the differentiation process are indicated (blue) and were immunodetected in the following experiments in order to confirm cell lineage (see Appendix 1: List of antibodies). The main connexins expressed by mature cell types are also indicated (green).

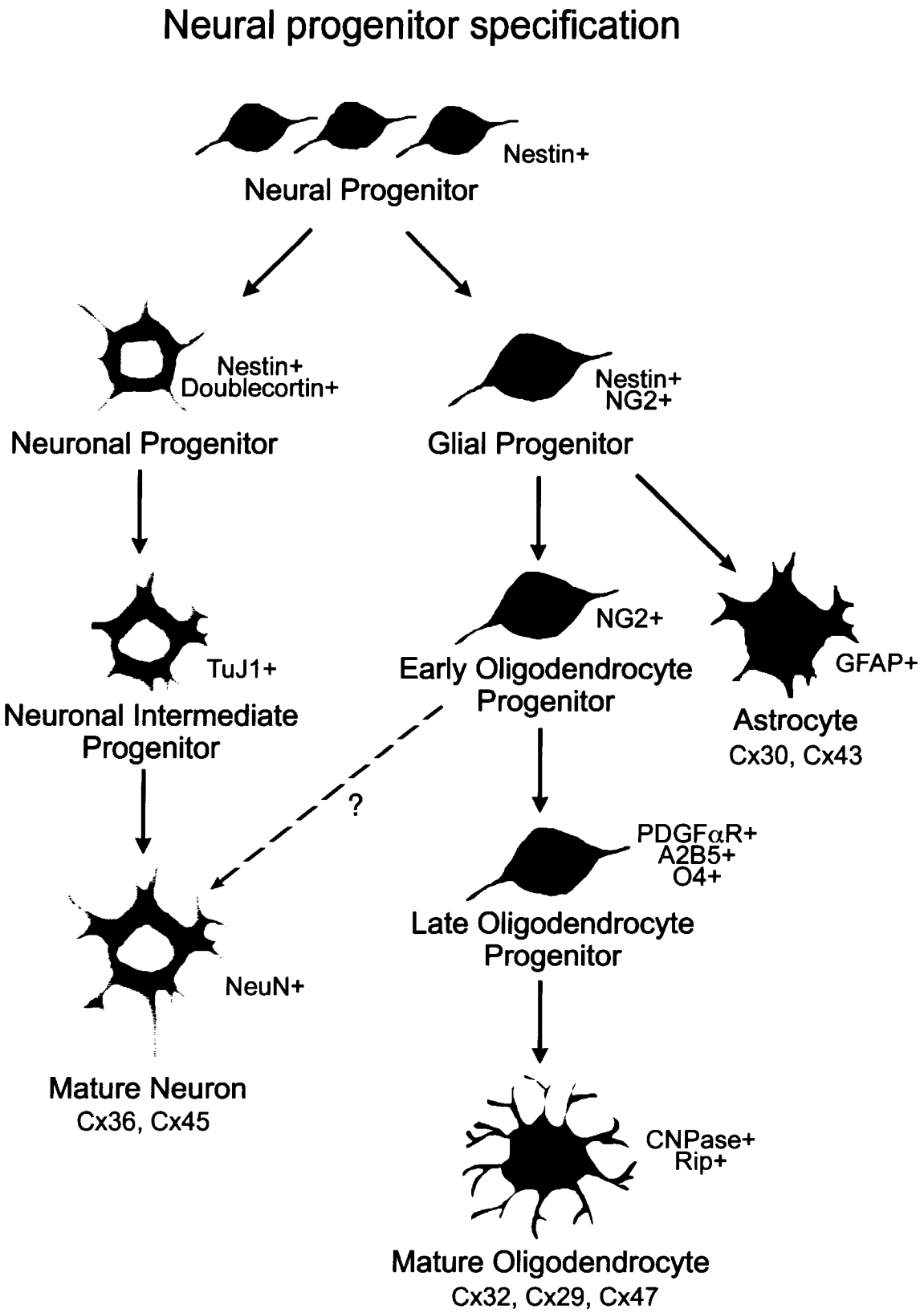
Neural progenitor specification
Nestin+
Neural Progenitor
Nestin+
Doublecortin+
Neuronal Progenitor
Nestin+
NG2+
Glial Progenitor
TuJ1+
Neuronal Intermediate
Progenitor
NG2+
Early Oligodendrocyte
Progenitor
GFAP+
Astrocyte
Cx30, Cx43
?
PDGFαR+
A2B5+
O4+
Late Oligodendrocyte
Progenitor
NeuN+
Mature Neuron
Cx36, Cx45
CNPase+
Rip+
Mature Oligodendrocyte
Cx32, Cx29, Cx47

Figure 1.1

progenitor subtypes. Multipotential stem cells produce transit amplifying daughter cells that expand the pool of neuronal progenitors before producing neuroblasts. Stem cells found in the SVZ are relatively quiescent, with a cell cycle of approximately 20 days, and give rise to actively proliferating progenitors, with a cell cycle lasting between 14 and 18 hours (Morshead et al., 1994; Smith and Luskin, 1998; Zheng et al., 2004). The latter are limited to few divisions and migrate along the rostral migratory stream to terminally differentiate and replenish olfactory bulb neurons (reviewed in Doetsch, 2003; Luskin, 1998). Commitment to an oligodendrocyte lineage is a more extensive process involving several cell intermediates. SVZ stem cells can generate $NG2^+$ glial progenitors that specify to platelet derived growth factor α receptor $(PDGF\alpha R)^+$ oligodendrocyte progenitors and become mature oligodendrocytes, retained locally within the striatum (Gritti et al., 2002).

It remains controversial whether the pool of precursor cells found in the adult SGZ also contains stem cells, or if it is strictly formed of progenitor cells (Becq et al., 2005; Gage, 2000; Seaberg and van der Kooy, 2002). *In vivo*, SGZ neural precursors migrate into the granule cell layer, where they differentiate to a mature granule neuron phenotype and are functionally integrated into hippocampal circuitry (Figure 1.2). These newly born neurons receive synaptic contact, develop dendritic processes reaching the molecular layer, and rapidly send appropriate axonal projections into the CA3 region of the hippocampus (Hastings and Gould, 1999; Markakis and Gage, 1999; Stanfield and Trice, 1988; Wang et al., 2000). Moreover, it has been reported that hippocampal $NG2^+$ glial progenitors are capable of both glio- and neurogenesis, with new neurons located predominantly to the dentate gyrus granule cell layer of P30 mice (Belachew et al., 2003).

The plasticity of these progenitors and their progeny is partially defined by

Figure 1.2. The hippocampal formation. Abbreviations: CA1,2,3, 3c Py, pyramidal cell fields of the hippocampus; DG, dentate gyrus; GrDG, granule cell layer of the dentate gyrus; PoDG, polymorphonuclear layer of the dentate gyrus; SGZ, subgranular zone of the dentate gyrus; Mol, molecular layer of the dentate gyrus; L.Mol, lacunosum moleculaire; Rad, stratum radiatum, Or, stratum oriens; SLu, stratum lucidum; GCL, granule cell layer. *A*) Cresyl violet-stained hippocampal formation of a 3 months old C57BL/6 WT mouse. Scale bar, 50 μm. *B*) Schematic diagram representing the hippocampal formation and the dentate gyrus (inset). *C*) Schematic diagram showing progenitor cell proliferation in the SGZ, followed by migration into the GCL and differentiation to a neuronal phenotype. Adapted from Gage F. H., 2000.

A

B

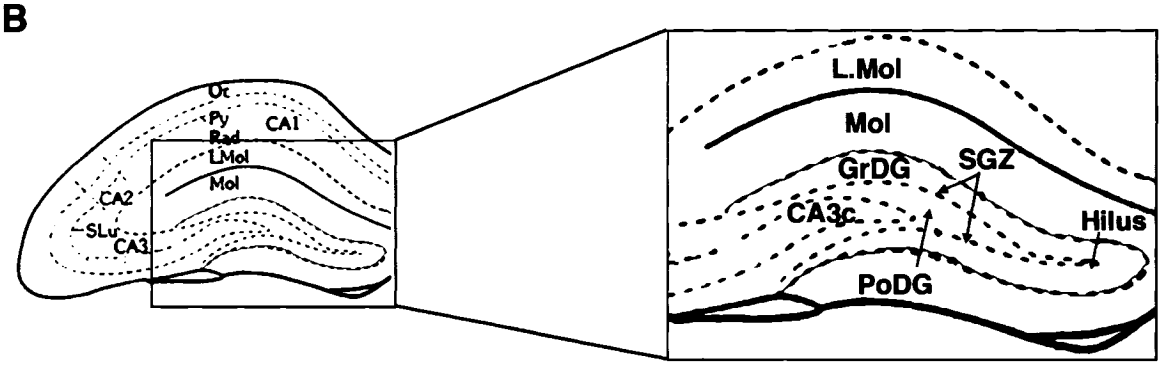

C

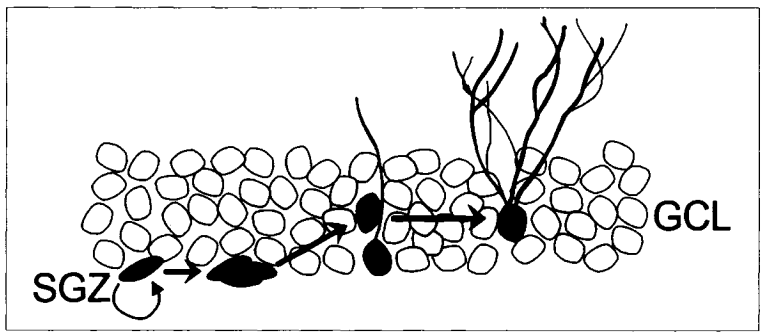

Figure 1.2

epigenetic control, transcriptional, post-transcriptional, as well as environmental regulation. Identifying (a) the genes active in postnatal progenitors that are gradually silenced in their increasingly committed progeny and (b) cell lineage-specific genes that are sequentially turned on in their place is crucial to our understanding of how multipotential progenitor cell number is regulated in adult brain (Gangemi et al., 2004). Several extrinsic environmental factors have also been shown to influence neurogenesis. For example, the production of stress-related adrenal steroids inhibits both progenitor proliferation and neuronal differentiation through an N-methyl-D-aspartate (NMDA) receptor-dependent pathway (Cameron and Gould, 1994; Cameron et al., 1995; Gould and Tanapat, 1999; Tanapat et al., 1998). Interestingly, the rate of formation of new neurons also declines with age, a phenomenon that could be due to a decrease in the number of precursors, a change in precursor cell properties, and/or a change in the levels of molecular factors influencing neurogenesis (Kuhn et al., 1996). Conversely, the presence of serotonin and estrogen, exposure to associative learning tasks, exercise, as well as an overall enriched environment have positive effects on neurogenesis (Brezun and Daszuta, 1999; Gould et al., 1999; Kempermann et al., 1997b; Tanapat et al., 1999; van Praag et al., 1999).

Relevant to the hypothesis underlying this thesis, there is now compelling evidence that direct cell-cell interactions between progenitors and astrocytes, oligodendrocytes, or neurons can also effectively control their proliferation, migration, and specification to different neural cell lineages (Lim and Alvarez-Buylla, 1999; Song et al., 2002). As such, this study focuses on elucidating the role of connexin-mediated communication in the control of neural precursor cell fate *in vitro* as well as *in vivo* in both injured and uninjured tissue.

1.3 Connexin-mediated communication.

1.3.1 Connexins are the structural units of gap junction channels

Gap junctions are specialized zones of direct cell-cell contact in which two cells are linked by a series of small intercellular channels that were first described in mouse cardiomyocytes and hepatocytes (Revel and Karnosvsky, 1967). The term 'gap junction' defines the morphology of several intercellular channels clustered in close proximity that span the plasma membrane of adjacent cells and allow metabolic and electrical coupling (Figure 1.3). Each channel subunit is composed of six structural connexin proteins that oligomerize to form a hemichannel or connexon, a pore-like structure anchored in the plasma membrane of a single cell. When two connexons expressed by neighbouring cells align, they create a single axial channel bridging the cell cytoplasms and providing a direct conduit for signaling molecules and ionic currents to pass between the cells. When clusters of connexons align, the plasma membranes of the two opposing cells are separated by a gap of ~2-3 nm from which the term gap junction is derived. These channels are essential for multiple biological functions. For example, in cardiac myocytes, electrical coupling through gap junctions is required for the coordinated and synchronized contractions of the heart (Beyer et al., 1987).

Specificity of molecular passage is determined by the connexin subunits comprising each channel. To date, at least 20 different connexins have been identified in rodents and humans. Each connexon hemichannel can therefore either be homomeric (composed of identical connexins) or heteromeric (composed of a combination of connexins). The intercellular channels created by connexon alignment can, in turn, either be homotypic (alignment of two identical connexons) or heterotypic (alignment of two different connexons; reviewed in Bruzzone et al., 1996; Willecke et al., 2002).

Figure 1.3. Three-dimensional schematic diagram of a gap junction cluster. This schematic diagram of a gap junction cluster was derived from X-ray diffraction, electron microscopy, and chemical data. Six connexins (yellow) assemble into a connexon (green), delineating an axial channel with a central pore. Apposed connexons form intercellular channels, linking the two cell cytoplasms. From a few to over 10^5 intercellular channels are found in packed aggregations termed gap junctions. The length of each connexin is about 7.5 nm, the diameter of each connexon is about 1.5-2.0 nm and the two connected cells are ~3 nm apart. Connexons are illustrated in various combinations (red & blue). From Makowski et al., 1977, modified by Dermietzel and and Spray, 1993.

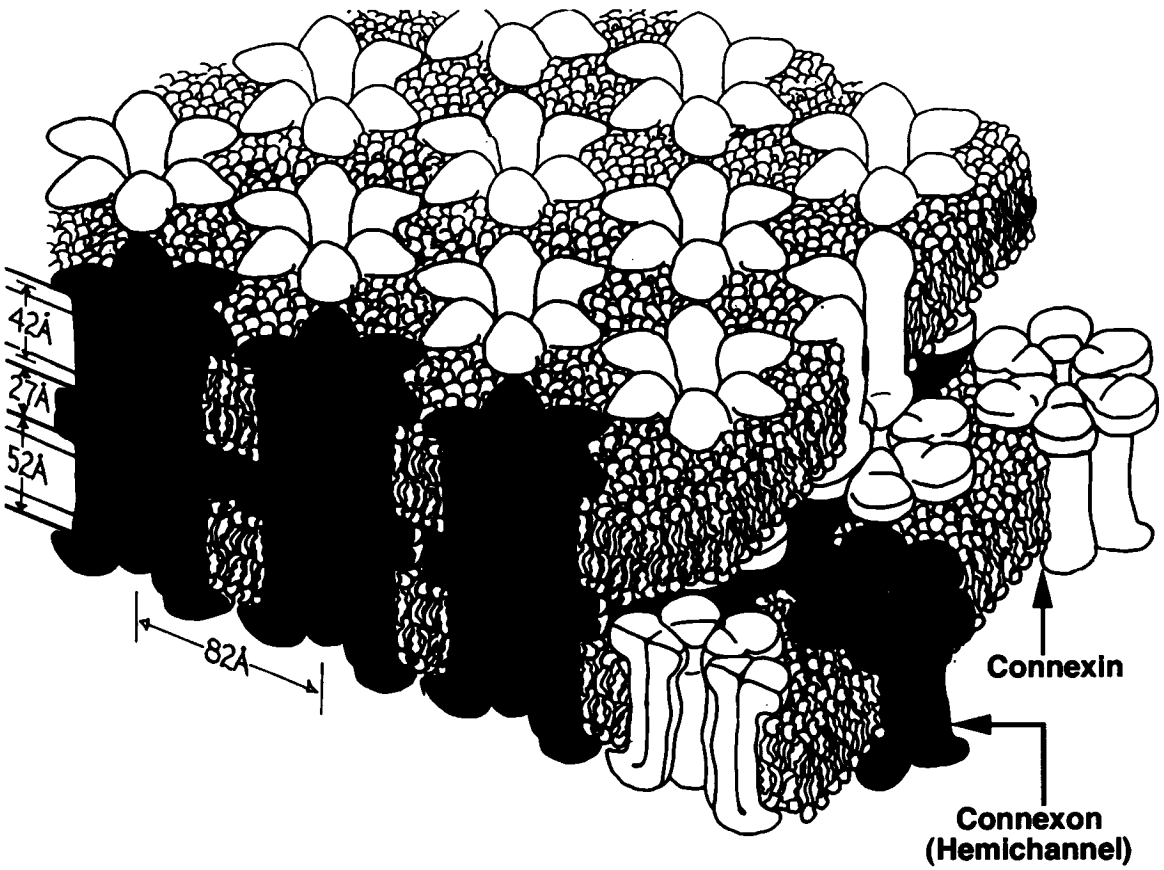

Figure 1.3

All of the connexin genes identified to date are single copy, but are localized to several different chromosomes. The majority are composed of two exons separated by an intron of variable size, with the complete open reading frame located on the second exon (Willecke et al., 2002). The structure of each connexin protein is characterized by four transmembrane domains (M1, M2, M3, and M4), flanked by two extracellular loops (E1, E2) and three cytoplasmic domains (N-terminus, cytoplasmic loop, and C-terminus; Goodenough et al., 1996; Milks et al., 1988; Yeager and Gilula, 1992; Zimmer et al., 1987). The connexin family shares about 50% amino acid homology overall, but the extracellular loops are uniformly conserved, with homology scores higher than 90% (Dahl et al., 1994). The majority of these proteins exhibit three cysteine residues in each extracellular loop that are believed to maintain the rigid tertiary structure required for oligomerization and pore formation (Haefliger et al., 1992; Kumar and Gilula, 1996; Rozental et al., 2000a).

Connexin nomenclature is based on their predicted molecular weight, ranging from 20 to 62 kDa (Willecke et al., 2002). Connexin subunits of each channel dictate the specificity of molecular passage (< 1kD) and ionic conductance (reviewed in Goldberg et al., 2004; Nicholson et al., 2000). Each connexin confers distinct biochemical and electrical properties to a connexon including selective permeability, voltage-sensitivity, and unitary conductance, allowing for molecules of different size and charge to be exchanged (Brissette et al., 1994; Dermietzel and Spray, 1993; Elfgang et al., 1995; Steinberg et al., 1994; Veenstra, 1996).

A Greek nomenclature is also employed to define connexin family subgroups based on the length of their cytoplasmic loop and their relative homology (Haefliger et al., 1992; Sohl et al., 1998). Group I (β) is composed of connexin25 (Cx25), Cx26, Cx30, Cx30.3,

Cx31, Cx31.1, and Cx32; group II (α) contains Cx33 (rodent only), Cx37, Cx40, Cx43, Cx46, Cx50, Cx57, Cx59, and Cx62; while Cx29, Cx36, Cx45, and Cx47 have been classified in the more divergent group III (γ) (Bruzzone, 2001; Goodenough et al., 1996; Rozental et al., 2000a; Willecke et al., 2002). Group III (γ) channels are unique in that they are more permeable to anions than other channels (Rozental et al., 2000b; Srinivas et al., 1999). While these subdivisions give some insight into protein compatibility, the capacity of different connexins to oligomerize into heteromeric connexons or to align to form heterotypic intercellular channels is dynamic and differs between connexins (Goodenough and Paul, 2003; White and Bruzzone, 1996). This selective process is thought to result from differences in the extracellular domain E2 that dictate the initial capacity of connexins to dock to one and other (Goodenough et al., 1996; White et al., 1994; White et al., 1995). As such, the changes in connexin expression observed over the course of CNS development and in response to environmental stimulation are predicted to alter the capacity of neural precursor cells to communicate with their progeny or with adjacent terminally differentiated "instructive cells" (neurons, astrocytes, and oligodendrocytes). These changes in connexin expression likely underlie the role of gap junctional intercellular communication in coordinating precursor cell activation, regional specification, axonal growth, axonal guidance, and synaptogenesis (Fulton, 1995; Guthrie and Gilula, 1989).

1.3.2 Functional hemichannels in non-junctional membranes

In addition to intercellular channels that provide direct cytoplasmic continuity between adjacent cells, recent studies indicate that unapposed connexons anchored in single plasma membranes can also be functional (reviewed in Contreras et al., 2004; Stout et al.,

2004). Rat Cx46, chicken Cx56, and mouse Cx50 expressed in *Xenopus* oocytes were first shown to insert in the plasma membrane and form functional hemichannels (Ebihara et al., 1995; Paul et al., 1991; Zampighi et al., 1999), with many of the properties similar to gap junction channels (Trexler et al., 1996). Subsequent reports identified the existence of Cx43 hemichannels at the plasma membrane of Novikoff cells, normal rat kidney cells, and Cx43-transfected HeLa cells (Li et al., 1996). In CNS cells, gated hemichannels in single plasma membranes localize to cytoplasmic processes and filopodia of subconfluent astrocytes, retinal horizontal cells, and human neural precursor cells (Boucher and Bennett, 2003; Hofer and Dermietzel, 1998; Kamermans et al., 2001; Stout et al., 2002). Dye-flux through hemichannels composed of Cx43 is proportional to the levels of connexin expression, providing further evidence of their functionality (Contreras et al., 2003b). In human teratocarcinoma-derived neural precursors (NT2 cells), maximal inducible hemichannel activity correlates with high expression of Cx43 and is substantially reduced following terminal differentiation to a mature neuronal phenotype corresponding with the loss of Cx43 expression (Boucher and Bennett, 2003).

Paired connexons in gap junction channels and functional hemichannels are found in either an open or closed conformation and switching between these two states requires a small cooperative rearrangement. The demonstration of critical connexon function in the absence of channel formation is surprising given that open hemichannels alter the permeability of individual cells and produce significant changes in cytoplasmic ionic concentrations that, if left open, can trigger death (Bennett et al., 2003; Paul et al., 1991). As such, biological relevance of hemichannel function *in vivo* is controversial (Bennett et al., 2003; Paul et al., 1991). Unpublished results from our laboratory indicate that induction

of Cx32-mediated hemichannel activity in rat pheochromocytoma (PC12) cells initially promotes neuritic extension, while excessive and sustained hemichannel activity triggers death. It is therefore not surprising that, under basal conditions, the majority of hemichannels are found in the closed formation (Stout et al., 2004).

Several stimuli can trigger channel opening. Cx43-containing hemichannels found in cardiac ventricular myocytes, Novikoff cells, and astrocytes are induced to open when exposed to low extracellular calcium concentrations, under conditions of metabolic inhibition, or following exposure to adenosine triphosphate (ATP) (Hofer and Dermietzel, 1998; John et al., 1999; Liu et al., 1995). Calcium itself modulates gap junction permeability and likely regulates hemichannel activity by inducing the tilting of the connexin subunits to a closed conformation (Unwin and Ennis, 1983; Unwin and Ennis, 1984). Other stimuli such as positive membrane potentials (Contreras et al., 2003a), intracellular kinase activity (Bao et al., 2004), and mechanical stimulation (Boucher and Bennett, 2003; Stout et al., 2002) trigger hemichannel opening, while negative membrane potentials, high concentrations of extracellular calcium (>1 mM), low intracellular pH (Trexler et al., 1999; Turin and Warner, 1977), and protein phosphorylation (Kim et al., 1999) close hemichannels (reviewed in Saez et al., 2003; Stout et al., 2004).

1.4 Connexin expression in the CNS

At least twelve connexins (Cx26, Cx29, Cx30, Cx32, Cx33 (rodent only), Cx36, Cx37, Cx40, Cx43, Cx45, Cx46, Cx47) are expressed in the mammalian CNS, found mainly in the cerebellum, cerebral cortex, hippocampus, hypothalamus, inferior olive, olfactory bulb, retina, and striatum (reviewed in Rouach et al., 2002; Rozental et al., 2000a). Gap

junctions in the CNS have been implicated in the control of multiple key biological activities such as buffering concentrations of metabolites or regulatory molecules and transmitting synchronous electrical signals (Barr et al., 1965; De Mello, 1987; Ledbetter and Lubin, 1979). Gap junctional communication between cells depends upon the unique repertoire of connexins expressed. Functional channel formation has been observed between neurons, oligodendrocytes, astrocytes, microglia, leptomeningeal and ependymal cells but not all cells are capable of communicating with each other as reviewed below (Dermietzel and Spray, 1993; Matsumoto et al., 1991; Parenti et al., 2002; Yamamoto et al., 1990a).

1.4.1 Connexins in neurons

Neurons are the functional cognitive cellular units of the nervous system, uniquely specialized to conduct nerve impulses that underlie "thought" and "action". Neurons communicate through synaptic connection. Two types of synapses, chemical and electrical, have been identified. Gap junctions are the structural units of the electrical synapse. Neuronal coupling via gap junctions has been well established, both *in vitro* and *in vivo* (Bani-Yaghoub et al., 1997; Dermietzel et al., 1989; Furshpan and Potter, 1959; Nadarajah et al., 1997; Rozental et al., 1998), with channels mainly localized to dendrites (Mollgard and Moller, 1975). Developing neurons express Cx40 and Cx43, while mature neurons express Cx36 and Cx45 as well as Cx26 and Cx37 with some controversy (Nakase and Naus, 2004; Venance et al., 2000). Expression of Cx32 mRNA by neurons has also been reported, but it is generally accepted that Cx32 protein is not present in the majority if not all neurons (Rash et al., 2000; Sohl et al., 2004).

In addition to synchronization of electrical activity, it has also been suggested that biochemical coupling through gap junctions (passage of small metabolites between cells) is an equally important, if not primary, mediator of coordinated neuronal activity (Kandler, 1997; Kandler and Katz, 1998). Both electrical and biochemical neuronal coupling are maximal during early development, decreasing in adult tissue, as neurons differentiate and as functional chemical synapses are formed (Christie and Jelinek, 1993; Connors et al., 1983; Hahnlein and Schuster, 1994; Kandler and Katz, 1995; MacVicar and Dudek, 1981; Walsh et al., 1989). These kinetics suggest that gap junctions are most important during the processes of neuronal specification and coordination of neuronal progenitor activity, and thus are required for events such as regulating the precision of developing synaptic circuits and defining neuronal domains in the developing brain (Peinado et al., 1993b).

1.4.2 Connexins in astrocytes

Astrocytes are the most prevalent cell type in the brain and their communication is fundamentally dependent upon connexin-mediated communication (Giaume and Mccarthy, 1996; Giaume and Venance, 1998). They constitute a metabolically and electrically coupled syncytium that plays an essential role in the metabolic, trophic, and structural support of neurons, notably by providing metabolic precursors and removing waste products. Key to these roles, astrocytes act as a buffer and maintain ionic homeostasis of the interstitial brain fluid through the regulation of extracellular ions (e.g., K^+ and H^+) arising from intense neuronal firing (Newman, 1986).

Gap junction channels are found abundantly between astrocytic processes surrounding synapses and nodes of Ranvier, and at astrocytic "endfeet" interacting with the

endothelium of blood vessels and regulating, in part, the blood brain barrier (Ochalski et al., 1997; Rouach et al., 2002; Yamamoto et al., 1990b). Connexin-mediated communication is proposed to underlie coordinated astrocytic activity required to achieve tasks such as potassium uptake, dissipation of neurotransmitters, as well as storage and delivery of glucose (Hofer and Dermietzel, 1998; Holthoff and Witte, 2000). Cx43 is the primary component of astrocytic gap junctions (Dermietzel et al., 1991; Giaume et al., 1991), but Cx26, Cx30, Cx40, and Cx46 have also been detected (Dermietzel et al., 2000). Astrocytes respond to a variety of stimuli by increasing their intracellular calcium concentration, either in individual cells or as waves propagated to surrounding cells, a function mediated by Cx43-containing channels (Charles, 1998; Charles et al., 1992; Nedergaard, 1994). In addition to gap junctional communication, Cx43-composed connexons can form functional gated hemichannels shown to control ATP release and the associated calcium signalling *in vitro* (Stout et al., 2002).

Many studies have described the predominance of heterotypic oligodendrocyte-astrocyte coupling (Kettenmann and Ransom, 1988). Heterologous gap junctions between these two cell types are localized between cell bodies, processes, and the external portion of myelin sheaths (Massa and Mugnaini, 1982). This panglial syncytium has been functionally described (Ransom and Kettenmann, 1990; Rash et al., 1997), with possible roles in the delivery of nutrients to oligodendrocytes and the reverse transfer of excess ions and waste products from oligodendrocytes to astrocytes, for discharge in brain microcapillaries (Nagy and Rash, 2000; Zahs, 1998). Heterocellular coupling has also been identified between neurons and astrocytes, although it is not as widespread (Froes and de Carvalho, 1998; Nedergaard, 1994). Such structures have been implicated in coordinated activity for bi-

directional calcium intercellular signalling (Pasti et al., 1997) as well as for neuronal differentiation (Froes et al., 1999).

1.4.3 Connexins in oligodendrocytes

Oligodendrocytes are the myelinating cells of the brain, insulating axons to allow an increase in conduction velocity. In the myelin sheath, gap junctions allow ions and nutrients to pass from the somata to all the layers of the myelin (Paul, 1995). Interestingly, non-myelinating oligodendrocytes have also been identified, with the same pattern of connexin expression, and with striking localization to the neural precursor rich regions of the adult CNS (i.e., along the non-myelinated mossy fibre pathway and bordering the SGZ or in the SVZ; Altevogt et al., 2002; Zerlin et al., 2004). Cx29, Cx32, and Cx47 can be found in oligodendrocytes throughout the brain and spinal cord (Dermietzel et al., 1997; Kunzelmann et al., 1997; Odermatt et al., 2003; Sohl et al., 2001a; Teubner et al., 2001). Cx32 is predominantly localized to Schmidt-Lanterman incisures and to the paranodal regions bordering the nodes of Ranvier of Schwann cells, the oligodendroglial cells myelinating the peripheral nerves (Bergoffen et al., 1993; Scherer et al., 1995). At the subcellular level, Cx32 protein is mainly found in the perikarya and processes of oligodendrocytes (Li et al., 1997). Although its distribution pattern is unique, Cx32 can be co-expressed with Cx47 in small myelin sheaths and with Cx29 in gray matter oligodendrocytes of the hippocampus (Kleopa et al., 2004). Connexin diversity and the specific expression pattern of each connexin in oligodendrocytes were suggested to define different subpopulations, characterized both by the caliber of the myelinated axon and a unique connexin expression profile (Altevogt et al., 2002). Each connexin may therefore serve a specialized but

overlapping role. This is reflected in the observation that Cx32 knockout (Cx32KO) and Cx47KO mice only show minimal CNS abnormalities, while the double-null mutant mice exhibit severe demyelination, leading to premature death (Odermatt et al., 2003). Furthermore, Cx32 may also be involved in the formation of reflexive gap junctions, channels allowing fast communication between adjacent paranodal loops (Scherer et al., 1995).

During oligodendrocyte differentiation in primary and secondary cell cultures from newborn and adult rat, ionic- and dye-coupling were observed between oligodendrocytes (Venance et al., 1995), although the presence of these inter–oligodendrocyte junctions *in vivo* has been debated (Rash et al., 2001). While most connexins are initially expressed during embryonic development, Cx32 is unique among connexins in that it is virtually exclusively expressed in postnatal brain (Dermietzel et al., 1989; Nadarajah et al., 1997). Cx32 mRNA is first detected in rodent brainstem around postnatal day 3 (P3) and is found at highest levels in the adult brain, with maximal expression detected in the hindbrain (Belliveau et al., 1995; Naus et al., 1990; Venance et al., 1995). Cx32 protein is detected at low levels between postnatal days 5-7 in rodent brain, with levels peaking around P14 - P21 and remaining high throughout adulthood (Belliveau et al., 1991; Nadarajah et al., 1997). Although this expression pattern closely corresponds to the time course of oligodendrocyte maturation, with the onset of oligodendrogenesis occurring during the first postnatal days and peaking around P14, (Belliveau et al., 1991; Dermietzel et al., 1989; Nadarajah et al., 1997; Parnavelas et al., 1983), the timing of Cx32 expression in differentiating oligodendrocyte progenitors had not yet been evaluated.

1.5 Connexin-mediated control of neural precursor cell fate

Functional indices of both electrical and metabolic coupling are widespread in the developing nervous system and it is likely that gap junctions represent the predominant means of cell-cell communication prior to the formation of chemical synapses (Lo Turco and Kriegstein, 1991; Peinado et al., 1993b). As discussed earlier, embryogenesis involves the transition of totipotent stem cells to multiple pluripotent and multipotent stem cells followed by progenitor cells. These latter progeny initiate specification in temporally defined 'waves' generating the mature cells of functional organs and integrated systems of the adult organism. This coordinated process requires extensive interaction between cells destined towards "like-lineage" as well as their segregation from neighbouring groups of cells induced by similar stimuli to specify to a different fate (Guthrie and Gilula, 1989). Gap junctional intercellular communication represents one of the underlying signaling mechanisms regulating this temporal patterning of stem cell progeny (Fraser and Bryant, 1985; Fraser et al., 1987; Furshpan and Potter, 1968; Lee et al., 1987; Warner et al., 1984). Patterning is dictated, in part, by the changing repertoire of connexins expressed by adjacent populations over the course of development, with expression of compatible connexins coordinating the specification of interconnected cell populations towards the same fate. Conversely, expression of incompatible connexins at the boundaries between these populations results in neighbouring groups adopting a different identity. Connexin-mediated intercellular communication and hemichannel formation are also believed to play a role in coordinating activity of neural precursors influencing tissue differentiation, progenitor migration, regional specification, axonal growth and guidance, and synaptogenesis during CNS development (Dermietzel and Spray, 1993; Fulton, 1995; Guthrie and Gilula, 1989;

Weissman et al., 2004).

Six (Cx26, Cx29, Cx32, Cx36, Cx43, Cx47) of the 12 connexin proteins identified in the CNS have been shown to be dynamically expressed over the course of cerebral development (Buniello et al., 2004; Gulisano et al., 2000; Hombach et al., 2004; Nadarajah et al., 1997; Nadarajah et al., 1998; Rouach et al., 2002; Sohl et al., 2001a; Sohl et al., 2001b). In embryonic brain, both Cx26 and Cx43 are expressed by neural precursors (Bittman and LoTurco, 1999; Duval et al., 2002; Nadarajah et al., 1997; Rozental et al., 1998; Rozental et al., 2000b). As precursors undergo neuronal differentiation, levels of Cx43 decline and an intermediate population of channels composed of Cx40 is detected (Bani-Yaghoub et al., 1997; Leung et al., 2002; Rozental et al., 1998). Phosphorylation of Cx43 is observed as protein levels drop and this reduction and post-translational modification have been proposed to play a crucial role in the program of neuronal differentiation (Dowling-Warriner and Trosko, 2000; Duval et al., 2002). Cx33 is also detected at this stage, although it may not be functional (Chang et al., 1996). Finally, terminal neuronal differentiation is accompanied by an upregulation of Cx36 expression (Rozental et al., 2000b).

Maintaining elevated levels of Cx43 over the course of P19 teratocarcinoma cell differentiation results in the inhibition of neuronal specification, while promoting differentiation to an astrocytic phenotype (Bani-Yaghoub et al., 2000; Belliveau et al., 1997). These observations were among the first to provide evidence that altering the repertoire of connexins expressed by progenitor cells is key to determining cell fate. However, several explanations have been suggested to account for the decrease in coupling strength of Cx43-containing channels observed during the progressive specification of

neuroblasts. First, channels formed by Cx43, Cx33, and Cx40 might not be functional, since it has been shown that Cx43 does not pair with Cx40 or Cx33 connexons (Rozental et al., 1998). Second, the different channels formed by newly expressed connexins may possess different biophysical properties, favouring the passage of different molecules. A third possibility is that coupling between astrocytes and progenitors may dictate neuronal differentiation. Direct cell-cell contact between astrocytes and SVZ or hippocampal precursors has been shown to induce the proliferation of these precursors and to direct their subsequent differentiation to migrating neuroblasts (Lim and Alvarez-Buylla, 1999; Song et al., 2002). Astrocytes produce a wide variety of intercellular signals implicated in CNS development that could diffuse through gap junctions (Zaheer et al., 1995). Since conditioned media did not provide the same supportive environment as astrocyte monolayers, direct contact was proposed to be required for neurogenesis (Song et al., 2002). Taken together, the studies reviewed above highlight the importance of defining the impact of connexin-mediated communication on neural progenitor cell fate and underlie the importance of regulated expression patterns of diverse connexin subtypes over the course of progenitor cell specification. Based on this compelling developmental evidence, I hypothesized that altering connexin expression could direct **adult** neural progenitor activation and specification *in vitro* as well as *in vivo*. To test this hypothesis, I focused on elucidating the role of postnatal Cx32 expression in regulating adult neural progenitor cell fate.

1.6 Cx32 in the control of adult neural progenitor cells

To establish the role of Cx32 in the control of adult neural progenitors, I performed a series of loss of function and gain of function *in vitro* and *in vivo* studies using uninjured and injured Cx32-null mutant mice. Cx32 was chosen as the ideal connexin for initial study based on its expression pattern. As with all other connexins, it is abundantly expressed outside of the nervous system, in cells such as hepatocytes, epithelial cells, and pancreatic acinar cells (Dermietzel and Spray, 1993; Nicholson and Bruzzone, 1997). However, while most connexins are initially expressed during embryonic development, Cx32 is the only connexin protein expressed exclusively in the postnatal and not embryonic brain (Dermietzel et al., 1989; Belliveau et al., 1991). Arguably, connexin-null mutant mice represent the best available means of examining the contribution of individual connexins to neural progenitor cell regulation. However, germ line deletions can elicit adaptive gene expression, compensation by other family members, and alteration of endogenous spatial-temporal gene regulation that could equally alter the phenotype (reviewed in Bockamp et al., 2002). Thus, I argue that Cx32 is the optimal candidate to initiate these investigations given that null mutation is not predicted to impact upon embryonic precursor populations. Furthermore, as mentioned in "1.4.3 Connexins in oligodendrocytes", Cx26, Cx43, and Cx32 protein levels fluctuate during postnatal development (Nadarajah et al., 1997). Whereas developmental regulation of Cx26 and Cx43 expression has been associated with embryonic progenitor cell fate (Bittman and LoTurco, 1999), the putative role of Cx32 in a progenitor population has not yet been investigated.

1.7 Research objectives

The **overall hypothesis** of my doctoral research was that alterations in Cx32 expression would affect adult progenitor cell proliferation or differentiation in postnatal rodent brain. To assess this hypothesis, I established: (1) the impact of Cx32-null mutation on adult hippocampal progenitor fate *in vitro* and *in vivo* in uninjured tissue, (2) the effect of these phenotypic alterations in progenitors on behavioural indices of learning and memory in healthy animals, (3) the effect of Cx32 loss of function on neurogenesis following excitotoxic injury *in vivo*, and (4) the cell-autonomous role of Cx32 in directing postnatal progenitor fate *in vitro*. These studies are described in the following four chapters. The specific objectives of each study are defined at the beginning of each chapter. The findings generated over the course of this research are then placed in context with our existing understanding of the potential role of connexin-mediated communication in the control of progenitor fate in a final summary chapter.

Chapter 2: Oligodendrocyte progenitor enrichment in the connexin32-null mutant mouse

2.1 Objectives

The overall goal of my research was to elucidate the role of connexin-mediated communication in determining progenitor cell fate and to exploit this understanding to promote regulated survival, expansion, and differentiation of stem and progenitor cells *in vitro* as well as *in vivo.* To this end, I first addressed two experimental objectives as part of my Ph.D research: **1)** determine whether Cx32 localizes to an adult progenitor population in the dentate gyrus of the hippocampal formation of C57BL/6 mice and **2)** determine whether the loss of Cx32 affects progenitor cell specification in the hippocampus.

2.2 Statement of collaborator contributions

I wish to thank Dr Klaus Willecke and Dr David Paul for providing the initial Cx32KO breeding pairs and Sandy Beyko for her contribution in the initial histological assessment of the Cx32KO mice.

2.3 Abstract

Prior to the establishment of chemical synapses, neural progenitors are often coupled by connexin-mediated gap junctions providing a robust mechanism for cell-cell communication in the developing brain. The present study was undertaken to determine if alterations in junctional coupling also affect neural progenitor proliferation, survival, and differentiation in the adult brain. In adult mice, we localized the Cx32 gap junction protein to a subset of $NG2^+$ and $PDGF\alpha R^+$ early oligodendrocyte progenitors in the dentate gyrus of the hippocampal formation. In Cx32KO mice, we found an increase in the total number of proliferating $nestin^+$ and $NG2^+$ progenitors in the SGZ, hilus, and polymorphonuclear layer of the dentate gyrus *in vivo* and in the total number of $nestin^+$ progenitors capable of clonogenic expansion *in vitro*. By bromodeoxyuridine labelling, lineage analysis, and terminal deoxynucleotidyl transferase nick end labelling, we demonstrated that the turnover of these cells is constitutively enhanced in the Cx32KO dentate gyrus thereby reflecting a dynamic defect in oligodendrogenesis in this population. Analyses of surviving bromodeoxyuridine-labelled cells at 1, 3, 5, 7, 14, and 28 days after injection revealed that the transient amplifying progenitor population fails to terminally differentiate and is likely deleted by an apoptotic-like mechanism within 3 days of labelling. These data provide empirical evidence to support the hypothesis that connexin expression influences adult progenitor number and specifically implicate Cx32-mediated signaling in the activation, survival, and differentiation of a subset of early oligodendrocyte progenitors in postnatal rodent brain.

2.4 Introduction

There is growing evidence indicating that passage of ions, metabolites, and second messengers between cells via connexin-mediated gap junctions alters neural progenitor fate (Bittman and LoTurco, 1999; Mercier and Hatton, 2001; Nadarajah et al., 1998; Rozental et al., 1998; Rozental et al., 2000b). *In vitro*, pharmacological inhibition of gap junctional-mediated intercellular communication decreases the percentage of embryonic progenitors that enter S-phase and inhibits terminal differentiation of embryonic carcinoma cells into neurons and glia (Bani-Yaghoub et al., 1999; Bittman et al., 1997). To address whether connexin-mediated communication regulates progenitor fate in adult brain, we began by evaluating glial progenitor activation in Cx32-null mutant mice. As described in Chapter 1, Cx32 expression closely corresponds to the time course of oligodendrocyte maturation (Belliveau et al., 1991; Dermietzel et al., 1989; Nadarajah et al., 1997; Parnavelas et al., 1983). In the peripheral nervous system, the significance of Cx32 expression by Schwann cells is underscored by the fact that Cx32 mutations result in a demyelinating peripheral neuropathy called X-linked Charcot-Marie-Tooth disease (CMTX) (Bergoffen et al., 1993; Bruzzone et al., 1994; Nicholson et al., 1999). One of the most common inherited neurological disorders, CMTX neuropathy affects both motor and sensory nerves and is often first manifested by weakness of the foot and lower leg muscles, with subclinical abnormalities in visual, acoustic, and motor pathways detected in most patients (Bahr et al., 1999). At least 90 different Cx32 mutations result in CMTX (Bergoffen et al., 1993). These mutations have a direct effect on channel activity (Bruzzone et al., 1994), although the direct deleterious mechanism of most Cx32 mutations remains unclear. They may cause a toxic gain of function in oligodendrocytes due to altered trafficking and/or accumulation of Cx32

in the Golgi or endoplasmic reticulum (Kleopa et al., 2004). On the other hand, some mutations may result in reduced connexin expression levels or altered properties, or create a dominant negative, thereby inhibiting other connexins (Bruzzone et al., 1994). Cx32KO mice exhibit a mild late-onset peripheral neuropathy characterized by thin myelin sheaths, cellular onion bulb formation, and enlarged periaxonal collars (Anzini et al., 1997), but only a slightly altered nerve conduction and no apparent muscle weakening or abnormality in CNS myelin (Scherer et al., 1998).

In this study, we evaluated Cx32 expression in the adult mammalian brain and determined the impact of the loss of Cx32 using a Cx32-null mutant mouse model. Our results implicate Cx32 in the activation, survival, and differentiation of a specific subset of early oligodendrocyte progenitors.

2.5 Materials and methods

2.5.1 Generation of Cx32KO mice

Breeding pairs of Cx32-deficient mice were initially obtained from Dr Klaus Willecke (Universitat Bonn, Germany). To insure uniformity in genetic background, animals were backcrossed to C57BL/6 wildtype (WT) mice (Charles River Laboratories, Wilmington, DE) for 12 generations. All animals used in this study were 2-4 months old.

2.5.2 Histology and lineage analyses

A total of n=46 Cx32KO and n=46 WT male mice were evaluated in this study. Animals were euthanized by lethal injection with sodium pentobarbital and transcardially perfused with 10 mM phosphate buffered saline (PBS; 10 mM sodium phosphate, 154 mM

sodium chloride) followed by 4% paraformaldehyde in 10 mM PBS. For histological analysis, brains were removed and post-fixed for 24 h in this same solution, transferred to 10 mM PBS, and paraffin-embedded according to standard histological procedure. Serial coronal sections (4 μm) were cut on a rotary microtome (Leica Microsystems Inc., Richmond Hill, ON). Sections were stained with Hoechst 33258 (2 μg/ml, Sigma, St. Louis, MO) or cresyl violet according to standard histological procedure. Cell number was established by counting Hoechst-stained nuclear profiles over three adjacent 4 μm sections. These values were averaged to yield a single parameter per animal. Layer thickness was determined by measuring the width of layered cell nuclei in the CA1 and CA3c pyramidal cells fields and the superior limb of the dentate gyrus using Image Pro Software v3.01 on a Nikon E800 microscope equipped for epifluorescence. Three measurements were taken in a 0.1 mm^2 field and averaged to yield a single value per animal.

Cell identity was determined by immunofluorescence. Brains were post-fixed for 24 h in 4% paraformaldehyde in 10 mM PBS, and cryoprotected in 20% sucrose solution in 10 mM PBS containing 0.001% sodium azide. Serial coronal sections (10 μm) were cryostat-cut (Leica Microsystems Inc.). Primary antibodies were anti-Cx32 (1ug/ml, Zymed, Burlington, ON), anti-nestin (1:50, Chemicon, Temecula, CA), anti-NG2 (1:200, Chemicon), anti-PDGFαR (1.5 μg/ml, BD Biosciences, Mississauga, ON), anti-A2B5 (1:2, ATCC, Manassas, VA), anti-O4 (1:50, Chemicon), anti-galactocerebroside (GalC, 1:50, Sigma), anti-proteolipid protein (PLP, 1:100, Biogenesis, Kingston, NH), cyanine-3 (Cy3)-tagged anti-glial fibrillary acidic protein (GFAP, 1:800, Sigma), and anti-NeuN (1:100, Chemicon). Secondary antibodies were Cy3- or fluorescein isothiocyanate (FITC)-conjugated anti-mouse IgG (1:800, 1:100, Jackson ImmunoResearch, West Grove, PA) or

IgM (1:600, Jackson ImmunoResearch), Cy3-conjugated anti-rat (1:400, Jackson ImmunoResearch), and Cy3- or FITC-conjugated anti-rabbit (1:600, 1:100 Jackson ImmunoResearch) IgG as appropriate. Antibodies were diluted in Ab buffer (10 mM PBS, 0.3% Triton-X 100, 3% bovine serum albumin). Immunofluorescence was evaluated using OpenLab Software v3.08 (Improvision, Lexington, MA) on a Leica DMXRA2 microscope equipped for epifluorescence. All other details were as described in (Bennett et al., 1998a; Bennett et al., 2000). All antibodies are listed in "Appendix 1: List of antibodies".

2.5.3 Western analyses

Mice were euthanized by lethal injection with sodium pentobarbital and decapitated. Hippocampal protein was extracted from n=2-4 animals per sample using Trizol reagent (Invitrogen, Burlington, ON). Protein concentration was measured with the BioRad DC assay kit (Mississauga, ON). Proteins (30 μg) were separated by sodium dodecyl sulphate (SDS)-polyacrylamide gel electrophoresis (SDS-PAGE) of 7.5% or 12.5% gels under reducing conditions and transferred to Immobilon membrane (Amersham-Pharmacia Biotech, Baie d'Urfé, PQ). Membranes were blocked in 10 mM PBS containing 1% casein. Anti-nestin (1:500, Chemicon), anti-GFAP (1:2000, Sigma), anti- GalC (1:200, Sigma), or anti-β-tubulin (1:400, Sigma) were diluted in the same solution. Secondary antibodies and tertiary reagents were biotinylated anti-mouse IgG (1:10,000, Sigma) and extravidin peroxidase (1:1000, Sigma) or extravidin alkaline phosphatase (1:300,000, Sigma), or peroxidase-conjugated anti-rabbit IgG (1:5000, Jackson ImmunoResearch; see "Appendix 1: List of antibodies"). Immunoreactivity was visualized by enhanced chemiluminescence following the protocol provided by the manufacturer (Pierce, Rockford, IL). Where

reprobing for β-tubulin is indicated, membranes were processed colourimetrically using BCIP/NBT Fast tablets (Sigma). All other details are as in (Bennett et al., 2000).

2.5.4 Bromodeoxyuridine labelling of mitotically active cells

In order to label actively dividing cells, bromodeoxyuridine (BrdU) (50 μg/g in sterile 10 mM PBS, pH 7.0) was administered intraperitoneally (Cooper-Kuhn and Kuhn, 2002). Animals received two daily injections (4-5 h apart) over two consecutive days and a single injection on the third day. Mice were sacrificed 24 h after the last injection and brains processed as described above. Cryostat-cut sections (10 μm) were incubated in 2 N hydrochloric acid for 1 h and neutralized in 0.1 M borate buffer (pH 8.5). BrdU incorporation was detected by immunofluorescence using mouse anti-BrdU (6 μg/ml, Roche) and Cy3- conjugated anti-mouse IgG as described above. Cell number was established by counting Cy3-$BrdU^+$ nuclear profiles over three adjacent 10 μm sections between bregma –1.68 and –2.08 in the CA1 and dentate gyrus of the hippocampal formation using the Measurement Module of OpenLab 3.08 software. Counts were performed by three independent investigators. Values were averaged to yield a single parameter per animal. The total area (mm^2) of each region was determined using OpenLab 3.17 Measurement Module. Data are expressed as the number of $BrdU^+$ cell profiles per 0.1 mm^2. Where double-labelling is indicated, a rat monoclonal FITC-conjugated anti-BrdU (1:20, Accurate Chemical, Westbury, NY) and anti-NeuN, anti-NG2, or anti-GFAP were employed as described above.

2.5.5 Terminal deoxynucleotidyl transferase-mediated dUTP nick end labelling

Dying cells were detected by terminal deoxynucleotidyl transferase (TdT)-mediated deoxy-uridine (dUTP) nick end labelling (TUNEL). Sections were permeabilized by a 15 min incubation in 0.1% Triton-X/0.1% sodium citrate on ice and a 2 min incubation in ethanol:acetic acid (2:1) on ice. Sections were rinsed for 2 min in 10 mM PBS and reacted for 1 h at 37°C with FITC–labelled dUTP in TdT buffer (30 mM Tris-HCl, pH 7.2, 140 mM sodium cacodylate, 1 mM cobalt chloride) and TdT according to the protocol provided by the manufacturer (Roche). TUNEL-reacted sections were double-labelled with NG2 as described above. Negative controls included sections incubated with FITC–labelled dUTP in the absence of TdT. The number of $TUNEL^+$ cells was determined as described above for $BrdU^+$ cells.

2.5.6 *In vitro* culture of progenitors isolated from Cx32KO and WT mice

Clonogenic assays were performed essentially as described for embryonic cultures in (Williams et al., 1997). Culture modifications to accommodate adult progenitors were as follows. Primary progenitor cultures were prepared from adult WT and Cx32KO mice at 3 months of age. Mice (n=3 animals/condition/experiment) were euthanized by lethal injection with sodium pentobarbital. The hippocampal formation from both hemispheres was dissected in Dissection Media (10 mM PBS, 154 mM sodium chloride, 2 mM glucose, 200 U/ml penicillin streptomycin) and rocked in Dissection Media on a clinical orbiter until all samples were collected. Tissue was transferred to sterile 15 ml polystyrene tubes containing 3 ml of 10 U/ml papain (Sigma) in Dissection Media brought to pH 7.0 with 1 N sodium hydroxide and passed repeatedly through a 5 ml pipette. 0.05% Trypsin/0.53 mM

ethylenediaminetetraacetic acid (EDTA; 3 ml, 1x, Invitrogen) was added and tubes were rotated at 37°C for 10 min. 0.5% Trypsin/5.3 mM EDTA (2.5 ml, 10x, Invitrogen) was added to each suspension and tubes were rotated at room temperature for an additional 10 min. Nine ml of Plating Media consisting of Neurobasal Media with B27 supplement (100 U/ml), 10% heat-inactivated fetal calf serum, 10% heat-inactivated horse serum, and 100 U/ml penicillin/streptomycin (Invitrogen) was added to each tube. Suspensions were transferred to sterile 50 ml polypropylene tubes and passed repeatedly through a 10, 5, and 1 ml pipette followed by trituration through a glass bore pasteur pipette. Cells were centrifuged and resuspended in 20 ml Plating Media. Trypan blue hemocytometer counts were performed. Cultures were not plated unless >95% of cells excluded the dye after the dissociation procedure. Primary cultures were plated at a density of $5x10^5$ cells/ml in 4 well Lab-Tek culture slides (1 ml/well) coated with poly-D-lysine (50 μg/ml in double distilled H_20). On the following day, the medium was changed to Maintenance Media consisting of Neurobasal Media with B27 supplement (100 U/ml), penicillin/streptomycin (100 U/ml), and basic fibroblast growth factor (bFGF; 20 ng/ml, Invitrogen). After 7 days of cultures, cells were fixed in 4% paraformaldehyde in 10 mM PBS for 10 min and immunoreacted as described above with polyclonal anti-enolase (1:10, Calbiochem, La Jolla, CA), Cy3-conjugated anti-GFAP, or monoclonal anti-nestin. Cultures were double-labelled with anti-enolase and anti-nestin using FITC and Cy3 conjugated secondary antibodies respectively as described above. Colonies > 7 cells were counted. To assess differentiation potential, colonies were treated for 7 days with bFGF and then exposed for 5 days to brain-derived neurotrophic factor (BDNF, 10 ng/ml, Invitrogen) in Neurobasal Media supplemented with B27 supplement (100 U/ml) and penicillin/streptomycin (100 U/ml).

2.5.7 Statistical analyses

Data are presented as the mean ± standard error of measurement (SEM). Data were analyzed by (a) Multiple analysis of variance (MANOVA) followed by *post hoc* Tukey tests to identify conditions that differed significantly from WT control or (b) Student's *t* tests as applicable. In each analysis, α was set at $p<0.05$.

2.6 Results

2.6.1 Generation of C57BL/6 Cx32KO and WT mice

Cx32KO mice, in a mixed genetic background of 129SVJ1 and C57BL/6 strains, were obtained from Dr Klaus Willecke (Nelles *et al.*, 1996). Because 129SVJ1 animals exhibit reduced neural progenitor proliferative capacity relative to other strains (Kempermann et al., 1997a), we placed the Cx32KO mice in a largely C57BL/6 genetic background by extensive backcrossing. At the F12 generation, a genetically matched inbred WT colony was derived from Cx32 heterozygote matings. Animals used in the present study were either F12 littermates or the progeny of time-matched pregnancies using the F12 C57BL/6 Cx32KO and WT colonies.

2.6.2 Hyperchromatic cells are found in the dentate gyrus of Cx32KO mice

In order to determine the histological profile of an adult C57BL/6 mouse brain developed in the absence of Cx32, we first evaluated Nissl-stained serial midbrain coronal sections from WT and Cx32KO 3 months old mice. No gross midbrain cytoarchitectural abnormality was noted in the Cx32KO animals. However, a closer morphological analysis of the dorsal hippocampal formation revealed a consistent expansion of hyperchromatic cell

profiles in the Cx32KO hippocampal formation. These cells were observed in the SGZ and hilus of the dentate gyrus and in the CA3c pyramidal layer of the hippocampus (Figure 2.1). Since the removal of Cx32 had a noticeable impact on one or more cell populations within the dentate gyrus, the precise cellular localization of Cx32 was investigated in the dentate gyrus of WT animals.

2.6.3 Cx32 localizes to oligodendrocytes and oligodendrocyte progenitors in adult WT dentate gyrus

Because Cx32 expression kinetics closely match the time course of CNS myelination (Dermietzel et al., 1997; Li et al., 1997; Parnavelas et al., 1983), loss of Cx32 could potentially affect the fate of oligodendrocyte progenitors present in the SGZ of the dentate gyrus. To explore this possibility, expression of Cx32 protein was evaluated by immunofluorescence. As expected, strong immunoreactivity was observed in small irregular diamond-shaped soma with long processes consistent with the morphology of terminally differentiated oligodendrocytes (Figure 2.2 *A,B, arrows*). Numerous immunoreactive cells with small cell bodies and shorter stellate processes were also detected in the SGZ and polymorphonuclear layer of the dentate gyrus (Figure 2.2 *A,B, arrowheads*). Finally, $Cx32^{+}$ cells with oblong cell bodies were observed in the SGZ. No labelling was detected in the Cx32KO negative control (Figure 2.2 *C,D*).

To evaluate Cx32 expression in progenitor populations, double immunostaining for Cx32 and two characteristic markers of glial and early oligodendrocyte progenitors, NG2

Figure 2.1. An increase in hyperchromatic cell profiles is detected in the SGZ of the Cx32KO dentate gyrus. Abbreviations: CA1,2,3, 3c, pyramidal cell fields of the hippocampus; GrDG, granule cell layer of the dentate gyrus; PoDG, polymorphonuclear layer of the dentate gyrus; SGZ, subgranular zone of the dentate gyrus; MolDG, molecular layer of the dentate gyrus; L.mol, lacunosum moleculaire; S.rad, stratum radiatum, S.oriens, stratum oriens. Cresyl violet-stained hippocampal sections from 3 months old C57BL/6 WT (*A, B*) and Cx32KO (*C, D*) mice. *A, C*) A sizable population of hyperchromatic Nissl-stained cells was observed in the SGZ and hilus of the dentate gyrus (arrows) and in the CA3c pyramidal cell layer (arrowheads) of Cx32KO mice. Scale bars, 100 μm. *B, D*) Morphology of the enriched cell type. Hyperchromatic cells were oblong or oval shaped in Cx32KO and WT mice (arrows), often with darkly stained short neuritic extensions in Cx32KO animals (arrowheads). Scale bars, 50 μm.

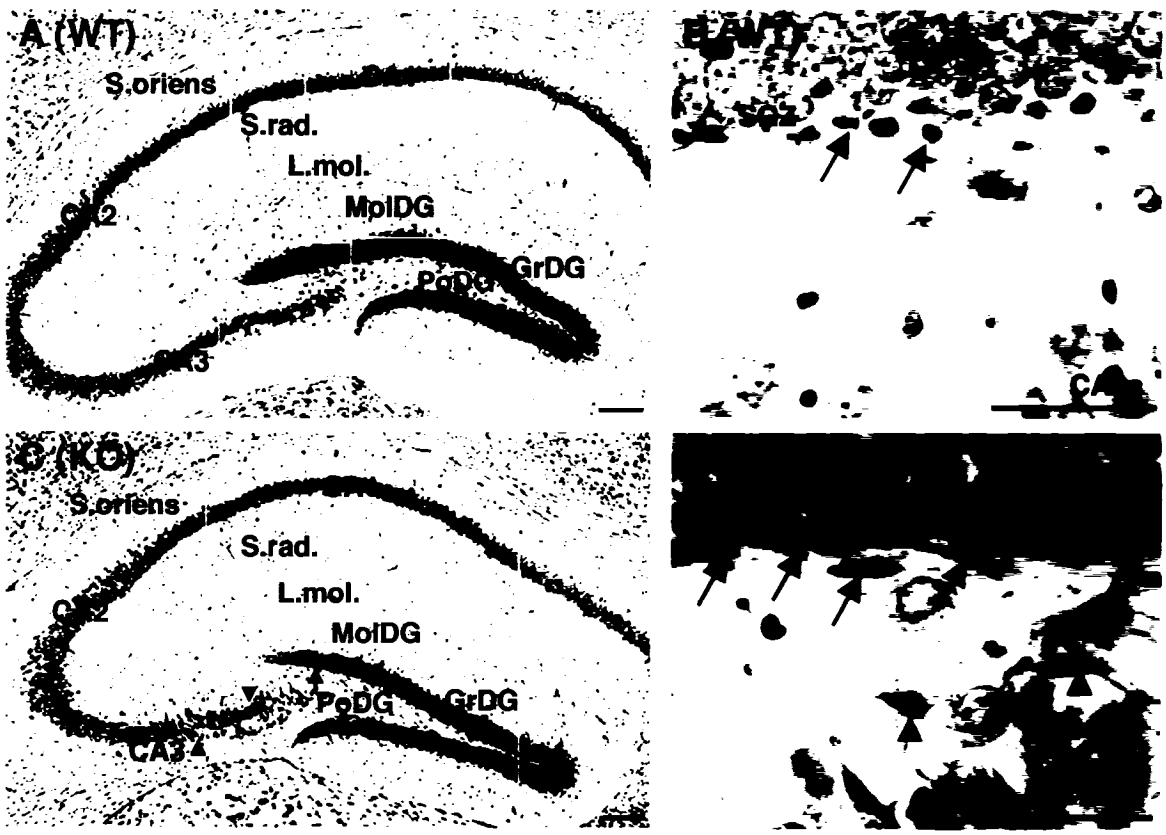
A (WT)
S.oriens
S.rad.
L.mol.
MolDG
GrDG
B (WT)
SGZ
C (KO)
S.oriens
S.rad.
L.mol.
MolDG
PoDG
GrDG
CA3

Figure 2.1

Figure 2.2. Cx32 localizes to cells with three distinct morphologies in WT dentate gyrus. Abbreviations are as defined in Figure 2.1. *A*) Cx32 is detected in cells in the GrDG with diamond-shaped soma (asterisks) and long processes (small arrows) typical of oligodendrocytes. Immunoreactive cells with small cell bodies and shorter stellate processes were also observed in the SGZ and PoDG (arrowheads). Larger $Cx32^{+}$ oblong cell bodies were consistently detected in the SGZ (large arrows). *B*) Higher power inset outlined in *A*. *C*) No labelling was detected in the Cx32KO negative control. *D*) Higher power inset outlined in *C*. Scale bars, 50 μm.

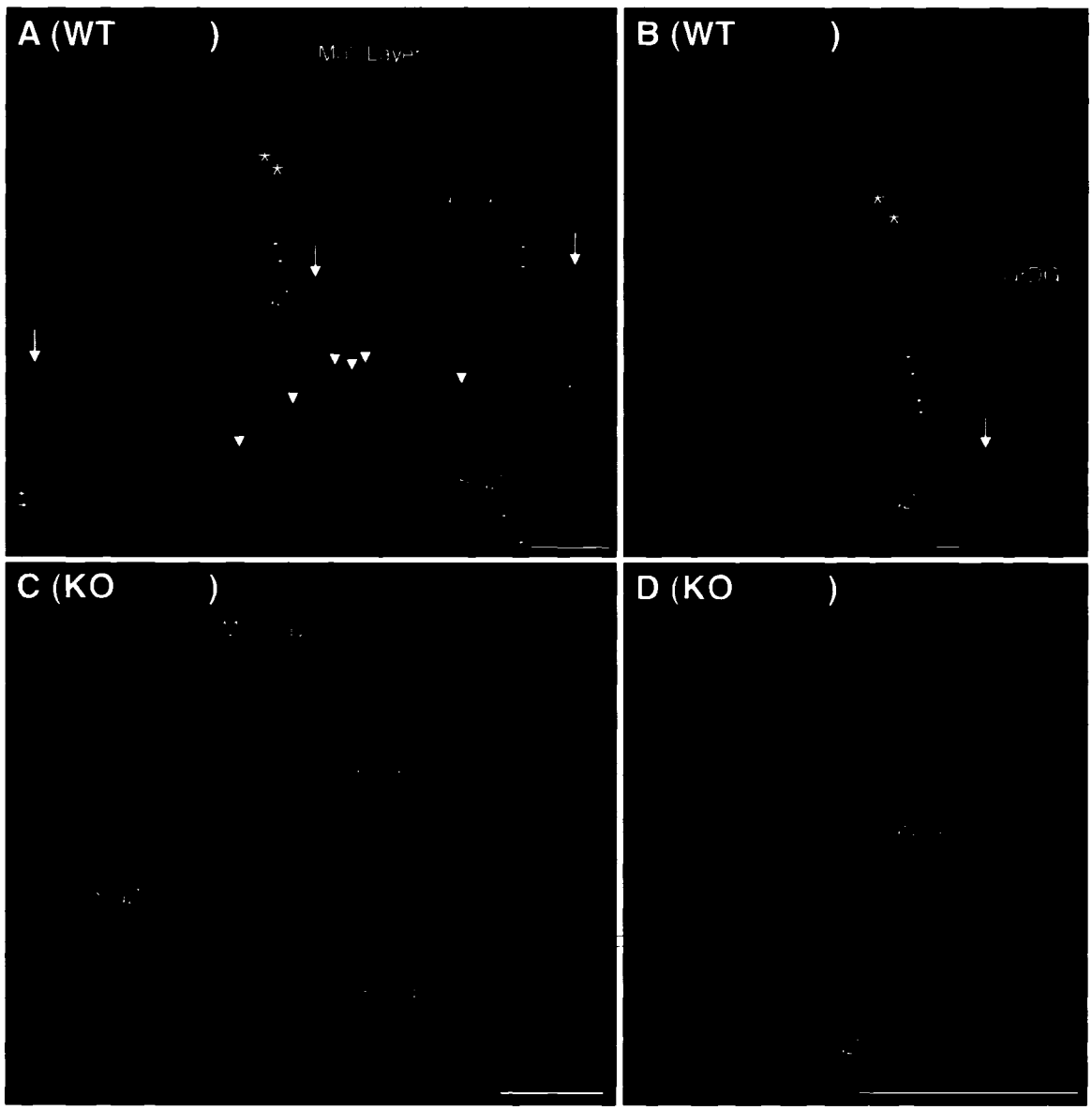

Figure 2.2

chondroitin sulfate proteoglycan and PDGFαR, was performed (Dawson, 2000; Kondo and Raff, 2000; Levine, 1993). Numerous $NG2^+$ cells with small cell bodies and stellate processes were $Cx32^+$ (Figure 2.3 *A,B*). Punctate Cx32 immunostaining characteristic of gap junctions was also clearly observed at the plasma membrane of larger oblong $PDGF\alpha R^+$ cells in the SGZ (Figure 2.3 *C-F*). Double-labelling with PLP and GFAP determined Cx32 expression in terminally differentiated glia. Cx32 was not detected in $GFAP^+$ astrocytes but was consistently detected in PLP^+ oligodendroglia as expected (data not shown). In order to investigate the role of Cx32 in these glial and early oligodendrocyte progenitor populations, we evaluated the effects of the absence of Cx32 using Cx32KO mice.

2.6.4 Cell proliferation is increased in the Cx32KO dentate gyrus

To determine whether loss of Cx32 alters proliferation in the SGZ, actively dividing cells were labelled with BrdU. Cx32KO and WT animals received five intraperitoneal injections of 50 μg/g BrdU over three consecutive days. Animals were sacrificed 24 h after the last BrdU injection. A statistically significant increase in the frequency of $BrdU^+$ cells was detected in the Cx32KO dentate gyrus compared to WT (Figure 2.4 *B*). Cx32KO animals exhibited 50% more BrdU-labelled cells than WT (*$p<0.05$, ANOVA, *post hoc* Tukey test). The number of $BrdU^+$ cells was also assessed in a region of low proliferative index, the CA1 pyramidal cell field, in order to confirm that the increase in BrdU incorporation was not a result of altered blood-brain barrier integrity. No difference in $BrdU^+$ cell profiles was observed in the CA1 region, suggesting that BrdU bioavailability within the hippocampal formation was comparable between genotypes (Figure 2.4 *B*).

Figure 2.3. Cx32 localizes to NG2$^+$ and PDGFαR$^+$ oligodendrocyte progenitors in WT dentate gyrus. Abbreviations are as defined in Figure 2.1. Locations of photomicrographs are indicated in the schematics of the hippocampal formation. *A)* Cx32 (red) is detected at the cell membrane of a subset of NG2$^+$ progenitors (green). *B)* Higher power magnification of inset in *A*. Arrows indicate Cx32 labelling on NG2$^+$ processes and cell bodies. *C, E)* Cx32 (green) is detected at the cell membrane of PDGFαR$^+$ cells (red) with oblong cell bodies in the SGZ (arrow). *D, F)* Higher power magnification of inset in *C* & *E*. Arrows indicate Cx32 labelling localizing to PDGFαR$^+$ cells. Scale bars in *A, C, E,* 50 μm. Scale bars in *B, D, F,* 12.5 μm.

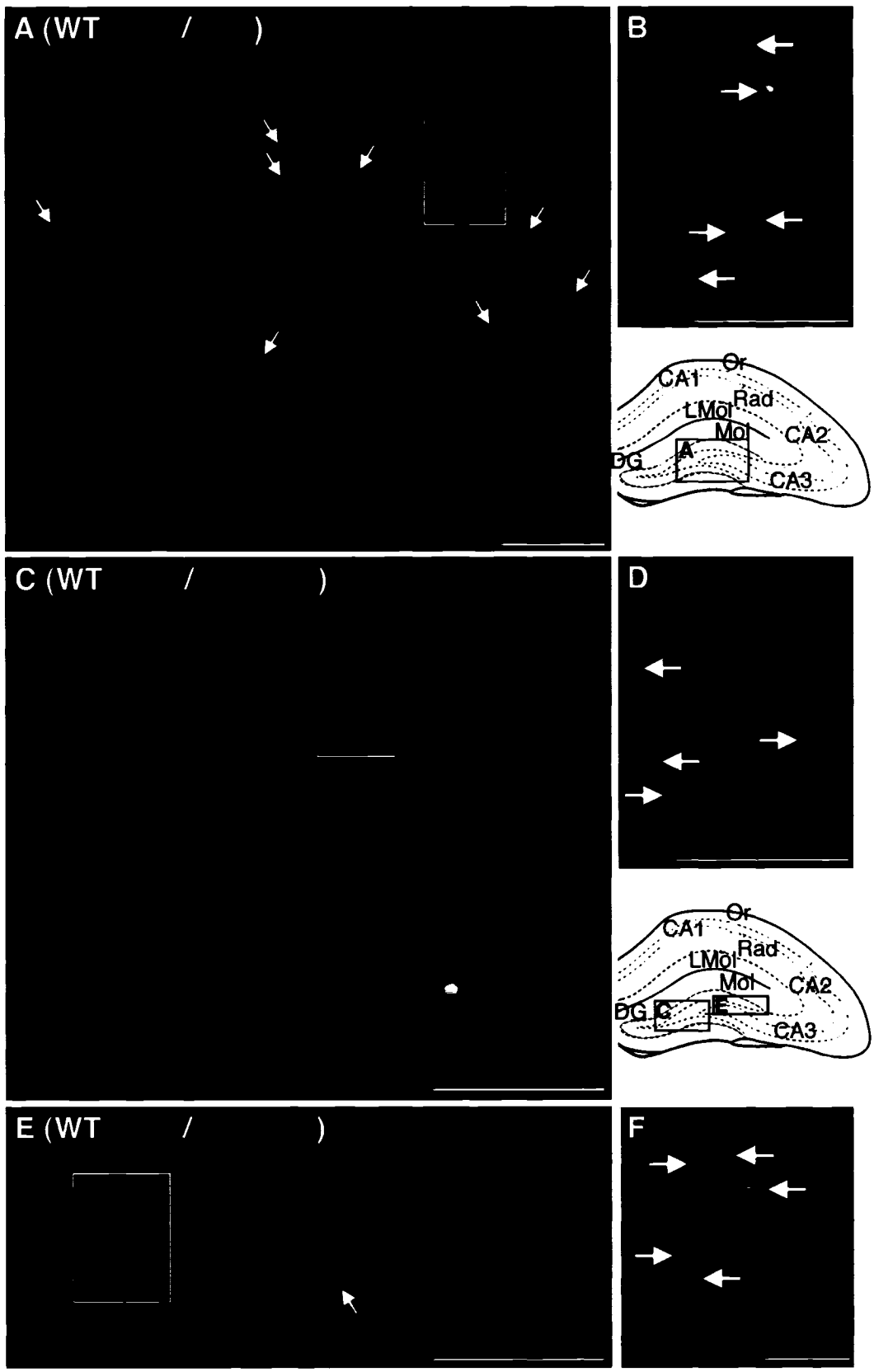
A (WT /)
B
Or
CA1
Rad
LMol
Mol
CA2
A
DG
CA3
C (WT /)
D
Or
CA1
Rad
LMol
Mol
CA2
DG
C
E
CA3
E (WT /)
F

Figure 2.3

Figure 2.4. Cell proliferation is increased in the Cx32KO dentate gyrus.
Abbreviations are as defined in Figure 2.1. *A*) Schematic of the hippocampal formation. The areas chosen for BrdU counts are outlined in dark grey (dentate gyrus) and light grey (CA1 pyramidal field). Locations of photomicrographs (*C-H*) are indicated in red. *B*) Quantitation of $BrdU^+$ cells in the dentate gyrus and CA1 pyramidal cell field in n=10 WT and n=7 Cx32KO mice. A statistically significant increase in the number of BrdU-labelled cells was detected in the Cx32KO dentate gyrus (left panel, *$p<0.05$, Student's *t* test), but not in the CA1 cell field (center panel). No difference in the overall area of the dentate gyrus was detected (right panel). *C-H*) Double-labelling for BrdU (green) and NeuN (red). Note that the increase in $BrdU^+$ cells is localized to the SGZ and hilus of the Cx32KO dentate gyrus with some infiltration into the granule cell layer. Proliferating cells in the SGZ and hilus are NeuN-negative. Inset in *H* depicts a typical pattern of BrdU labelling in a Cx32KO cell nucleus. Scale bars, 25 μm.

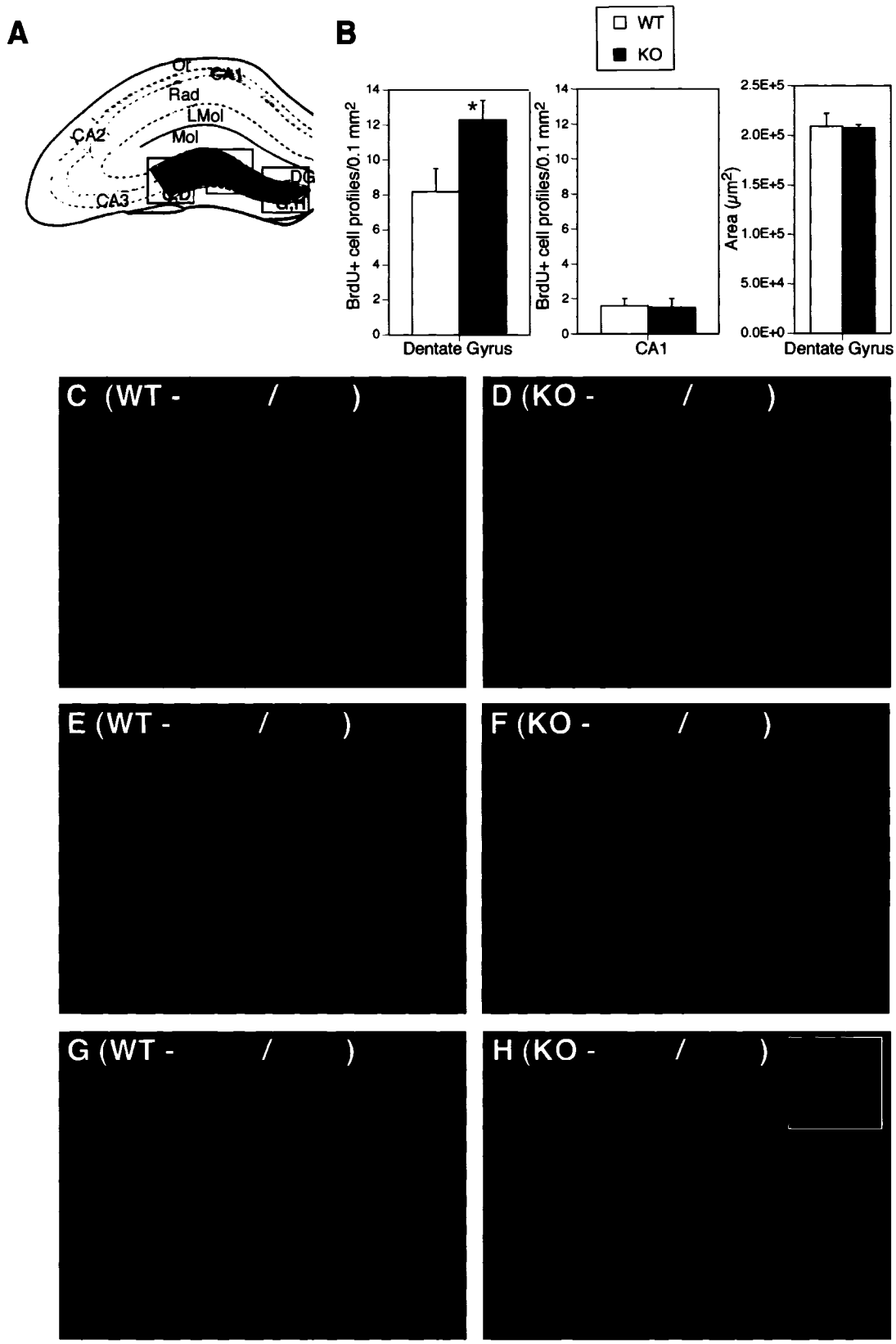
A
B
WT
KO
Or
CA1
Rad
LMol
Mol
CA2
CA3
DG
BrdU+ cell profiles/0.1 mm2
Dentate Gyrus
CA1
Area (μm2)
C (WT - /)
D (KO - /)
E (WT - /)
F (KO - /)
G (WT - /)
H (KO - /)

Figure 2.4

The increase in BrdU-labelled cells did not alter overall anatomical size or cytoarchitectural organization of the Cx32KO dentate gyrus. Total area was comparable between WT and Cx32KO groups (Figure 2.4 *B*). Furthermore, the distribution of labelled cells was similar between Cx32KO and WT mice with the enriched population of $BrdU^+$ cells in the Cx32KO localized primarily to the SGZ and polymorphonuclear layer of the dentate gyrus (Figure 2.4 *C-H*).

2.6.5 Progenitor numbers are enhanced in the Cx32KO dentate gyrus

To identify BrdU-labelled cells in Cx32KO mice and determine whether these were, in fact, progenitor cells, expression of nestin, NG2, PDGFαR, A2B5, O4, PLP, GalC, GFAP, and NeuN was evaluated by immunofluorescence. Nestin is a marker of neural and glial progenitors (Lendahl et al., 1990). NG2 is expressed by glial and early oligodendrocyte progenitors (Dawson, 2000). PDGFαR, A2B5 and O4 are detected in various populations of oligodendrocyte progenitors (Dawson, 2000; Kondo and Raff, 2000; Reynolds, 1997). PLP and GalC label committed oligodendrocytes (Spassky, 2001). Increases in nestin (Figure 2.5 *B-E*) and NG2 (Figure 2.5 *G,H*) immunoreactivity were detected in the SGZ, polymorphonuclear layer, granule cell layer, and hilus of the Cx32KO dentate gyrus as compared to WT. Elevated nestin protein levels were confirmed by immunoblotting (Figure 2.5 *F*). Double-labelling with BrdU demonstrated that more $NG2^+$ progenitors were actively proliferating in the Cx32KO dentate gyrus than WT (Figure 2.5 *G,H, inset*). Dual immunofluorescence for BrdU and nestin was not possible as the denaturation steps required for BrdU detection markedly reduced nestin

Figure 2.5. Cx32KO mice exhibit a higher frequency of nestin$^+$ and NG2$^+$ progenitors in the polymorphonuclear layer and SGZ of the dentate gyrus than WT. Abbreviations are as defined in Figure 2.1. *A*) Schematic of the hippocampal formation. Locations of photomicrographs are indicated in green (NG2 immunostaining) and red (nestin immunostaining). *B-E*) An increase in nestin immunostaining (red) was detected in the SGZ and hilus of the Cx32KO dentate gyrus. *F*) Increased nestin expression was confirmed by Western analysis. Blots were reprobed with β-tubulin as a loading control. *G, H*) An increase in NG2 immunostaining (green) was detected in the PoDG with enhanced infiltration of NG2$^+$ cells into the granule cell layer in Cx32KO mice. Double-labelling with BrdU (red) indicated that more NG2$^+$ progenitors in the Cx32KO dentate gyrus are actively proliferating than in the WT (arrows and inset). Scale bars, 25 μm.

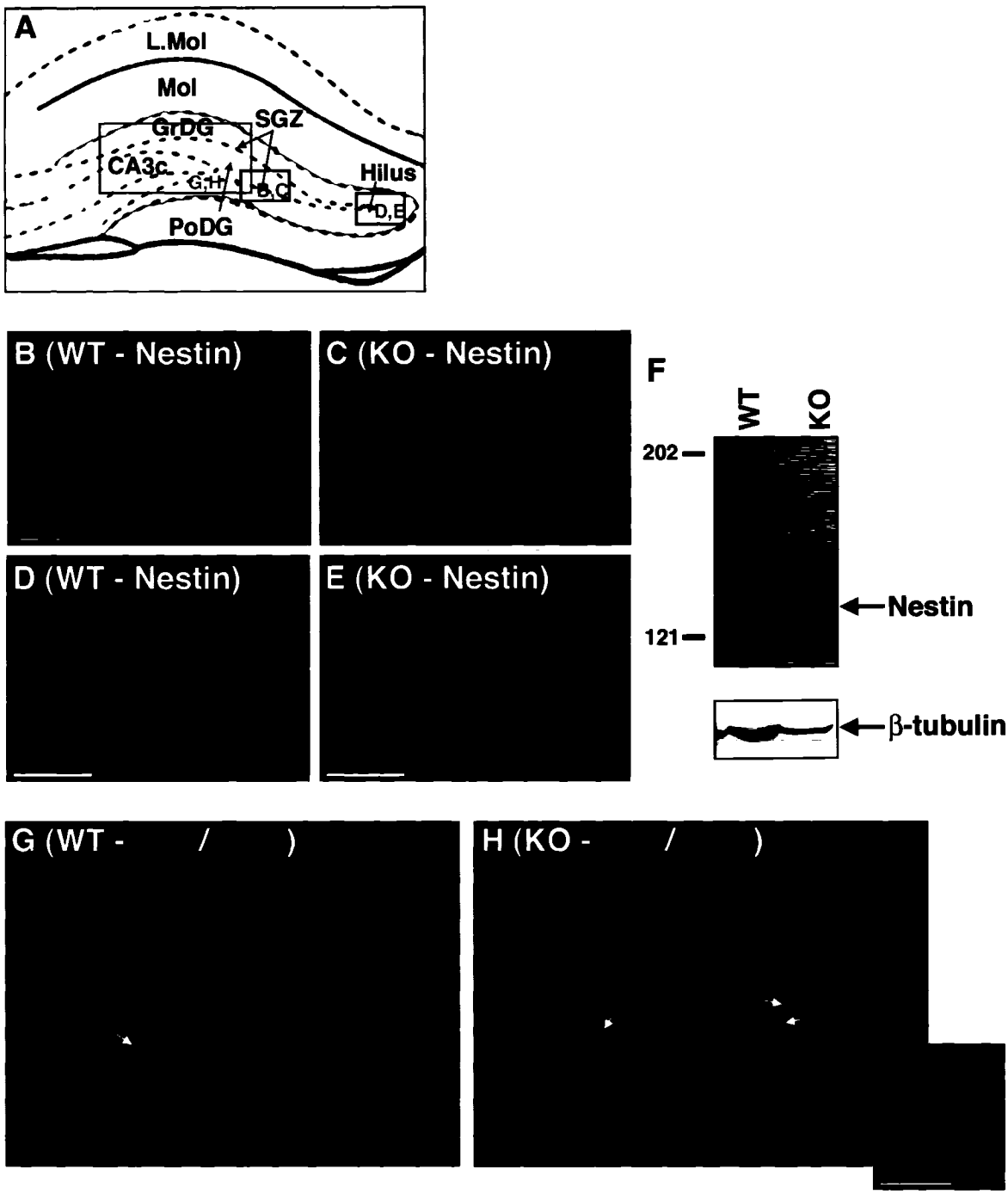
A
L.Mol
Mol
GrDG
SGZ
CA3c
G,H
B,C
Hilus
D,E
PoDG
B (WT - Nestin)
C (KO - Nestin)
D (WT - Nestin)
E (KO - Nestin)
F
WT
KO
202
121
Nestin
β-tubulin
G (WT - /)
H (KO - /)

Figure 2.5

immunoreactivity to the point that co-localization could not be reliably assessed. No obvious change in the number, distribution, or proliferative index of PDGFαR$^+$, A2B5$^+$, O4$^+$, PLP$^+$, or GalC$^+$ cells was detected. Representative A2B5 immunofluorescence (Figure 2.6 *A,B*) and GalC immunoblots (Figure 2.6 *C*) are depicted. There was also no change in the frequency or localization of NeuN$^+$ neurons in the granule cell layer (Figure 2.4 *C-H*) or GFAP$^+$ astrocytes in the molecular and polymorphonuclear layers of the dentate gyrus (Figure 2.6 *C-E*). The extent of BrdU$^+$/GFAP$^+$ double-labelling in Cx32KO and WT mice was also comparable (Figure 2.6 *F,G*). Taken together, these data suggest that the loss of Cx32 results in increased proliferation of a subset of nestin$^+$ and NG2$^+$ progenitors in adult Cx32KO dentate gyrus.

2.6.6 Progenitor turnover is enhanced in the Cx32KO dentate gyrus

The increase in progenitor number could be due to a general increase in neurogenesis during early postnatal development. Thus, the loss of Cx32 could result in the retention of a subset of nestin$^+$/NG2$^+$ progenitors over the course of development. According to this hypothesis, adult progenitor fate might not mechanistically depend upon Cx32 but rather be a consequence of increased progenitor number at earlier developmental time points. Alternatively, expression of Cx32 may be actively required for successful commitment of a subset of nestin$^+$/NG2$^+$ progenitors to an oligodendrocyte lineage in adult brain. In the absence of Cx32 protein, these progenitors would proliferate but fail to terminally differentiate. According to this hypothesis, Cx32 plays an active role in regulating commitment of specific progenitor populations in adult brain. Clearly, these two hypotheses

Figure 2.6. The expanded cell population in the Cx32KO SGZ does not express immunogenic markers of late oligodendrocyte progenitors, terminally differentiated astrocytes, or oligodendrocytes. Abbreviations are as defined in Figure 2.1. *A, B*) No significant change in A2B5-immunostaining (late oligodendrocyte progenitors) was detected in the dentate gyrus between WT and Cx32KO mice. *C*) Western analysis of GalC (oligodendrocytes) and GFAP (astrocytes) demonstrated comparable protein levels between Cx32KO and WT. *D, E*) No change in gliosis was detected between WT and Cx32KO mice. *F, G*) The majority of BrdU-labelled proliferating cells (green) in both WT and Cx32KO dentate gyrus were GFAP-negative (red). A small number of cells in both groups were $GFAP^+$ (arrows). Scale bars, 50 μm.

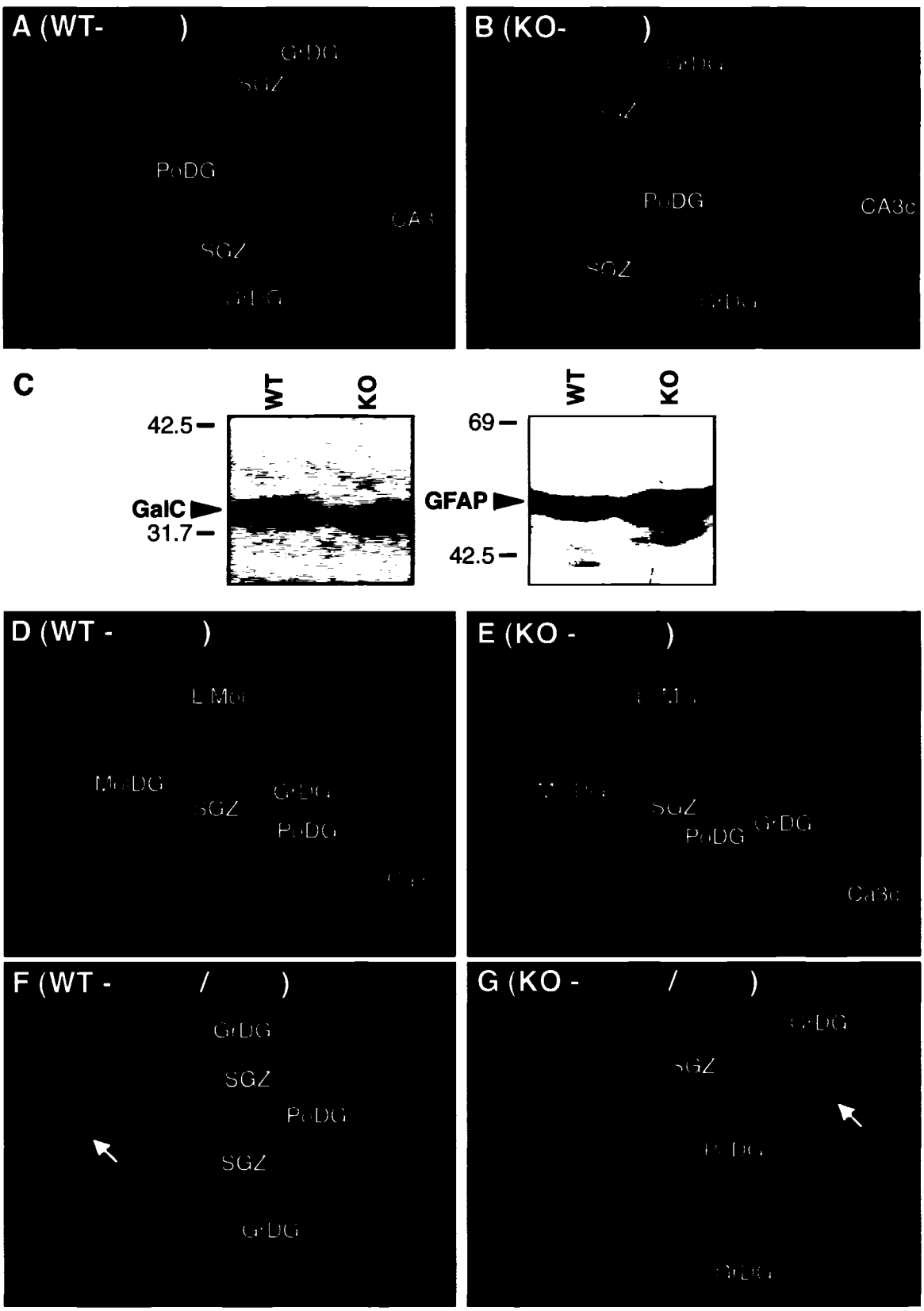

Figure 2.6

must be reconciled before the molecular mechanisms underlying Cx32-mediated progenitor fate can be determined. To address this issue, we evaluated total cell number, layer thickness, cell density, progenitor turnover, progenitor survival, and progenitor differentiation in hippocampi of Cx32KO and WT mice.

If loss of Cx32 results in a general increase in neurogenesis or gliogenesis over the course of development, then the extra progenitors would most likely be manifested as an increase in total cell number, layer thickness, or cell density. These parameters were examined in Hoechst 33258-stained sections between bregma -1.68 to bregma -2.08 (Figure 2.7). Thicknesses of cell layers in the CA1 field (Figure 2.7 *C,D*), CA3c field (Figure 2.7 *E,F*), and dentate gyrus (Figure 2.7 *G,H, arrows)* were comparable between WT and Cx32KO mice. However, in both the CA3c cell field and the dentate gyrus granule cell layer, an increased frequency of small oblong brightly stained nuclei in the SGZ was detected in Cx32KO animals (Figure 2.7 *F,H*). Cell number in the CA3c field was calculated to determine whether these cells increased overall packing density. No significant difference in cell number was observed between Cx32KO and WT mice (Figure 2.7 *I*). Furthermore, no obvious differences in the overall cytoarchitecture of the dentate gyrus (Figure 2.1), in total area (Figure 2.4 *B*), or in frequency and localization of terminally differentiated $NeuN^+$ neurons (Figure 2.4 *C-H*) or $GFAP^+$ astrocytes (Figure 2.6 *D-G*) were observed. Thus, the increase in progenitor number and proliferation exhibited by adult Cx32KO mice is not accompanied by evident increases in cell number or significant changes in developmentally dependent differentiation, migration, or localization of neurons and glia.

Given that the proliferative index of progenitors is enhanced in the Cx32KO SGZ but

Figure 2.7. No difference in layer thickness or cell density is detected in the hippocampal formation of Cx32KO and WT mice. *A, B*) Cresyl violet-stained WT and Cx32KO dorsal hippocampal formations. The areas chosen for nuclear counts and measurements are indicated in the photomicrographs. *C-H*) Adjacent sections were stained with Hoechst 33258. Layer thickness was measured in n=5 animals/condition in the WT CA1 cell field (*C*), Cx32KO CA1 cell field (D), WT CA3c cell field (E), Cx32KO CA3c cell field (F), WT GrDG (G). and Cx32KO GrDG (H). Average layer thickness $\pm$ SEM is indicated beside each photomicrograph. Scale bars, 5 μm. No difference in layer thickness was detected in any of the cell fields. A higher frequency of small oblong brightly stained nuclei was detected in the CA3c pyramidal cell field of the hippocampus and granule cell field of the dentate gyrus in Cx32KO as compared to WT animals *(arrows)*. *I*) Nuclei in the CA3c pyramidal cell field in 3 adjacent sections were counted in n=5 animals/condition. Values were averaged to yield a single measurement per animal. No significant difference in nuclei number was detected ($p>0.05$, Student's *t* test).

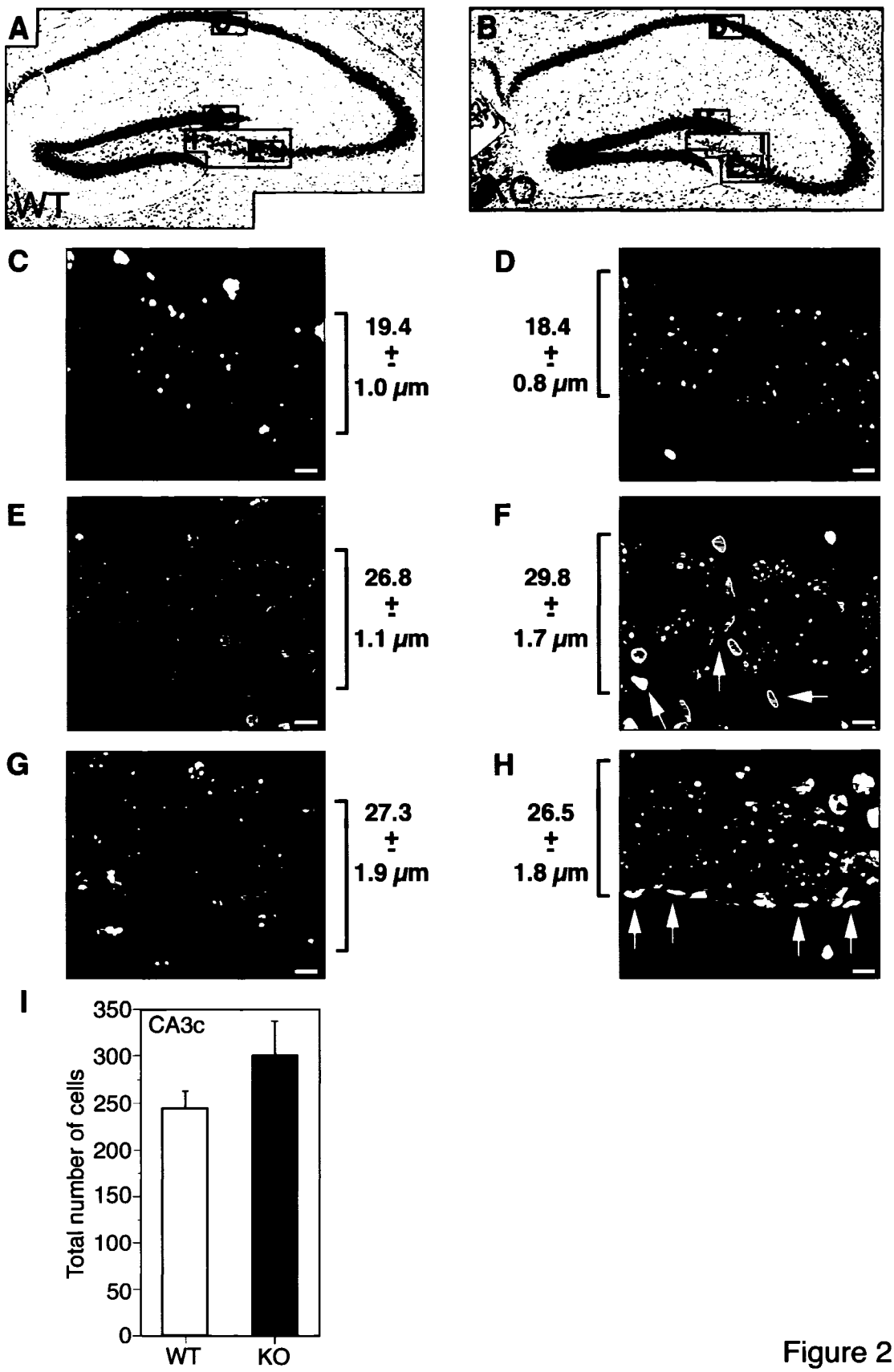
A
WT
B
KO
C
19.4
±
1.0 μm
D
18.4
±
0.8 μm
E
26.8
±
1.1 μm
F
29.8
±
1.7 μm
G
27.3
±
1.9 μm
H
26.5
±
1.8 μm
I
CA3c
Total number of cells
350
300
250
200
150
100
50
0
WT
KO

Figure 2.7

overall cell number remains constant, the kinetics of progenitor survival in adult dentate gyrus were established. The number of BrdU-labelled cells was assessed 1, 3, 5, 7, 14, and 28 days after the last BrdU injection (Figure 2.8). As reported above, a significant increase in BrdU-labelled cells in the dentate gyrus of Cx32KO mice was detected 24 h after injection compared to WT. However, surviving cell number decreased rapidly in Cx32KO dentate gyrus and was comparable to WT within 3 days of BrdU injection. Survival of BrdU-labelled cells was significantly reduced 28 days after injection in both WT and Cx32KO dentate gyrus (Figure 2.8; *$p<0.05$, **$p<0.01$, MANOVA, *post hoc* Tukey test). WT mice exhibited an 85% reduction in BrdU-labelled cell number over the 28 day survival period, while Cx32KO mice exhibited a 92% reduction.

Since a decrease in the number of BrdU-labelled cells was observed in Cx32KO animals 3 days after labelling, TUNEL assays were performed to establish whether these cells were deleted as a result of cell death or whether the BrdU label became diluted 72 h after injection as a result of hyperproliferation and therefore labelled progeny were not detected. In order to determine the identity of the $TUNEL^+$ dying cells, double-labelling was performed using various lineage markers. A significant increase in the number of $TUNEL^+$ cells was detected in the Cx32KO dentate gyrus relative to WT (Figure 2.9 *A,B,D*; *$p<0.05$, Student's *t* test). $TUNEL^+$ cells were predominantly $NG2^+$ progenitors (Figure 2.9 *C*). This 3-fold increase in $TUNEL^+$ cells in the Cx32KO dentate gyrus and the equivalent overall cell number in Cx32KO and WT hippocampi indicate that hyperproliferation is balanced by cell death. Taken together, these findings suggest that, in the absence of Cx32, progenitor proliferation is constitutively enhanced in the adult SGZ but that the $NG2^+$ progeny are deleted prior to differentiation. Deletion occurs through an

Figure 2.8. The enriched subset of BrdU-labelled progenitors in Cx32KO mice is deleted within 3 days of BrdU injection. Survival of $BrdU^+$ cells was assessed 1, 3, 5, 7, 14, and 28 days after the last BrdU injection. A statistically significant increase in BrdU-labelled cells was detected in the Cx32KO dentate gyrus 1 day after the last BrdU injection as reported in Figure 2.4. Surviving cell number markedly decreased within 3 days of labelling in Cx32KO dentate gyrus compared to WT. No difference in BrdU-labelled cell number between Cx32KO and WT was detected 3 (n=3 WT, n=3 Cx32KO), 5 (n=7 WT, n=3 Cx32KO), 7 (n=3 WT, n=3 Cx32KO), 14 (n=4 WT, n=3 Cx32KO), and 28 days (n=6 WT, n=10 Cx32KO) after the last injection (*$p<0.05$, **$p<0.01$, MANOVA, *post hoc* Tukey test).

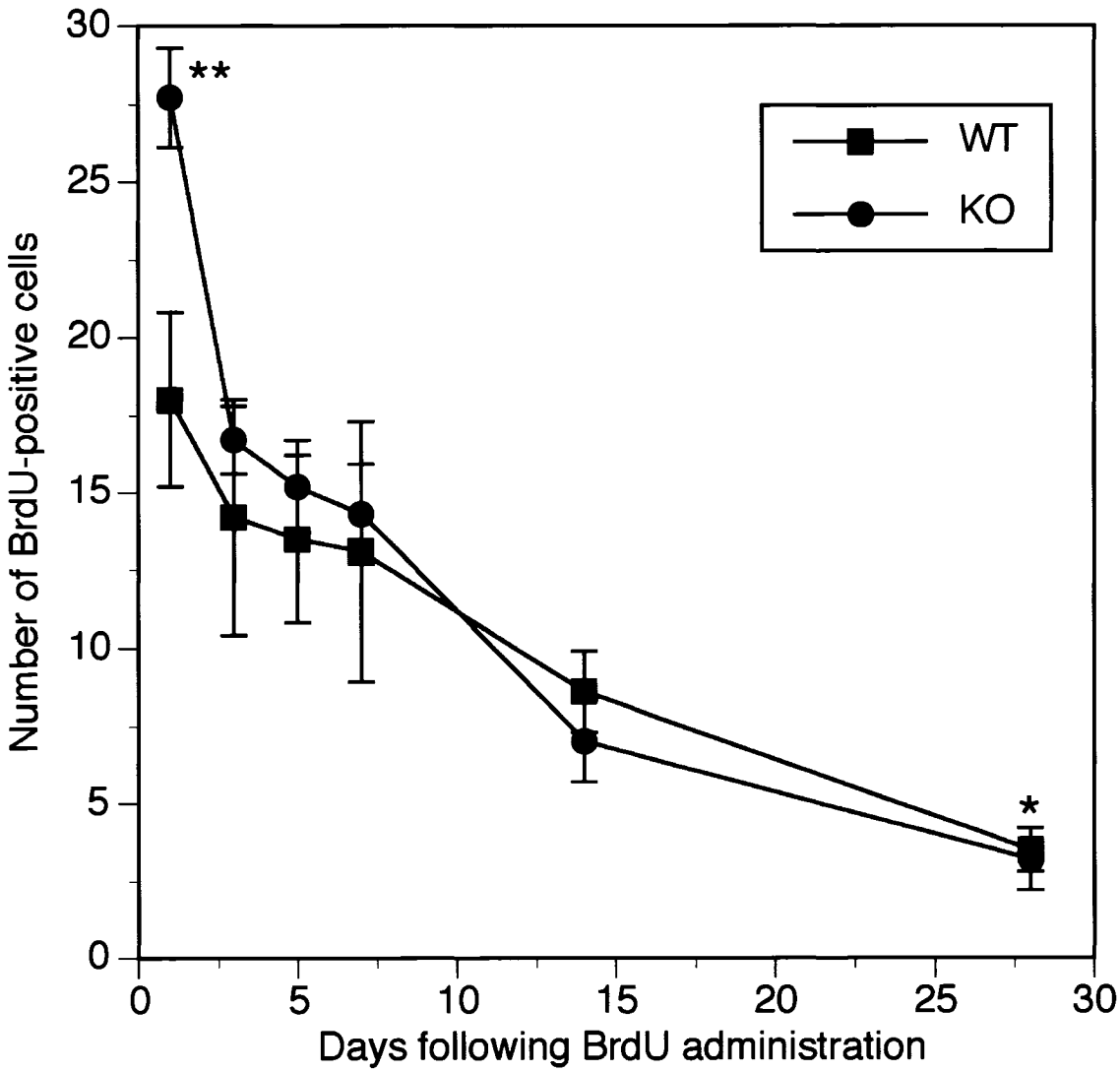
30
25
20
15
10
5
0
**
*
WT
KO
Number of BrdU-positive cells
0
5
10
15
20
25
30
Days following BrdU administration

Figure 2.8

Figure 2.9. Cell death of NG2$^+$ progenitors is increased in the Cx32KO dentate gyrus. Abbreviations are as defined in Figure 2.1. The location of photomicrographs is represented in the schematic of the hippocampal formation. *A*) TUNEL labelling of DNA strand breaks in WT animals (green). *B*) An increased frequency of TUNEL$^+$ cells was consistently detected in Cx32KO dentate gyrus. *C*) TUNEL$^+$ cells (green) are primarily NG2$^+$ (red) progenitors (arrowheads). Inset depicts higher magnification of TUNEL$^+$/NG2$^+$ cells. Scale bars, 50 μm. *D*) Quantitation of TUNEL$^+$ cells in the granule cell layer and polymorphonuclear layer of the dentate gyrus (grey area in the schematic) from n=5 animals/group. A statistically significant increase in TUNEL$^+$ cells was detected in Cx32KO mice (*$p \leq 0.05$, Student's *t* test).

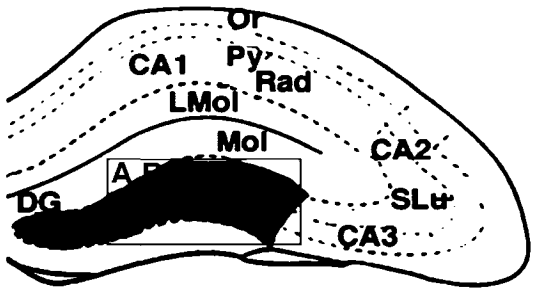
Or
CA1
Py
Rad
LMol
Mol
CA2
DG
SLu
CA3

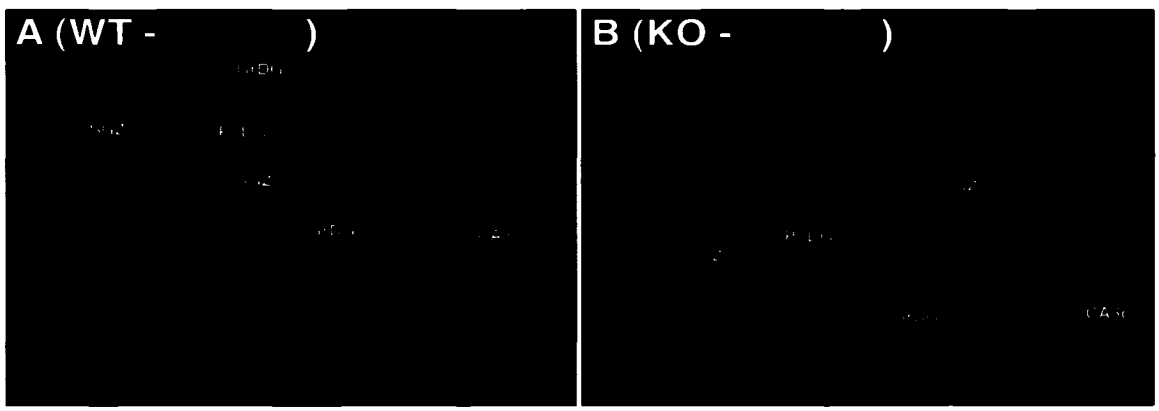
A (WT -)
B (KO -)

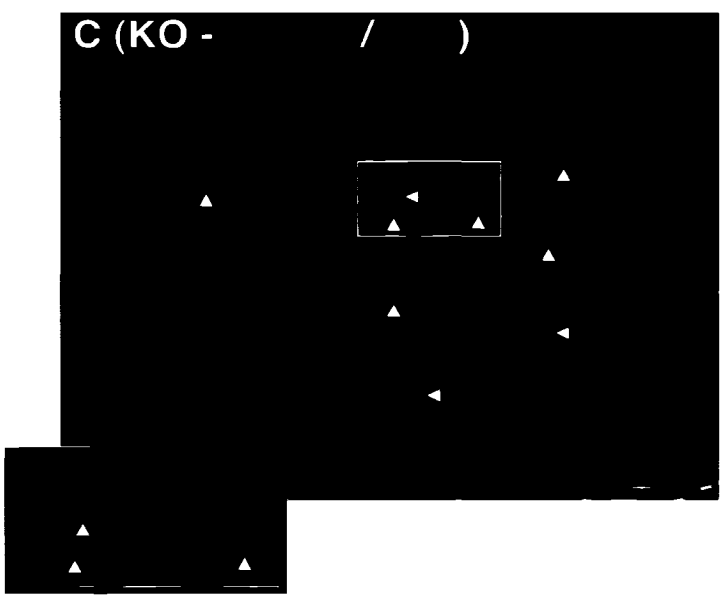
C (KO - /)

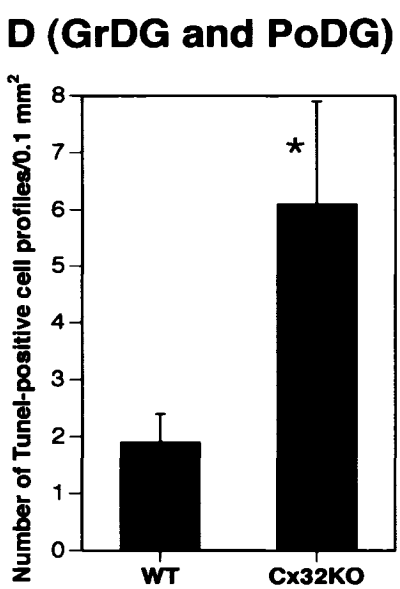
D (GrDG and PoDG)
Number of Tunel-positive cell profiles/0.1 mm2
0
1
2
3
4
5
6
7
8
*
WT
Cx32KO

Figure 2.9

apoptotic-like mechanism involving nuclear and chromatin condensation (Figure 2.7), cytoplasmic condensation, pyknosis, hyperchromaticity (Figure 2.1), and DNA fragmentation (Figure 2.9), in the absence of significant gliosis (Figure 2.6).

2.6.7 *In vitro* proliferation and differentiation of Cx32KO progenitors

Nestin$^+$ progenitors are capable of self-renewal and differentiation into functional neurons and glia *in vitro*. Because we performed BrdU/NG2 double-labelling but not nestin/BrdU double-labelling due to technical considerations, we were unable to establish definitively whether loss of Cx32 increases nestin$^+$ progenitor proliferation in adult brain. To confirm nestin$^+$ progenitor enrichment *in vitro*, clonogenic assays were performed on cultured primary hippocampal cells. Cx32KO and WT dissociated cell suspensions were plated on poly D-lysine coated dishes, cultured for 7 days in bFGF, fixed, and double-labelled with anti-nestin and anti-enolase (Figure 2.10 *A,D,E*). Colonies >7 cells in size were counted. In three separate experiments, the ratio of Cx32KO colonies to WT was consistently 4:1 or a 3-fold increase in colony formation (Figure 2.10 *A*; ** $p<0.01$, Student's *t* test). The majority of Cx32KO colonies were nestin$^+$ and enolase$^-$, confirming that they were progenitor cells and not adult neurons or glia. The nestin$^+$/enolase$^-$ cells found in colonies were large phase-dark oblong cells often exhibiting blunt neuritic extensions, characteristic of progenitor cells (Figure 2.10 *C-E)*. WT colonies (~1 colony/well) were nestin$^-$ and enolase$^+$ and thus were likely pre-existing adult neurons that had plated in close proximity to progenitors, or progeny of committed progenitors that differentiated within 7 days of plating. These data indicate that a larger

Figure 2.10. More Cx32KO than WT progenitors cultured *in vitro* are capable of clonal expansion in the presence of bFGF and neuronal differentiation in the presence of BDNF. *A*) Dissociated single cell suspensions prepared from the hippocampal formation of n=3 WT and n=3 Cx32KO mice/experiment (n=2 experiments) were plated on poly-D-lysine-coated glass microscope slides and cultured for 7 days in serum-free media containing 20 ng/ml bFGF as described in Materials and methods. Cultures were double-labelled for nestin (progenitor marker) or neuron-specific enolase (neuronal marker). Colonies (> 7 cells) were counted. Data are expressed as the mean number of colonies/well $\pm$ SEM. A 3-fold increase in colony formation was detected in Cx32KO cultures (Total; ** $p<0.01$, Student's *t* test). Cells in Cx32KO colonies were nestin$^+$ indicative of progenitors (Nestin$^+$ colonies). The rare WT colonies were enolase$^+$ indicative of terminally differentiated neurons (Enolase$^+$ colonies). *B*) Dissociated cell suspensions were plated on poly-D-lysine-coated glass microscope slides and cultured for 7 days in serum-free media containing 20 ng/ml bFGF followed by 5 days in media containing 10 ng/ml BDNF. A three-fold increase in colony formation was again detected in Cx32KO cultures (Total, ** $p<0.01$, Student's *t* test). The majority of cells differentiated to a neuronal lineage (Enolase$^+$ colonies) following BDNF treatment. *C*) High power magnification phase microscopy of Cx32KO cultures treated for 7 days with bFGF. *D, E*) Cells are nestin$^+$ (red) and enolase$^-$ (green). *F*) High power magnification phase microscopy of Cx32KO cultures treated for 7 days with bFGF followed by 5 days with BDNF. *G, H*) Cells are nestin$^-$ (red) and enolase$^+$ (green) with long neuritic extensions.

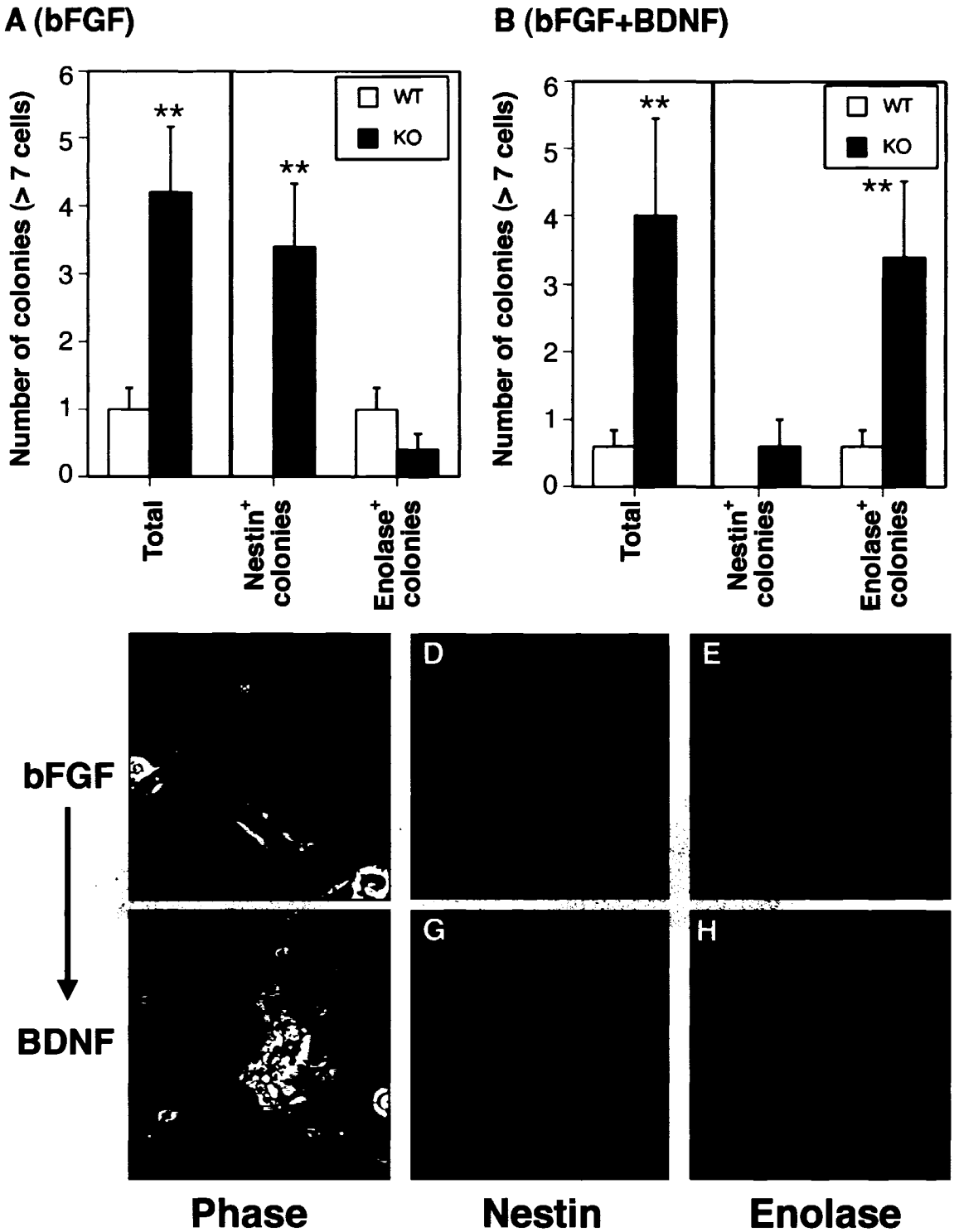
A (bFGF)
B (bFGF+BDNF)
Number of colonies (> 7 cells)
WT
KO
**
Total
Nestin+ colonies
Enolase+ colonies
bFGF
BDNF
D
E
G
H
Phase
Nestin
Enolase

Figure 2.10

percentage of cells dissociated from Cx32KO than WT hippocampus are nestin$^+$ progenitors capable of clonogenic expansion *in vitro*.

In vivo, the enriched population of progenitors in the Cx32KO SGZ fails to differentiate to oligodendrocytes and instead is rapidly deleted. To definitively establish whether the increased population of proliferating nestin$^+$ progenitors could differentiate into a lineage other than oligodendrocytes, cells dissociated from Cx32KO and WT hippocampi were treated for 7 days with bFGF to promote clonal expansion and then incubated with BDNF for an additional 5 days to induce neuronal differentiation. Cultures were double-labelled with anti-nestin and anti-enolase (Figure 2.10 *G,H*). Colonies (> 7 cells) were analyzed. A 3-fold increase in colony formation was again observed in Cx32KO cultures relative to WT, consistent with the increased number of nestin$^+$ progenitors detected *in vivo* (Figure 2.10 *B*). Significantly, following BDNF treatment, the majority of Cx32KO progenitor colonies differentiated into enolase$^+$/nestin$^-$ neurons (Figure 2.10 *B,G,H*; ** $p<0.01$, Student's *t* test). Differentiated enolase$^+$ cells were phase-bright, with small cell bodies and elaborate neuritic processes, characteristic of neurons (Figure 2.10 *F*). These data confirm our *in vivo* observations that loss of Cx32 results in expansion of nestin$^+$ and NG2$^+$ progenitors, but does not significantly affect the capacity of these cells to differentiate to a lineage other than oligodendrocytes.

2.7 Discussion

2.7.1 Summary of hippocampal changes associated with defective oligodendrogenesis in the absence of Cx32

In this study, we show, for the first time, that Cx32 is expressed by a subset of early oligodendrocyte progenitors in the murine dentate gyrus and that the loss of Cx32 prevents differentiation of these progenitors to oligodendroglia. In adult C57BL/6 mice, we localized Cx32 protein to subpopulations of $NG2^+$ and $PDGF\alpha R^+$ oligodendrocyte progenitors as well as terminally differentiated populations of oligodendroglia, located in the dentate gyrus of the hippocampal formation. To determine whether the loss of Cx32 is associated with a defect in adult oligodendrogenesis in the dentate gyrus, we evaluated activation, survival, and differentiation of progenitors in adult Cx32KO mice. Constitutive loss of Cx32 protein resulted in an overproliferation of $nestin^+$ and $NG2^+$ progenitors. The majority of these progenitors do not survive for an extended period of time, given a substantive loss of BrdU label within 3 days of injection. To establish whether the reduction in BrdU labelling resulted from either hyperproliferation and hence label dilution or cell death in the Cx32KO dentate gyrus, we evaluated cell number, layer thickness, and apoptotic index. We did not detect any overall increase in cell number or layer thicknesses in the Cx32KO relative to the WT. However, a significant increase in the number of $TUNEL^+$ cells localizing predominantly to $NG2^+$ progenitors was observed in Cx32-null mutant mice. We conclude that, in the absence of Cx32 protein, a subset of $NG2^+$ progenitors fail to terminally differentiate. Proliferation is enhanced constitutively, likely in an attempt to compensate for this failure in differentiation, and defective progeny are subsequently deleted through an apoptotic-like mechanism (Figure 2.11).

Figure 2.11. Summary of changes associated with defective oligodendrogenesis in Cx32KO mice. In the absence of Cx32, the turnover of a population of early oligodendrocyte progenitors is constitutively enhanced. These cells hyperproliferate and are rapidly deleted through an apoptotic-like mechanism. *In vitro*, more hippocampal progenitors can be expanded from Cx32-null mutant mice. Furthermore, these progenitors are capable of neuronal specification when treated with a neurogenic stimulus (dotted line).

Summary of changes associated with defective oligodendrogenesis in Cx32KO mice

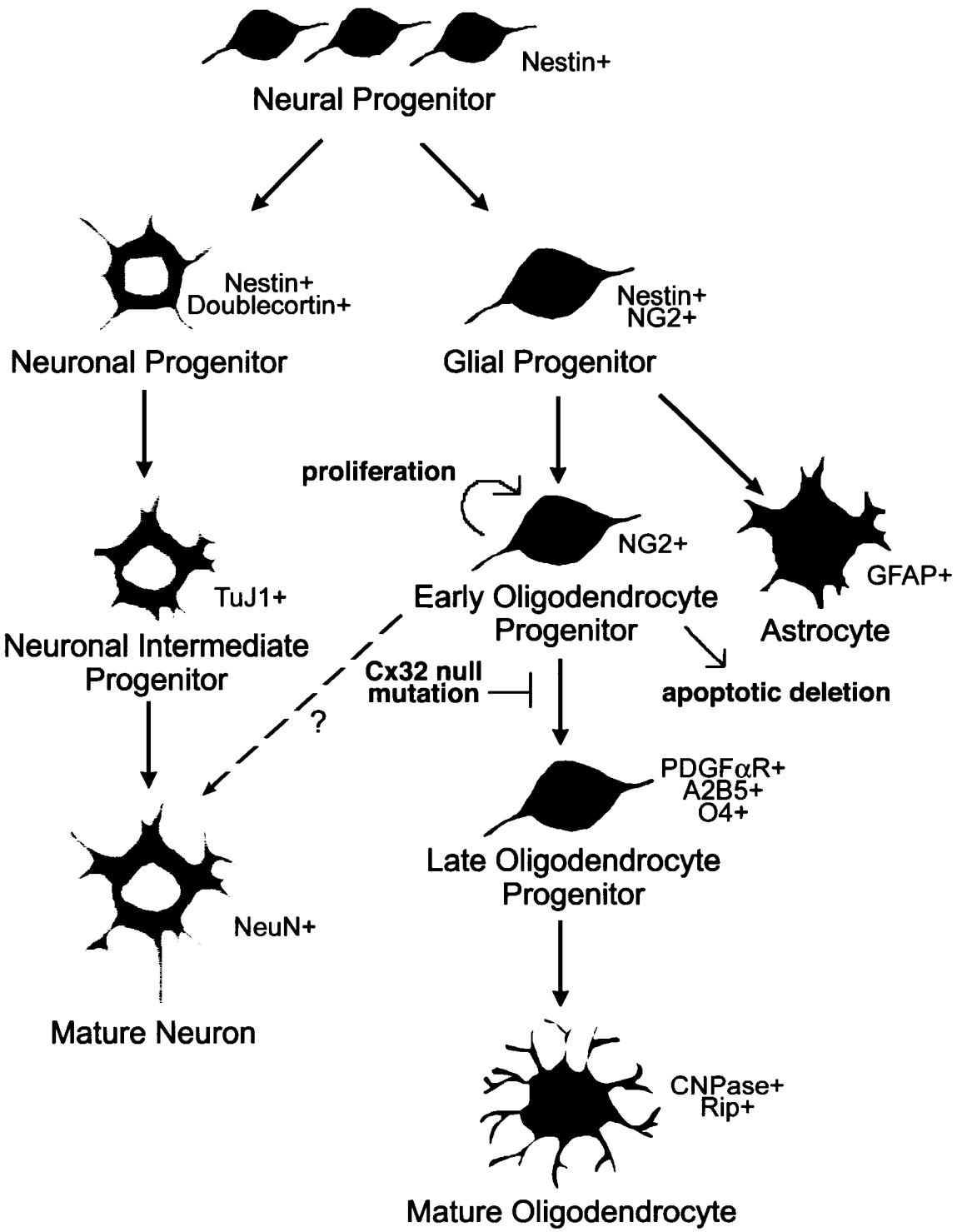

Figure 2.11

While we cannot definitively distinguish between $NG2^+$ glial progenitors or early oligodendrocyte progenitors, the affected population of cells is likely composed of oligodendrocyte progenitors. Three lines of evidence attest to the competency of neural and glial progenitor populations in the adult Cx32KO mice. First, no significant difference in the frequencies of $GFAP^+$ terminally differentiated astrocytes and $A2B5^+$, $GalC^+$, or PLP^+ oligodendroglia was observed in Cx32KO mice, suggesting that the majority of glial and oligodendrocyte progenitors are capable of differentiation. Second, we show that differentiation is blocked and turnover is enhanced in a transiently enriched population of $NG2^+$ cells. Third, our *in vitro* data demonstrate that the actively proliferating progenitors in the Cx32KO retain their multipotential capacity to differentiate to neurons. *In vivo*, no obvious difference in neuron number, neuronal localization, or cytoarchitecture was detected in the Cx32KO mice. Together, these findings indicate that, in the absence of Cx32, multipotential and bipotential progenitors are apparently competent but hyperactive and that null mutation inhibits differentiation of a subset of early oligodendrocyte progenitors.

2.7.2 Alternative explanations for the increase in early oligodendrocyte progenitor number in the Cx32KO mouse

Connexin-null mutant mice represent the best available means of examining the contribution of individual connexins to neurogenesis, gliogenesis, and neural differentiation. Typically, KOs are obtained in a mixed genetic background of 129SVJ1 and C57BL/6 strains. However, 129SVJ1 animals exhibit reduced neural progenitor number relative to other strains that might obscure the effects of altering connexin levels (Kempermann et al. 1997). To address this issue, we backcrossed extensively to the N12 generation to produce a

Cx32KO in a largely C57BL/6 genetic background. Regardless, in both mixed (data not shown) and backcrossed animals, Cx32KOs exhibit more proliferating progenitors than WT controls.

The hyperproliferation of progenitors in the Cx32KO dentate gyrus may also be due to a general increase in neurogenesis or gliogenesis during development. Because significant Cx32 expression is not detected in embryonic brain (Belliveau et al., 1991; Dermietzel et al., 1989; Nadarajah et al., 1997; Parnavelas et al., 1983), it is unlikely that mutation would impact on the retention of embryonic progenitor populations. However, the loss of Cx32 during postnatal oligodendrogenesis could potentially result in enhanced survival of $NG2^+$ progenitors. To address this possibility, we evaluated total cell number, layer thickness, cell density, progenitor turnover, progenitor survival, and progenitor differentiation in hippocampi of our C57BL/6 Cx32KO and WT mice. We did not detect an increase in overall cell number, layer thickness, or cell density as would be expected if additional progenitor populations were retained over the course of development. Furthermore, our analysis of BrdU-labelled cell survival indicates that constitutive progenitor turnover is a dynamic process in adult brain. Both the proliferation and concomitant apoptotic deletion of cells are markedly enhanced in the adult CX32KO dentate gyrus. Thus, the changes in proliferation and in nestin and NG2 immunoreactivity detected in the adult Cx32KO mouse reflect an ongoing defect in the absence of Cx32 protein rather than an earlier event in development. It will be important to evaluate whether this defect is site-specific by determining changes in early oligodendrocyte progenitor turnover in other brain regions.

2.7.3 Connexin-mediated control of oligodendrocyte progenitor fate

Cx32-null mutant mice have been previously shown to exhibit deficits in peripheral nerve myelination, resulting in reduced nerve conductance velocity (Anzini et al., 1997; Scherer et al., 1998). Our data add to these well-established experimental and clinical studies and extend these observations by localizing Cx32 to a specific subset of oligodendrocyte progenitors, providing an explanation for the apparent sparing of CNS myelinating glia in CMTX patients. Our data involve Cx32 in oligodendrocyte specification and leave open the possibility that other connexins may also play a role in directing early oligodendrocyte progenitor commitment and differentiation. Two other connexins, Cx29 and Cx47, are expressed by mature oligodendrocytes with Cx32 and Cx29 often localizing to different subsets of terminally differentiated oligodendroglia (Altevogt et al., 2002; Dermietzel et al., 1997; Sohl et al., 2001a). It will be essential to determine whether this cell-specific localization also applies to discrete oligodendrocyte progenitor populations in different brain regions. Connexin-specific expression in distinct populations of early oligodendrocyte progenitors may be responsible for specific defects in CNS myelination following mutation. Furthermore, other connexins expression might be upregulated in response to Cx32 deletion, providing another possible explanation for the relatively intact CNS myelination in Cx32-null mutant mice.

2.7.4 Possible mechanisms underlying the defect in oligodendrogenesis in the Cx32KO mouse

Although we have yet to identify the signals and associated transduction mechanisms responsible for the failure of a subset of early oligodendrocyte progenitors to differentiate in

the absence of Cx32, two general mechanisms can be elaborated. The first utilizes orthodox junctional communication to transmit signals related to differentiation. The majority of gap junctions made by oligodendrocytes are with astrocytes and, to a lesser extent, with other oligodendrocytes (Li et al., 1997; Massa and Mugnaimi, 1982; Rash et al., 2001; Wasman and Black, 1984). While this is the first study to localize Cx32 to oligodendrocyte progenitors, it is reasonable to assume that the same relationship will hold in other progenitor populations. Song et al (2002) have provided elegant evidence that contact between progenitors and "instructive glia" *in vitro* can direct progenitor fate down specific lineages. Gap junctional intercellular communication may be one of the molecular mechanisms responsible for this control. Thus, in the absence of Cx32, affected early oligodendrocyte progenitors would be unable to interact with neighbouring "instructive cells" and pass necessary second messengers required for further lineage progression.

A second possible mechanism involves the formation of hemichannels, connexin-based channels that are active in single plasma membranes. Cx26, Cx32, Cx43, and Cx45 are known to induce large, non-selective, voltage-gated conductances in single plasma membranes facilitating passage of metabolites and second messengers to and from extracellular space (Castro et al., 1999; Kammermans et al., 2001; Stout et al., 2002; Valiunas, 2002). These channels thereby provide a robust mechanism by which progenitors could sample and respond to changes in the extracellular environment in the absence of functional synapses and ligand-gated ion channels. This hypothesis represents an unexplored role for connexin-mediated hemichannels *in vivo*.

Chapter 3: Connexin32 knockout mice exhibit behavioural impairments in a standard learning and memory task

3.1 Objectives

In Chapter 2, I determined that the hippocampal formation of Cx32KO mice contains an enriched pool of early oligodendrocyte progenitors with enhanced turnover. The next objective was to establish whether this dynamic defect in progenitor proliferation and specification in the adult Cx32KO hippocampus influences behavioural criteria of learning and memory.

3.2 Statement of collaborator contributions

Behavioural testing was conducted with the help of Dr Andrea Hebb, a postdoctoral fellow, and Misagh Ziaei, an undergraduate summer student in the Bennett laboratory. I wish to thank Dr Andrea Hebb for her invaluable assistance in the experimental design.

3.3 Abstract

The purpose of this study was to further characterize connexin-mediated control of progenitor cell function by evaluating the impact of enhanced progenitor turnover on hippocampal function in Cx32KO mice. To achieve this, WT and Cx32KO animals were tested in the radial arm maze, a standard learning and memory task used to monitor prefrontal cortical and hippocampal function. In the habituation portion of this task, food was placed at the end of all 8 arms of the maze. Animals were required to enter each arm and retrieve the food reward. In the acquisition paradigm, only 6 out of the 8 arms were baited. The number of repeat entries into arms already entered during the test (working memory errors) and the number of entries into arms that did not contain food (reference memory) were monitored. The number of trials required to meet performance criteria was recorded. We demonstrate that both genotypes exhibited similar behaviour in the habituation portion of this task, linked to the prefrontal cortex activity, in which WT and Cx32KO mice show no phenotypic differences. However, Cx32KO mice display an obvious impairment in the acquisition portion of the maze, linked to hippocampal activity. We show that Cx32KO mice exhibit reference memory but not working memory deficits. This phenotype cannot be attributed to an impairment in motor activity, as both WT and Cx32KO animals traverse the maze within comparable time periods and, in a separate motoric paradigm, are capable of equivalent sustained running wheel activity. This study provides the first demonstration that increases in progenitor cell turnover and/or impaired connexin-mediated communication specifically impact on hippocampal function.

3.4 Introduction

Based on data presented in Chapter 2, I hypothesized that Cx32 expression in progenitors acts as a molecular switch, influencing commitment of multipotent progenitors to an oligodendrocyte lineage. In Cx32KO adult hippocampus, we demonstrated an enrichment of transiently amplifying early oligodendrocyte progenitors that fail to differentiate to mature oligodendroglia (Melanson-Drapeau et al., 2003). Here, we sought to determine whether the increase in hippocampal $NG2^+$ progenitor proliferation and/or the dynamic defect in specification of these progenitor cells in the absence of Cx32 affect behavioural criteria of learning and memory.

The hippocampal formation is pivotally involved in memory and navigation, playing a crucial role in the integration of information received through the perforant path (reviewed in Jones, 1993; Wang et al., 1997). Hippocampal progenitor number and responsivity have been shown to influence behavioural indices of learning and memory in adult animals and it is hypothesized that progenitor activation, migration, and subsequent differentiation may underlie the formation of new memories, specifically spatial memories (Macklis, 2001; Taupin, 2005). However, it has yet to be determined whether increases in progenitor turnover impact on hippocampal function.

Recent studies have demonstrated that connexin alterations impact on behavioural indices of cognition. More precisely, the deletion of astrocytic Cx43 and the subsequent altered communication between neurons and astrocytes results in increased exploratory activity and impaired motor capacities (Frisch et al., 2003). The deletion of Cx30, another astrocytic connexin, results in anxiogenic behaviour as well as reduced exploratory activity (Dere et al., 2003). Mechanistic insight is still forthcoming. Here, we assessed the effect of

Cx32-null mutation on hippocampal associated cognitive function. Since Cx32KO mice show an enhanced pool of progenitors in the hippocampal formation, we chose a behavioural test involving the hippocampus - the radial arm maze. A well-established paradigm of spatial learning and memory, this maze allows us to evaluate reference as well as working memory, thereby assessing hippocampal and prefrontal cortical function (Toumane et al., 1988). We found that Cx32KO mice exhibit specific defects in memory consolidation and learning. We show that Cx32-null mutation does not impact on habituation to the radial arm maze, a measure of working memory, but that Cx32KO mice exhibit impaired reference memory in the acquisition portion of maze testing.

3.5 Materials and methods

3.5.1 Animals

Two weeks prior to radial arm maze testing, WT (n=9) and Cx32KO (n=14) 2 months old male mice were removed from the breeding colony, individually housed and maintained on a reverse 12 h dark:light schedule (lights on at 19:00). Mice were also introduced to the food rewards (i.e., sunflower seeds) that were eaten while in the home cage. One week prior to testing, animals were food deprived to 85% of their body weight. Mice were maintained at this reduced body weight for the duration of testing, relative to age-matched mice given free access to food. All animal manipulations were performed in compliance with approved institutional protocols and according to the strict ethical guidelines for animal experimentation established by the Canadian Institute of Health Research.

3.5.2 Radial arm maze apparatus

Testing occurred in a modified eight-arm radial maze (Figure 3.1 *A*). The maze arms were constructed from Acrylonitrile-Butadiene-Styrene (ABS) pipe (5 cm diameter) connected to a circular plastic hub (26 cm diameter). The walls of the central platform were 11.5 cm high above a circular horizontal floor. The equally spaced radiating arms were 35 cm long and bisected the circular wall 1 cm above the hub floor. The maze was elevated a maximum of 2.5 cm above the table by the ABS pipe elbows and food cups. Three rows of seven holes (1.3 cm diameter) located on the top and along opposing sides of the arms allowed the investigator to video the progress of the animal through the arms and monitor successful retrieval of the food reward from the food cups. Spatial cues consisting of hand-drawn spirals, X's, and various shapes were mounted above each arm opening. Tactile cues consisting of 100-grit sandpaper were placed at the entrance of, and leading into, arms 3 and 7 (facing each other). The spatial cues above these arms were identical. Olfactory cues included shapes coloured with a Sanford aroma accent highlighter. The central hub of the apparatus was covered with a plexiglass shield during testing. Food rewards were single unsalted, roasted sunflower seed placed at the bottom of the arm elbows in food cups. The maze body was positioned on a stainless steel table 65 cm above the ground in a testing room illuminated by a single 40-W desk-lamp. The positioning and features of the maze, including the position of the light source and experimenter, remained the same for each trial.

3.5.3 Radial arm maze testing

Testing took place in morning (8:00-12:00) and afternoon blocks of time (1:00-5:00). The order of mice tested was varied randomly from day to day. Experimenters were blinded

as to the genotype of the test subject. Following each block of testing time (morning and afternoon), the maze was washed with soap and water. Animals were first subjected to the shaping paradigm. WT and Cx32KO mice were placed in the maze for a period of 15 minutes, on three consecutive days, in order to get familiarized with the experimental apparatus. Food rewards were scattered randomly throughout the maze and the time it took the mice to initiate eating (i.e., neophobia) was recorded. Animal behaviour was videotaped using a Sony Hi8 video camera mounted above the maze.

After 3 days of shaping, mice were moved to the habituation protocol. In the habituation phase, mice accessed the maze for 15 min (maximum) sessions (from trials 1 - 7) or 10 min sessions (from trials 8 - 24). Each of the eight arms was baited with a food reward. Animals were placed in the central area of the maze facing the same direction in each session. The order of arm entry was recorded for each mouse by the experimenter present in the room. Mice were removed from the maze when they had successfully traversed all eight arms and consumed the food reward or had exceeded the time limit. Working memory errors were recorded, defined as reentry into an arm in which a reward had already been retrieved, a measure of spatial working memory. Time to complete the trials, order of arm entry, as well as number of treats eaten were also recorded. To reach habituation criteria, mice were required to consume the food reward placed at the end of all 8 arms, making 8 out of 9 correct arm choices (allowed 1 working memory error) on 2 out of 3 consecutive days. Mice were then moved to the acquisition protocol, in which two of the eight arms (arms 3 and 7) were unbaited. During trials 1 - 7, mice were permitted 10 min to retrieve and consume all 6 treats. On each trial, the order of arm choice, number of working and reference memory errors and total running time were recorded. Reference memory

errors were defined as entry into an arm that never contained a food reward (arms 3 and 7). Mice were removed from the maze once they had retrieved all 6 treats or 10 min had elapsed. During trials 8 - 24, maze access was reduced to 5 min. During trials 25+, mice were removed from the maze after entry into an unbaited arm (reference memory error). This was done in order to discourage chained or sequenced behaviour that involves a particular motor response and does not rely on spatial cues or memory. Acquisition criteria was fulfilled when mice entered all of the baited arms without making a reference memory, making 6 out of 7 correct arm choices (allowed 1 working memory error) over 3 out of 4 consecutive trials. At the end of the completed behavioural paradigms (shaping, habituation, acquisition) animals were given unlimited access to food until the normal body weight was achieved (3-5 days).

3.5.4 Voluntary exercise

To establish whether behavioural differences observed in the radial arm maze were the result of an impairment in motor activity, a separate cohort of WT and Cx32KO mice between 2 and 3 months of age were tested in a voluntary exercise paradigm. Mice were given unlimited access to running wheels for 5 days a week, over a 4 week period. The distance ran was recorded by digital counters, reset daily. Animals tested in the running wheel paradigm received *ad libitum* access to food and water.

3.5.5 Statistical analyses

Data are presented as the mean $\pm$ SEM and were analyzed by one-way analysis of variance (ANOVA), followed by *post hoc* Tukey tests.

3.6 Results

3.6.1 Cx32KO mice exhibit impaired spatial learning and memory

In the habituation portion of the test, the number of working memory errors was recorded and criteria was set as 8 correct choices out of the 9 first arm entries. No significant difference was detected between genotypes. WT and Cx32KO mice required comparable number of trials (average of 16 trials) to reach habituation criteria (Figure 3.1 *B*, *Habituation*). In the acquisition portion, both working and reference memory errors were recorded. Since only 6 out of 8 arms were baited, reference memory errors were defined as entry into an unbaited arm. Mice were considered to have failed the trial and were removed from the maze as soon as they (a) committed a reference memory error or two working memory errors, or (b) exceeded the preset time limits. While WT mice reached criteria within 8 trials on average (on 3 out of 4 consecutive trials), Cx32KO mice required approximately 30 trials to achieve the same goal (Figure 3.1 *B*, *Acquisition*; $^{**}p<0.01$, ANOVA, *post hoc* Tukey test).

3.6.2 Motor activity is not impaired in Cx32KO mice

Since Cx32 mutations cause a peripheral neuropathy in humans resulting in altered motor function, the decreased performance of Cx32KO mice in the radial arm maze could result from impaired motor abilities preventing Cx32KO mice from entering all of required arms within the time constraints imposed. However, we found that Cx32KO mice traversed the same number of arms and spent equivalent time in the maze as WT mice before removal due to memory errors (Figure 3.2 *A*). To further establish that Cx32-null mutation does not impact on motor function, mice were tested in a voluntary exercise paradigm. Placed in an

Figure 3.1. Cx32KO mice exhibit an obvious impairment in the acquisition portion of the radial arm maze. *A*) A modified version of the radial arm maze apparatus was used to assess learning and memory in WT (n=9) and Cx32KO (n=14) mice. *B*) The number of trials needed to achieve criteria was determined for each genotype. Note that both WT and Cx32KO animals reach criteria within a comparable number of trials in the habituation portion of this task, while Cx32KO mice are significantly impaired in the acquisition portion of the maze (**$p<0.01$, ANOVA, *post hoc* Tukey).

A

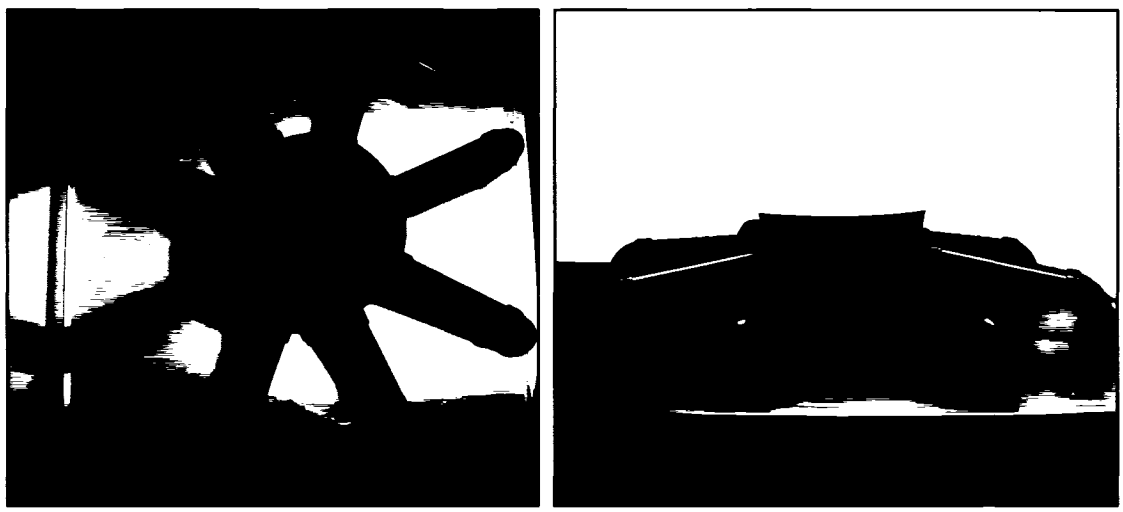

B

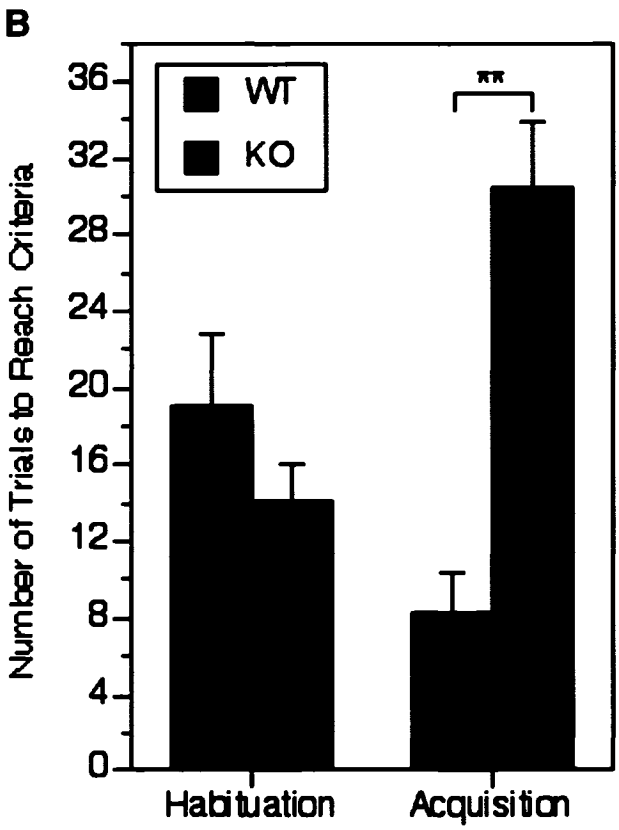
WT
KO
**
Number of Trials to Reach Criteria
0
4
8
12
16
20
24
28
32
36
Habituation
Acquisition

Figure 3.1

Figure 3.2. Cx32KO mice are not motorically impaired. *A*) Average time spent in the radial arm maze per session was recorded for each trial in i) the three trials in which animals reached habituation and ii) the first six trials of acquisition. Animals were removed from the maze when they successfully completed the task (habituation) or traversed 6 arms (acquisition). Note that WT (n=9) and Cx32KO (n=14) mice spend the same amount of time to traverse all arms in the habituation task and the same amount of time to traverse 6 arms in the acquisition phase. However, Cx32 KO mice commit a reference memory error within this time-frame while WT mice learn the task within an average of six trials. *B*) WT and Cx32KO mice were given access to a running wheel and the total distance ran was recorded after 1 week or after a 4 weeks period. Note that mice from both genotypes consistently run the same distance.

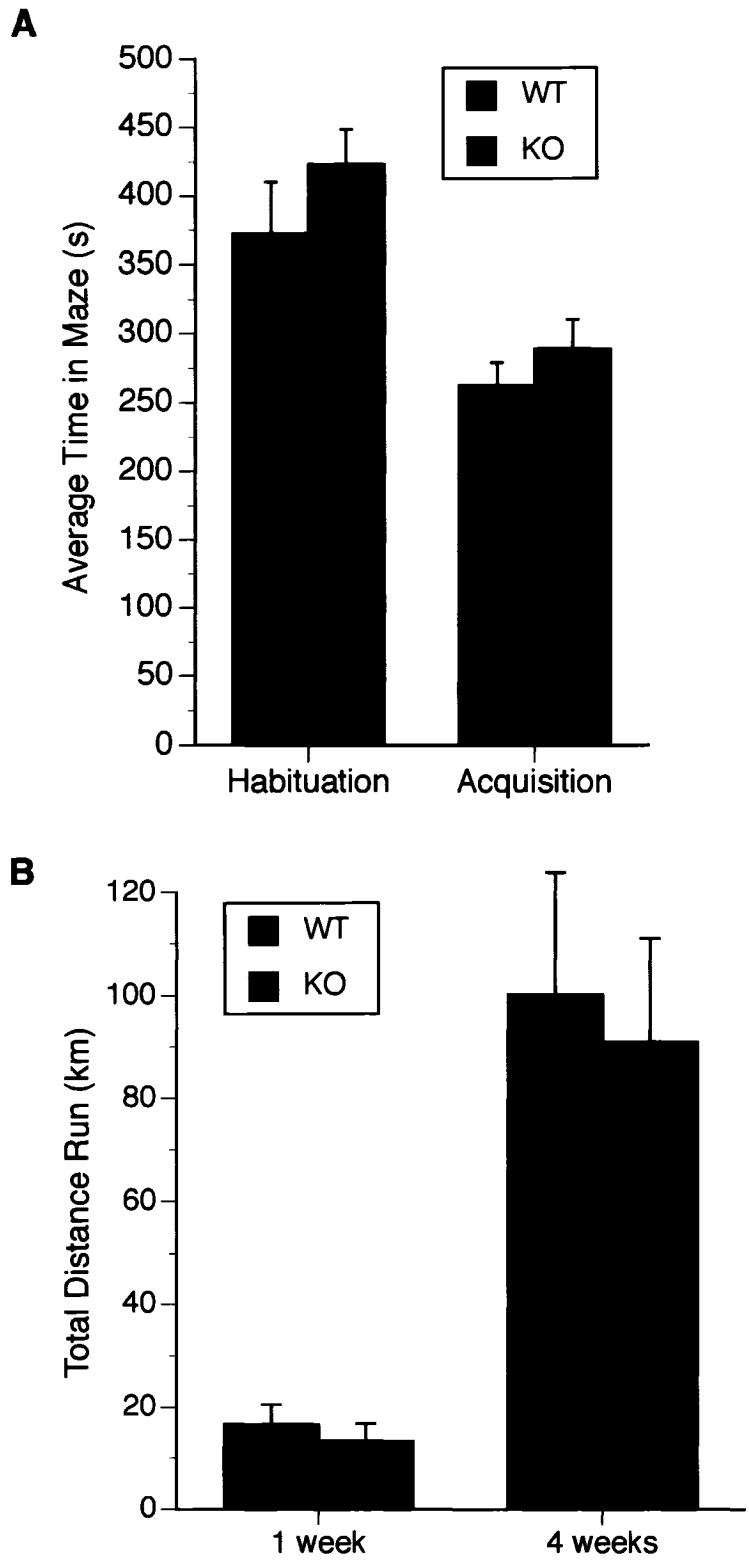
A
500
450
400
350
300
250
200
150
100
50
0
Average Time in Maze (s)
WT
KO
Habituation
Acquisition
B
120
100
80
60
40
20
0
Total Distance Run (km)
WT
KO
1 week
4 weeks

Figure 3.2

enriched environment, animals had free access to a running wheel, 5 days a week, and running behaviour was recorded for 1 week or over a 4 week period. The number of meters ran every day was recorded and compared between genotypes. In average, mice ran a total distance of 18 km in the one week period, and 90 – 100 km over the 4 week period (Figure 3.2 *B*). No difference was observed between genotypes in either group, suggesting that adult Cx32KO (3-4 months of age) mice are not motorically impaired.

3.7 Discussion

Results from this study show that Cx32-null mutation impacts on hippocampal function without altering motor function. Cx32KO mice exposed to a novel environment are capable of mastering a hippocampal-dependent learning and memory paradigm to the same extent as WT mice. However, when the paradigm criteria are altered, Cx32KO mice commit more reference memory errors than WT, indicative of a specific learning and memory deficit.

The hippocampus plays a crucial role in the acquisition and storage of information, received mainly from the entorhinal cortex (Nadel and Moscovitch, 1998). Previous studies have shown that, during the habituation phase of the radial arm maze, neurons within the CA1, CA3 as well as the dentate gyrus regions exhibit increasing activation, defined by enhanced metabolic activity (Ros et al., 2005; Toumane et al., 1988). The CA3 pyramidal cell field is hypothesized to be the hippocampal region most implicated in the acquisition and short-term storage of information when the animal is placed in a new environment (Lassalle et al., 2000), while the CA1 and dentate gyrus are primarily involved in the acquisition of information that is retrieved after a long-term absence in a familiar

environment (Lee and Kesner, 2002). Deficits in working memory are often attributed to deficits in CA3 to CA1 connectivity (Schmitt et al., 2005). Deficits in reference memory or strategy flexibility when paradigm criteria are altered have been linked to impairment of dentate granule cell innervation of the CA3 pyramidal cell field (Xavier et al., 1999). In the present study, Cx32KO mice, which show an enhanced turnover of progenitors in the dentate gyrus of the hippocampus, exhibited an impaired performance in a spatial learning and memory task. More specifically, Cx32KO mice showed a decreased performance in the switching of strategies. While they successfully completed the habituation task, they required almost three times more trials than WT mice to adapt to a paradigm shift in the acquisition phase of the radial arm maze and were unable to learn a new task in the same environment due to reference memory errors. Although the contribution of progenitors to new memory formation remains unclear (Taupin, 2005), the enhanced turnover of progenitors in the dentate gyrus is the only hippocampal phenotype detected in Cx32-null mutant mice and, thus, likely underlies this deficit.

Cx32KO mice show decreased conductance velocity in peripheral nerves, as measured by electrophysiology (Scherer et al., 1998). In order to confirm that the altered performance of these mice was not due to motor impairment, the time spent in the radial arm maze and the distance ran in a running wheel were assessed. Since no difference was observed between genotypes, we can conclude that the decreased performance of Cx32KO mice in the radial arm maze is not due to the inability of the mice to traverse the maze, and is instead most likely a direct or indirect result of impaired connexin-mediated communication.

Acquisition of hippocampal dependent learning tasks and exposure to an enriched environment (such as exercise) increase SGZ progenitor proliferation (Kempermann et al., 1997b). The resulting enhanced neurogenesis in the dentate gyrus has, in turn, been proposed to ameliorate spatial learning (Nilsson et al., 1999). However, it has also been suggested that, because progenitor cells are unspecialized cells with the potential to generate new neurons and glia but unable to participate in brain function, progenitor activation may be stimulated by hippocampal learning paradigms but does not impact upon cognition (reviewed in Taupin, 2005). Cx32-null mutant mice do not display an overt hippocampal phenotype other than enhanced progenitor turnover (proliferation and deletion). Here, we show, for the first time, that unscheduled progenitor activation is sufficient to impact upon learning and memory. While the impaired performance of Cx32KO mice cannot, at the moment, be attributed to a precise mechanism, further analysis of this behavioural data is currently being conducted. Several behavioural parameters are being evaluated. Both arm bias and spatial strategy set are under investigation, as well as the fate of activated progenitors over the course of the learning paradigm. These analyses will allow us to speculate on the type of reference memory deficit observed in Cx32KO animals and to determine how unscheduled progenitor cell activation resulting from alterations in connexin-mediated communication in uninjured brain contributes to this impairment.

Chapter 4: Altering connexin32 expression promotes hippocampal neuroregeneration following excitotoxic injury

4.1 Objectives

In Chapters 2 and 3, I determined that loss of Cx32 affects a subset of early oligodendrocyte progenitors in rodent uninjured brain with behavioural consequences, and that progenitors isolated from Cx32KO hippocampi can be induced to differentiate into neurons *in vitro*. In these next experiments, my objective was to assess the capacity of hippocampal progenitors to proliferate and differentiate into a particular cell type *in vivo*, in the presence or absence of Cx32, following brain injury. This objective entailed four specific aims: **(1)** establish the kainic acid sensitivity and seizure threshold of WT and Cx32KO mice, **(2)** determine the kinetics of degeneration and regeneration in the hippocampal formation of WT and Cx32KO mice following kainic acid-induced seizure, **(3)** evaluate progenitor cell activation at different time points following seizure, and **(4)** evaluate progenitor specification post-seizure.

4.2 Statement of collaborator contributions

This study was conducted with the assistance of Mario Morin. As part of his Honour's project, he performed all the NeuN immunostainings and TUNEL assays, as well as the quantitation of these results. The methyl green pyronine Y quantitation was performed with the help of Mario Morin and Siba Haykal (an undergraduate summer student).

4.3 Abstract

Systemic injection of kainic acid produces a well-defined pattern of seizure activity resulting in hippocampal neuronal loss. This experimental model of brain injury was chosen as it has previously been shown that endogenous SGZ progenitor cells are activated and partially regenerate hippocampal tissue following excitotoxic injury. The sensitivity of Cx32KO mice to kainic acid-induced seizure and seizure severity were comparable to that of WT mice. By methyl green pyronine Y, TUNEL, and fluorojade staining, as well as NeuN immunolabelling, cell viability of granule neurons in the dentate gyrus was found to be transiently compromised 1 week after seizure induction without significant cell loss. Conversely, significant excitotoxic cell death and neuronal degeneration were observed in the CA3a/b pyramidal cell field of both WT and Cx32KO mice 0.5 - 2 weeks after kainic acid administration. While WT mice exhibited only partial restoration of neuronal number 4.5 weeks following seizure, Cx32KO animals showed a complete regeneration of pyramidal and interneurons in the CA3a/b layer, as determined by antigenic lineage analysis of neuronal subtype. To provide mechanistic insight into how altering Cx32 expression promotes hippocampal pyramidal neuron regeneration, progenitor cell activation and specification were tracked by BrdU labelling and lineage analysis over time following kainate seizure. Proliferating cell number peaked significantly 0.5 week after seizure in the CA3a/b layer and 1 week after seizure in the SGZ of both Cx32KO and WT mice. Four weeks after labelling, the majority of actively dividing cells of the SGZ differentiated to a calbindin$^+$ neuronal phenotype and localized to the granule cell layer of the dentate gyrus. In the CA3a/b region. the majority of proliferating cells activated following seizure were identified as NG2$^+$ progenitors. Colleagues in the Bennett laboratory demonstrated that

neuronal specification of these proliferating $NG2^+$ cells increased significantly in Cx32KO mice. Overall, these results strongly suggest that connexin-mediated communication plays a role in directing $NG2^+$ progenitor specification following injury.

4.4 Introduction

4.4.1 Why study Cx32-null mutation in injured brain?

Recent literature has shown that proliferating cells isolated from non-neurogenic regions can be induced to differentiate into neurons *in vitro* or after grafting into neurogenic environments (Kondo and Raff, 2000; Palmer et al., 1999; Shihabuddin et al., 2000; Weiss et al., 1996). These observations provide compelling evidence that multipotential neural precursor cells may exist in larger numbers than previously anticipated in the adult CNS, but that local environmental factors restrict their plasticity, commitment, and fate (Song, 2002). The molecular mechanisms underlying local environmental control of progenitor fate are not well understood, but one possible influence is gap junctional intercellular communication, which may enable neural precursors to coordinate their survival, differentiation, and deletion in response to environmental changes. In Chapters 2 and 3, we demonstrated that Cx32 is involved in adult progenitor proliferation and specification, and that removing Cx32 results in altered hippocampal function. *In vitro*, we showed that the differentiation of hippocampal progenitors towards a neuronal phenotype was enhanced in the absence of Cx32. In the present study, we decided to further assess the role of Cx32 in dictating adult progenitor cell fate *in vivo*. We therefore sought to determine whether Cx32-mediated control of neural progenitor fate could be harnessed to enhance cell replacement following injury. Previous studies have shown that endogenous hippocampal cell replacement is increased by

intraventricular infusion of paracrine growth factors (Nakatomi et al., 2002). In this study, we investigated whether alterations in juxtracrine signaling mechanisms (i.e., loss of Cx32) would potentiate cell injury or facilitate cell replacement.

4.4.2 The role of connexins following brain injury

Gap junctions have been implicated in both the resistance to cell death as well as the propagation of damage following brain injury. Inter-astrocytic channels have been suggested to stabilize cellular calcium homeostasis and to dissipate oxidative stress, resulting in the protection of neurons from oxidative cell death (Blanc et al., 1998). The protective effects of connexins may be mediated independently of gap junction channel function, possibly by their contribution to the cytoskeletal organization. Connexin expression can induce phenotypic transformations such as cellular flattening and actin organization into parallel arrays of stress fibers, and therefore influence cellular resistance via changes in cell geometry (Chen et al., 1997; Cotrina et al., 1998). This mechanism is proposed to underlie protection of C6 glioma cells in various models of cell injury following Cx32, Cx40, and Cx43 ectopic expression (Lin et al., 2003).

Alternatively, several converging lines of evidence suggest that an increase in connexin expression is associated with enhanced cerebral injury. In *in vivo* models of traumatic injury, global ischemia, and in *in vitro* models of cellular injuries such as oxidative stress, connexin expression increases neuronal vulnerability and amplifies cell injury (Frantseva et al., 2002a; Lin et al., 1998; Rami et al., 2001). For example, in neuronal cells of the CA3 region of the rat hippocampus, Cx26 and Cx45 mRNAs were induced from 6 to 48 hr after kainic acid administration, co-localizing with cells undergoing apoptosis

(Condorelli et al., 2003). Furthermore, not only do gap junctions expressed by neurons play a role in their vulnerability to cell death, but glial gap junctions also affect neuronal viability following brain injury. In non-neuronal cells of the hippocampus, Cx32 and Cx45 mRNA and protein were found to be upregulated from 24 to 72 hours post-kainate treatment (Condorelli et al., 2003). In a model of global transient ischemia, elevated levels of Cx43 were detected in reactive astrocytes and a higher density of gap junctions was detected in the CA1 cell field of the hippocampus, the region most vulnerable to global ischemia. Furthermore, a reduction in neuronal cell death was achieved by inhibiting gap junction permeability (Rami et al., 2001). Furthermore, in models of ischemia and traumatic injury, injection of antisense oligodeoxynucleotides to block Cx32 and Cx26 mRNA expression resulted in significant neuroprotection, whereas partial reduction of Cx43 was sufficient to decrease cell death following hypoxic injury (Frantseva et al., 2002a; Frantseva et al., 2002b). These findings not only suggest that connexins might be implicated in apoptotic cell death, but also that they might play a role in the reactive glial cell response to brain injury.

In this study, to further elucidate the role of connexins in neurodegeneration and regeneration, we compared cellular damage, death, and recovery following kainic acid-induced hippocampal injury in WT and Cx32KO mice.

4.4.3 Seizure-induced hippocampal damage

Kainic acid is a glutamate analog that binds to kainate (KA) and alpha-amino-3-hydroxy-5-methyl-4-isoxazolepropionic acid (AMPA) receptors, resulting in strong epileptic activity and subsequent hippocampal damage (Ben-Ari, 1985; Kizer et al., 1977; Nadler, 1981; Nadler et al., 1980). Neuronal apoptotic cell death has been extensively described in the hippocampus of kainic acid-treated rodents, with the appearance of nuclear chromatin

condensation and DNA fragmentation with a typical ladder pattern as key apoptotic features (Humphrey et al., 2002; Pollard et al., 1994). However, necrotic cell death is also evident in organotypic hippocampal slice cultures treated with kainic acid (Holopainen et al., 2004). Regardless of the mode of cell death, it is generally accepted that neuronal damage triggers progenitor cell proliferation and subsequent specification (Dong et al., 2003; Gray and Sundstrom, 1998; Nakagawa et al., 2000; Yoshimura et al., 2001). For this reason, the kainate model was employed in the present study.

4.5 Materials and methods

4.5.1 Induction of kainic acid seizures

A total of n=42 WT and n=48 Cx32KO 2-4 months old male mice were evaluated in this study. Each animal received an intraperitoneal injection of 25 mg/kg kainic acid (Ocean Produce International, Nova Scotia). Seizure intensity was established according to a standard 5 point behavioural scale (Mckhann et al., 2003; Royle et al., 1999) previously employed in our laboratory (Cheung et al. 2005): stage 1: reduced locomotion and sedation; stage 2: automatisms such as head bobbing, scratching and repetitive face washing; stage 3: tremors and "wet-dog shakes"; stage 4: intermittent followed by continuous rearing with forelimb clonus and falling behaviour; stage 5: severe limbic seizures with respiratory difficulty, often lethal. Animals reaching stage 4 were injected with diazepam (5 mg/kg) within 5 minutes of staging to limit convulsions. Only the mice that reached stage 4 were included in this study. Mice were euthanized with sodium pentobarbital 3, 9, 15, 28, or 35 days after kainic acid-induced seizure and transcardially perfused with 10 mM PBS and 4% paraformaldehyde in 10 mM PBS as described in Chapter 2.

4.5.2 Quantitative analyses of cell death and degeneration

Brains were removed and processed as described in Chapter 2. For histological analysis, sections were stained with methyl green pyronine Y (MGPY) as described in (Moffitt, 1994), hematoxylin and eosin (H&E), or cresyl violet as described in (Bennett et al., 1995). In MGPY-stained sections, DNA is stained blue and RNA is stained pink. Cells defined as viable exhibited a light blue nucleus, confirming nuclear integrity, and a pink cytoplasm, indicative of RNA transcription (metabolic activity). Cells with hyperchromatic nucleus and/or lack of cytoplasmic (RNA) staining were identified as damaged cells (Al-Hazzaa and Bowen, 1998). Quantitative analyses were performed on MGPY-stained sections using the Advanced Measurement Module of Openlab 3.1.7 software (Improvision). The number of viable cells was assessed in the superior limb of the granule cell layer of the dentate gyrus and in the CA3a/b pyramidal cell field. Data are expressed as number of cells/0.1mm^2. Quantitative observations were confirmed by qualitative assessment of H&E and cresyl violet stained adjacent sections, in which pyknotic, eosinophilic, or hyperchromatic cells with amorphous or fragmented nuclei were defined as damaged cells. Cells with oval nuclei, prominent nucleoli lacking eosinophilic cytoplasm and homogenously stained by hematoxylin or cresyl violet were defined as healthy cells (Bennett et al., 1995; Bennett et al., 1998b). Edematous tissue was identified as area exhibiting macroscopic swelling, vacuolization, and herniation of neuropil (Bennett et al., 1995).

Cells dying through an apoptotic-like mechanism were identified by TUNEL, as described in Chapter 2. Degenerating neurons damaged through a non-apoptotic mechanism were identified by fluorojade B staining. Slides were incubated in a solution of 1% sodium

hydroxide in 80% alcohol for 5 min, followed by 2 min washes in 70% alcohol and distilled water and a 10 min incubation in a 0.06% potassium permanganate solution. Slides were rinsed in distilled water and stained in a 0.0004% fluorojade staining solution for 20 minutes. The number of $TUNEL^+$ or $fluorojade^+$ cells were determined by two independent evaluators, using the Measurement Module of the Openlab 3.1.7 software, and counts were averaged to yield a single parameter per animal. Data are expressed as the percentage of cells per 0.1 mm^2 exhibiting TUNEL or fluorojade reactivity.

4.5.3 BrdU labelling and antigenic lineage analysis

BrdU (50 μg/g in sterile 10 mM PBS, pH 7.0) was administered intraperitoneally. Following kainate treatment, animals received 5 injections of BrdU over 72 consecutive hours and were sacrificed 3 to 24 hours after the last injection. Animals were sacrificed following this protocol 0.5 (n=7 WT, n=4 KO), 1 (n=5 WT and 7 KO), 2 (n=3 WT and 3 KO) and 4 (n=3 WT and 3 KO) weeks after seizure induction, and were compared to uninjured controls (n=10 WT and 7 KO). Brains were processed and progenitor proliferation was assessed by BrdU immunodetection, as described in Chapter 2. For lineage analysis, animals received 5 injections of BrdU on days 6, 7, and 8 after the kainate administration and were sacrificed on day 9 or day 35. Cell identity was established by immunolabelling using anti-BrdU conjugated to FITC and antibodies to the specific lineage markers. Following this protocol, antibodies used for double-labelling were mouse anti-NeuN, Cy3-tagged anti-GFAP, mouse anti-CNPase (1:200, Sigma), rat anti-F4/80 (1:100, Abcam, Cambridge, MA), and rat anti-NG2, followed by Cy3-conjugated anti-mouse IgG or anti-rat IgG. Concentrations are as described in Chapter 2, Materials and Methods and see

"Appendix 1: List of antibodies". Double-positive cells were counted in the dentate gyrus and expressed as % double-positive cells ± SEM.

Mature neurons were detected by immunofluorescence. Coronal sections of animals sacrificed 0, 0.5, 1, 2, 4, or 5 weeks post-seizure were treated with anti-NeuN followed by a Cy3-conjugated anti-mouse IgG secondary. The number of $NeuN^+$ cells was counted in the dentate gyrus and CA3 region and expressed per $0.1mm^2$. To identify neuronal subtypes, sections were also stained with either rabbit anti-calbindin (1:200, Chemicon), rabbit anti-parvalbumin (1:1000, SWANT, Bellinzona, Switzerland) along with anti-NeuN, or with mouse anti-parvalbumin alone (1:2000, Sigma), followed by Cy3-conjugated anti-rabbit and FITC-conjugated anti-mouse or Cy3-conjugated anti-mouse IgG. Concentrations are as described in Chapter 2, Materials and methods.

4.5.4 Statistical analyses

Data are presented as the mean ± SEM and were analyzed MANOVA, followed by *post hoc* Tukey tests.

4.6 Results

4.6.1 WT and Cx32KO mice exhibit comparable kainic acid sensitivity and seizure activity

The following experiments were aimed at determining whether hippocampal progenitors could be induced to specify and adopt a neuronal fate *in vivo* to repopulate damaged tissue, in the presence or absence of Cx32. However, before this hypothesis could be tested using an excitotoxic seizure paradigm, the extent of the seizure intensity as well as the degree of resulting damage needed to be assessed and judged equivalent between genotypes to permit interpretation of subsequent cell replacement results. As discussed in Chapter 2, transgenics are typically in a polygenic background of mixed 129SVJ1 and C57BL/6 strains. Because 129SVJ1 mice exhibit an extremely low seizure threshold as well as a reduced neural progenitor proliferative capacity, we placed the Cx32KO mice into a C57BL/6 lineage by extensive backcrossing (see Chapter 2, Results). For this study, 42 WT and 48 Cx32KO mice received a dose of 25 mg/kg of kainic acid, previously shown to induce hippocampal damage without causing death in C57BL/6 mice (Royle et al., 1999; Schauwecker et al., 2000). Seizure induction was evaluated using a standard five point behavioural scale previously utilized in our laboratory (Cheung et al., 2005). Seizure activity was allowed to progress to stage 4, necessary to obtain significant neuronal loss (Bennett et al., 1995), and then was stopped by the administration of diazepam, an anti-convulsant, to minimize mortality. We found that this concentration of kainic acid elicited stage 4 seizures in ~90% of WT and Cx32KO mice (37/42 WT mice vs 42/48 Cx32KO mice). Of mice reaching stage 4, 12 WTs and 12 Cx32KOs died. The remaining 12% of mice from each genotype only reached stage 1-3 and were therefore discarded from this

study. These data are summarized in Table 4.1 and indicate that our congenic C57BL/6 Cx32KO and WT mice exhibit the same seizure susceptibility, seizure staging, and mortality rates following systemic injection of kainic acid.

4.6.2 Excitotoxic damage in the hippocampal formation of Cx32KO and WT mice is equivalent following kainic acid-induced seizure

The kinetics of excitotoxic cell death were established in WT and Cx32KO mouse hippocampus following kainic acid-induced seizure. MGPY, H&E, and cresyl violet histological analyses were first performed to determine cell viability, followed by TUNEL assay and fluorojade staining to measure the percentage of apoptotic and degenerating cells respectively (Figures 4.1 - 4.3). In MGPY-stained sections, the number of viable cells was assessed in the granule cell layer of the dentate gyrus and the CA3a/b pyramidal cell field of WT and Cx32KO mice sacrificed 0, 0.5, 1, 2, and 4.5 weeks after the seizure (Figure 4.1 *A1-8,B1-16,E,F*). Quantitative observations were confirmed by qualitative assessment of H&E (Figure 4.1 *C1-16*) and cresyl violet (Fig 4.1 *D1-16*) stained adjacent sections. In the granule cell layer of the dentate gyrus, cell viability was compromised 1 week after seizure induction, as indicated by a decrease in metabolic activity (Figure 4.1 *B9-10, arrows, E*; **$p<0.01$, MANOVA, *post hoc* Tukey test), the occurrence of hyperchromatic cells (Figure 4.1 *C9-10, arrowheads*), and the presence of vacuoles (Figure 4.1, *D9-10, large arrows*). However, further assessment of cell death revealed that the cell damage observed 1 week post-seizure did not translate into significant granule cell loss. In WT and Cx32KO mice, the number as well as morphology of viable granule cells found in the dentate gyrus 2 and 4.5 weeks post-seizure were similar to that of controls (Figure 4.1 *B,C&D13,E*).

Table 4.1. WT and Cx32KO mice exhibit comparable seizure intensity. Seizure induction was evaluated following intraperitoneal injection of 25 mg/kg kainic acid. The intensity of seizure was staged using a standard five point behavioural scale (Cheung et al., 2005). Note that WT and Cx32KO animals exhibit comparable kainic acid sensitivity and seizure intensitiy.

	Behavioral scale					
Genotype	**1**	**2**	**3**	**4**	**Mortality**	**Total number of mice**
WT	2 (5%)	2 (5%)	1 (2%)	25 (60%)	12 (28%)	42
Cx32 KO	2 (4%)	0 (0%)	4 (8%)	30 (63%)	12 (25%)	48

Figure 4.1. Kinetics of cellular degeneration and recovery in the hippocampus of WT and Cx32KO mice following kainic acid-induced seizure. Animals were sacrificed 0.5 (n=7 WT, n=4 KO), 1 (n=5 WT and 7 KO), 2 (n=3 WT and 3 KO) and 4.5 (n=8 WT and 8 KO) weeks after seizure induction, and were compared to uninjured controls (n=10 WT and 7 KO). Abbreviations: CA3a/b, pyramidal cell fields; DG, dentate gyrus; KA, kainic acid. *A-D*) Hippocampal sections were stained with MGPY (*A, B*), H&E (*C*) and cresyl violet (*D*). Boxes in *A* outline areas magnified in insets *B-D*. Scale bars *A*, 150 μm; Insets *B-D*, 50 μm. Arrows in B, C & D7-8 designate the CA3a/b region exhibiting significant degeneration at week 0.5 as compared to control (week 0; similar for both genotypes). In B, C, & D9-10, arrows show the decreased metabolic activity, arrowheads designate hyperchromatic cells and large arrows demonstrate the presence of vacuoles. Arrows in B, C & D15 denote the partial regeneration observed in the CA3 region of WT mice 4.5 weeks post-seizure. *E, F*) The number of viable cells was quantitated in the DG (*E*) and CA3a/b (*F*) of MGPY-stained WT and Cx32KO hippocampal sections. Data are expressed as mean number of viable cells ± SEM per $0.1mm^2$. Note that cell number is restored in the dentate gyrus of both genotypes, but that only Cx32KO mice exhibit complete cell recovery 4.5 weeks post-seizure (MANOVA, *post hoc* Tukey, * $p<0.05$, ** $p<0.01$).

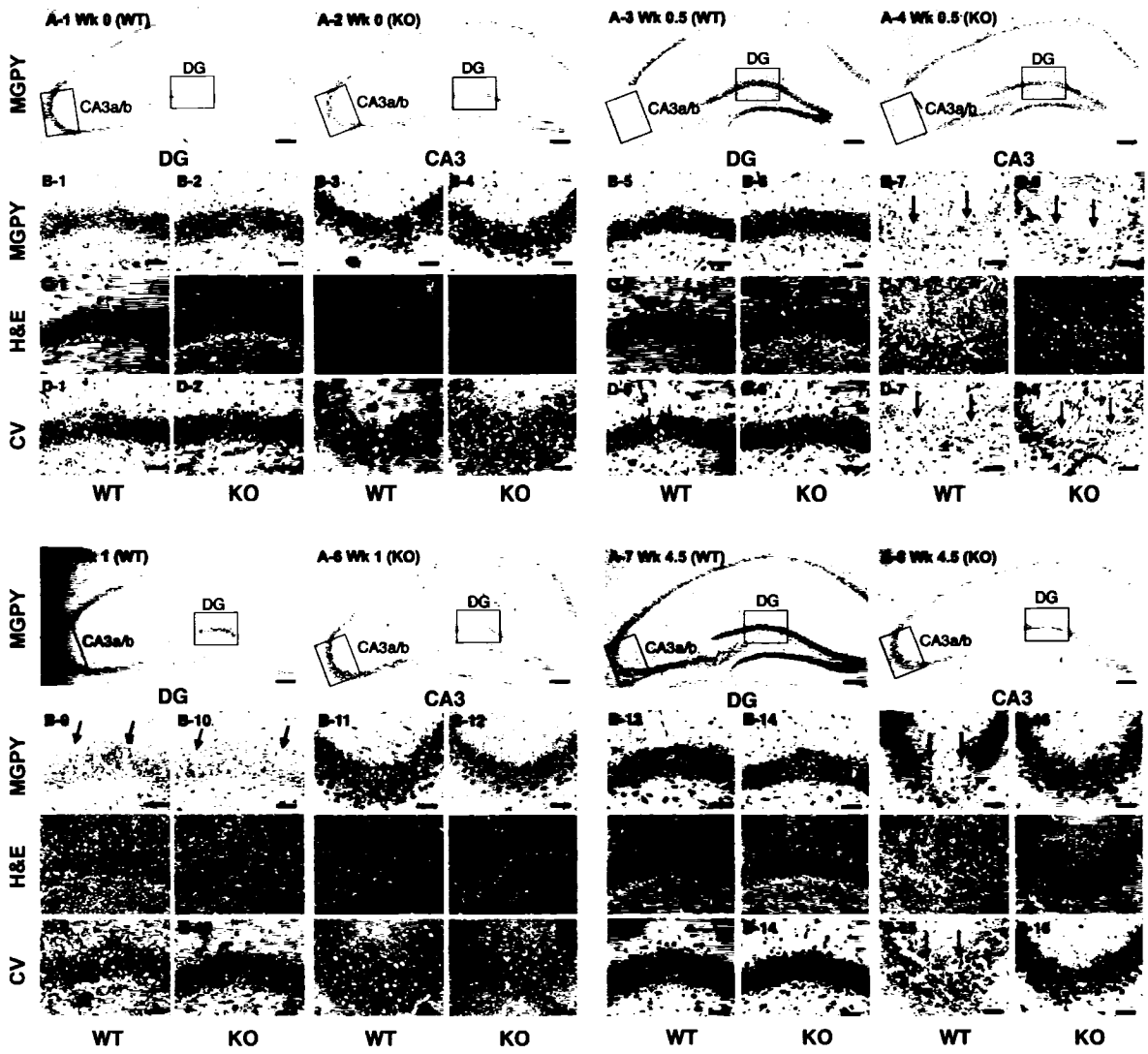
A-1 Wk 0 (WT)
A-2 Wk 0 (KO)
A-3 Wk 0.5 (WT)
A-4 Wk 0.5 (KO)
A-5 Wk 1 (WT)
A-6 Wk 1 (KO)
A-7 Wk 4.5 (WT)
A-8 Wk 4.5 (KO)
DG
CA3a/b
CA3
MGPY
H&E
CV
WT
KO

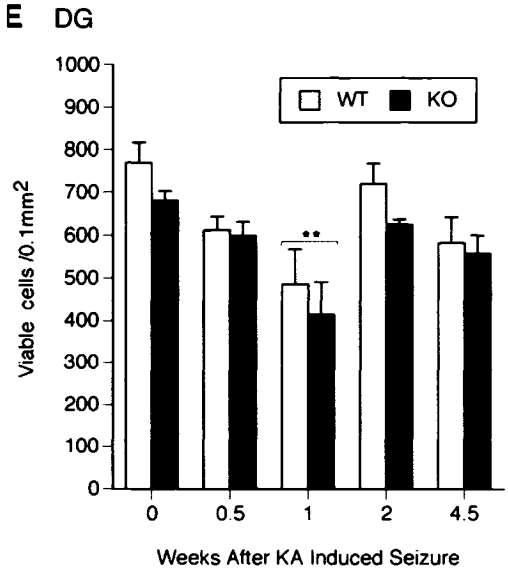
E DG
WT
KO
Viable cells /0.1mm2
Weeks After KA Induced Seizure

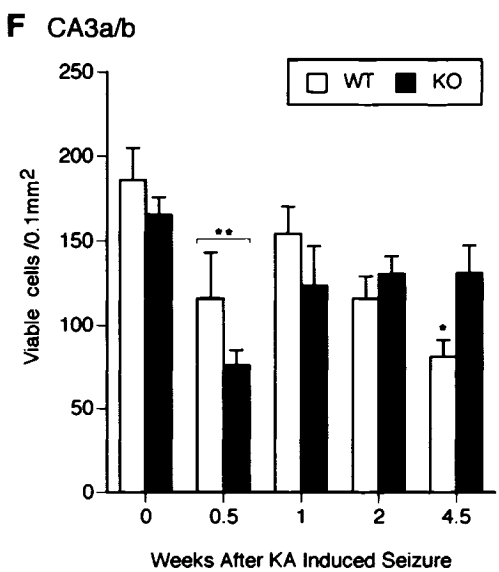
F CA3a/b
WT
KO
Viable cells /0.1mm2
Weeks After KA Induced Seizure

Figure 4.1

No apoptotic-like cell death was observed in the dentate gyrus by TUNEL reactivity at any time point following seizure (Figure 4.2 *A,C*). Fluorojade staining further confirmed the absence of degenerating neurons in the dentate gyrus of the hippocampus up to 4.5 weeks following kainic acid-induced injury (Figure 4.2 *B,D*).

By contrast, significant cell death was observed in the CA3a/b pyramidal cell field of both WT and Cx32KO mice. A substantial reduction in cell number was observed in the CA3 pyramidal layer 0.5 week after kainic acid administration, indicated by loss of MGPY (Figure 4.1 *B7-8, arrows*), H&E (Figure 4.1 *C7-8, arrows*), and cresyl violet (Figure 4.1 *D7-8, large arrows*) staining. Remaining cells in the CA3 area exhibited a pyknotic morphology (Figure 4.1 *C7-8,D7-8, arrowheads*). In MGPY-stained sections, the number of viable cells in both WT and Cx32KO mice was significantly reduced by 42% in WT animals and 54% in Cx32KO animals 0.5 week after kainic acid administration (Figure 4.1 *B7-8,F*; **$p<0.01$, MANOVA, *post hoc* Tukey test). TUNEL analysis and fluorojade staining confirmed these observations. Approximately 20% of cells in the CA3 region of both genotypes were $TUNEL^+$ at the 0.5 week time point, indicative of apoptotic-like cell death (Figure 4.3 *A,C*; *$p<0.05$, MANOVA, *post hoc* Tukey test). An additional 25-30% of cells were $fluorojade^+$, indicative of cells dying through a non-apoptotic mechanism (Figure 4.3 *B,D*, *$p<0.05$, MANOVA, *post hoc* Tukey test).

Taken together, these data demonstrate that the loss of Cx32 does not impact upon the degree of cell damage in the dentate gyrus or cell death in the CA3 pyramidal layer of the hippocampus following kainic acid-induced seizure. Significant cell loss is observed in the CA3a/b pyramidal cell field, with WT and Cx32KO mice exhibiting similar neuropathology with comparable kinetics.

Figure 4.2. No cell death is observed in the dentate gyrus of WT and Cx32KO mice following kainic acid-induced seizure. Animal numbers and abbreviations are as defined in Figure 4.1. *A*) Apoptotic cells in the dentate gyrus were labelled by TUNEL (green). *B*) Degenerating neurons dying through a non-apoptotic mechanism were identified by fluorojade B staining (green). Scale bars *A-B*, 100 μm. *C, D*) The number of $TUNEL^+$ or $fluorojade^+$ cells and the total number of cells in each field were counted and expressed as % apoptotic cells or % degenerating neurons ± SEM. Note that the basal apoptotic index is slightly higher in Cx32KO compared to WT animals as previously reported in Chapter 2. No statistically significant increase in TUNEL or fluorojade labelling is observed at any time point after injury.

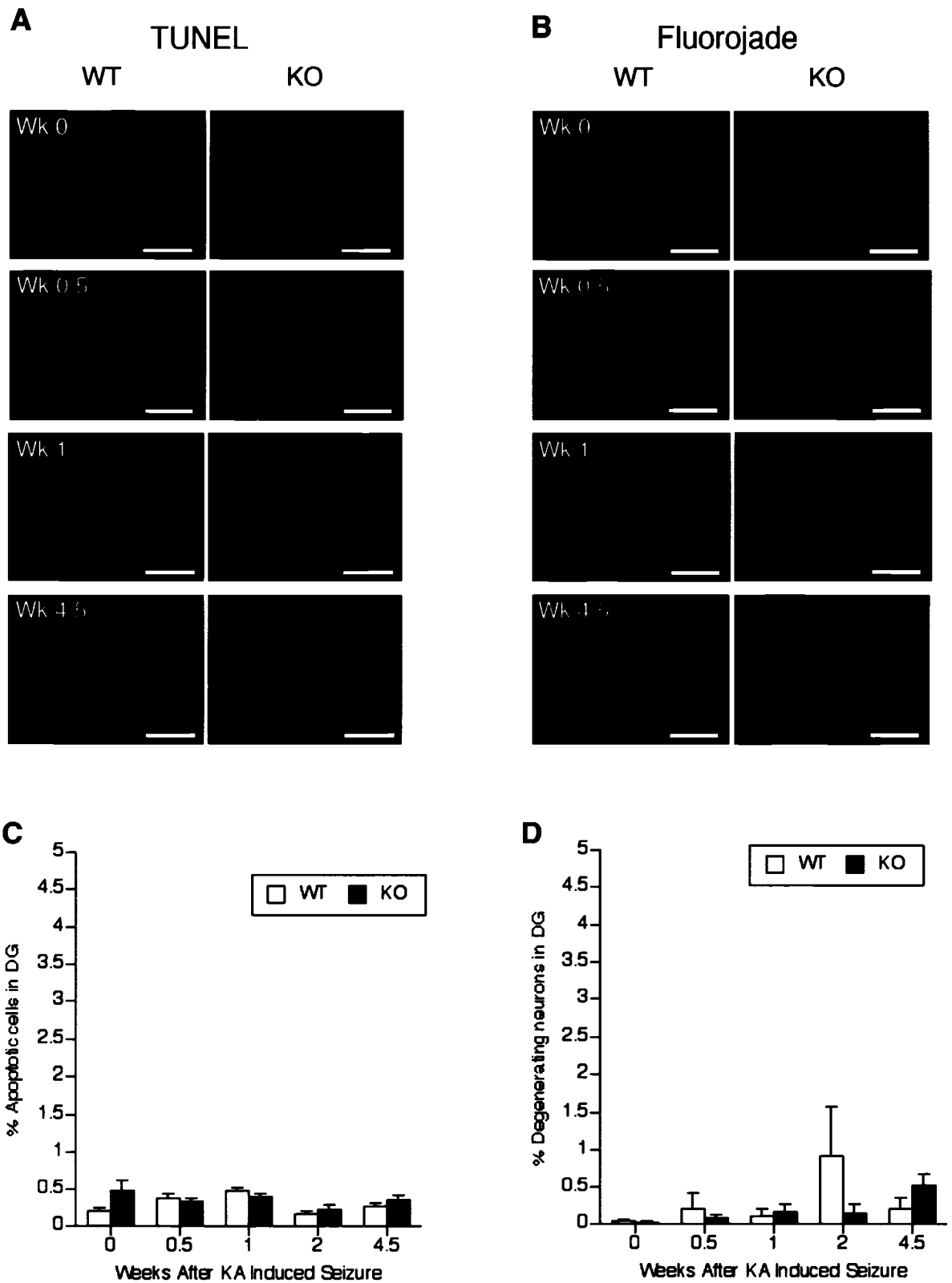
A
TUNEL
WT
KO
Wk 0
Wk 0.5
Wk 1
Wk 4.5
B
Fluorojade
WT
KO
Wk 0
Wk 1
C
WT
KO
% Apoptotic cells in DG
0
0.5
1
1.5
2
2.5
3
3.5
4
4.5
5
0
0.5
1
2
4.5
Weeks After KA Induced Seizure
D
WT
KO
% Degenerating neurons in DG
0
0.5
1
1.5
2
2.5
3
3.5
4
4.5
5
0
0.5
1
2
4.5
Weeks After KA Induced Seizure

Figure 4.2

Figure 4.3. Apoptotic-like cell death in the CA3 pyramidal cell field following kainic acid-induced seizure is comparable between WT and Cx32KO mice. Animal numbers and abbreviations are as defined in Figure 4.1. *A*) Apoptotic cells in the CA3 pyramidal cell field were labelled by TUNEL (green). *B*) Degenerating neurons dying through a non-apoptotic mechanism were identified by fluorojade B staining (green). Scale bars *A-B*, 100 μm. *C, D*) The number of $TUNEL^+$ or $fluorojade^+$ cells and the total number of cells in each field were counted and expressed as % apoptotic cells or % degenerating neurons ± SEM. Note that the basal apoptotic index is comparable between WT and Cx32KO and that both genotypes exhibit an increase in apoptotic-like cell death and non-apoptotic neuronal degeneration 0.5 week after seizure (*$p<0.05$, MANOVA, *post hoc* Tukey). The percentages of $TUNEL^+$ and $fluorojade^+$ cells are greater in WT compared to Cx32KO 4.5 weeks post seizure (~$p<0.07$, MANOVA, *post hoc* Tukey).

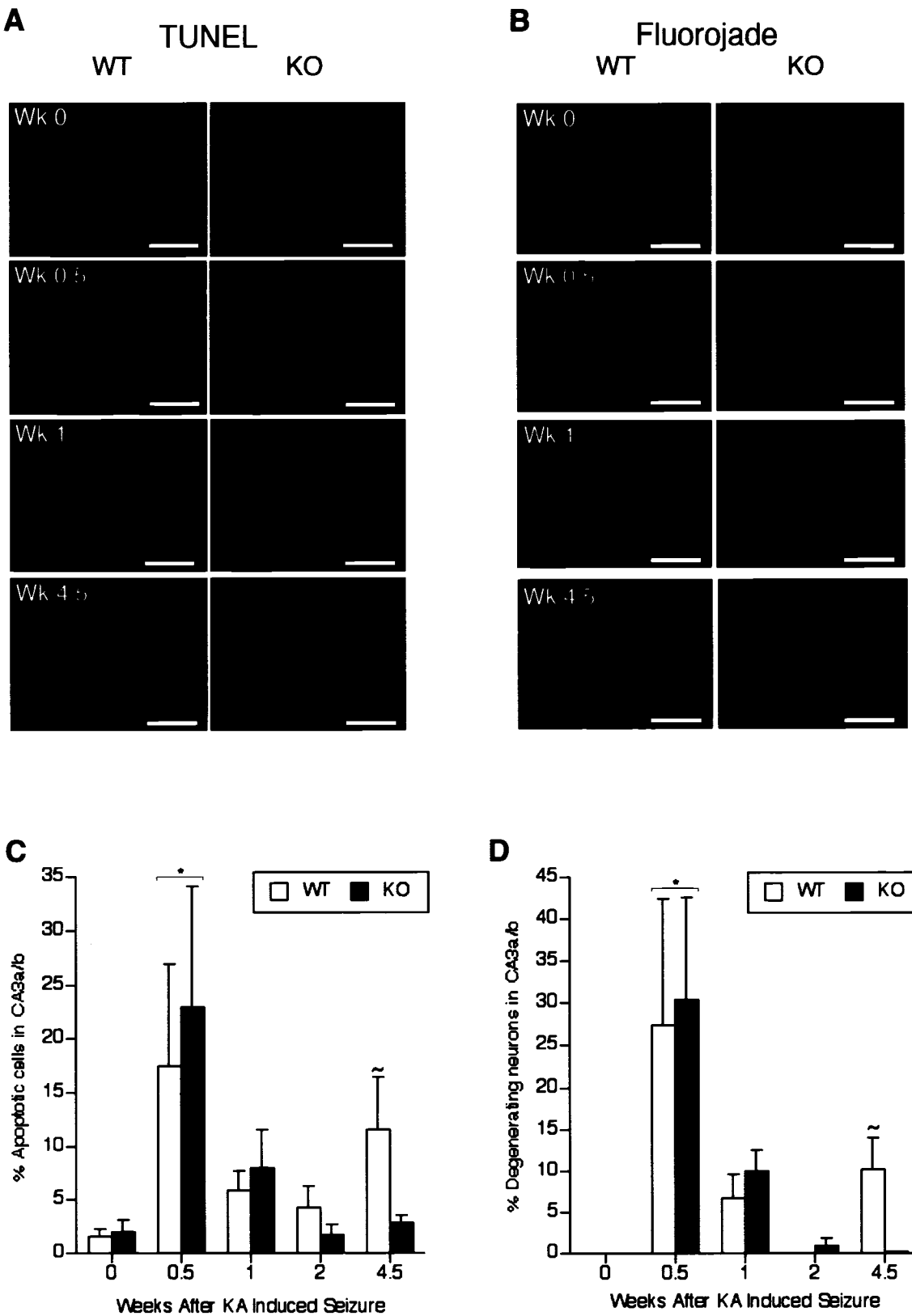
A
TUNEL
WT
KO
Wk 0
Wk 0.5
Wk 1
Wk 4.5
B
Fluorojade
WT
KO
Wk 0
Wk 0.5
Wk 1
Wk 4.5
C
WT
KO
% Apoptotic cells in CA3a/b
35
30
25
20
15
10
5
0
*
≈
0
0.5
1
2
4.5
Weeks After KA Induced Seizure
D
WT
KO
% Degenerating neurons in CA3a/b
45
40
35
30
25
20
15
10
5
0
*
≈
0
0.5
1
2
4.5
Weeks After KA Induced Seizure

Figure 4.3

4.6.3 The CA3 pyramidal cell field is partially recovered in WT mice and completely regenerated in Cx32KO animals following kainate injury

Partial regeneration of hippocampal neurons has been described previously in WT animals 4 to 5 weeks following seizure (Dong et al., 2003; Parent et al., 1997; Wang et al., 2004; Yoshimura et al., 2001). In this study, the number as well as morphology of viable granule cells found in the dentate gyrus of WT and Cx32KO mice 4.5 weeks post-seizure was similar to that of controls (Figure 4.1 *B,C&D13,E*). Conversely, in the CA3 pyramidal cell field, WT and Cx32KO animals exhibited significantly different trends. Although, MGPY-stained cell number rebounded in both genotypes 1-2 weeks after kainic acid injection, viable cells were only maintained to control levels in Cx32KO mice (Figure 4.1 *F)*. In WTs, the total number of MGPY-stained cells in the CA3 pyramidal layer was significantly reduced 4.5 weeks after seizure, as compared to control animals (Figure 4.1 *F*; *$p<0.05$, MANOVA, *post hoc* Tukey test). Moreover, an obvious cell loss and reduction in histological staining could be observed throughout the CA3 layer (Figure 4.1 *B,C&D15, arrows*) with residual neurons showing hyperchromatic and pyknotic features (Figure 4.1 *D15, arrowheads*). By contrast, in Cx32KO mice, the number of viable cells in the CA3 region was effectively restored, with viable cell morphology and number similar to uninjured controls (Figure 4.1 *B,C&D16,E*). TUNEL analysis revealed a difference between genotypes in apoptotic-like death, detected in the CA3 pyramidal layer 4.5 weeks after kainic acid-induced seizure, that approached statistical significance (Figure 4.3 *C*; ~ $p<0.07$, MANOVA, *post hoc* Tukey test). Increased cell death was noted in the WT CA3 region, whereas the Cx32KO animals showed a very low percentage of $TUNEL^+$ cells at this time

point. Fluorojade staining also revealed elevated levels of degenerating neurons in WT as compared to Cx32KO mice 4.5 weeks post seizure (Figure 4.3 *D*).

4.6.4 Neuronal regeneration of the CA3 pyramidal cell field is increased in Cx32KO as compared to WT mice

To identify the lineage of the $MGPY^+$ cells compromised following seizure, sections from WT and Cx32KO mice sacrificed at various time points following injury were stained with NeuN, a marker of terminally differentiated neurons. The number of $NeuN^+$ neurons was counted in the granule cell layer of the dentate gyrus and the CA3a/b pyramidal cell field at various time points after kainic acid injection (Figure 4.4). In the dentate gyrus, the overall number of $NeuN^+$ granule neurons was not altered at any time point following kainic acid-induced seizure (Figure 4.4 *A,B*). These results are consistent with the TUNEL analysis and fluorojade staining, suggesting that cell viability is only transiently compromised and that damaged granule neurons recover without significant cell death. In the CA3 region, a 30% decrease in neuronal number was observed 0.5 and 1 week post-seizure (Figure 4.4 *C*; *$p<0.05$, MANOVA, *post hoc* Tukey test). Neuronal loss was >50% in both genotypes within 2 weeks of kainic acid injection (Figure 4.4 *A,C*; $p<0.01$, MANOVA, *post hoc* Tukey test). Despite extensive cell loss in both genotypes, neuronal number was effectively restored in the CA3 pyramidal cell field 4.5 weeks after seizure induction in Cx32KO but not WT mice. A small increase in $NeuN^+$ neurons was observed in the CA3 region of WT mice (Figure 4.4 *A,C*), however, neuronal number remained significantly lower than controls (Figure 4.4 C; *$p<0.05$, MANOVA, *post hoc* Tukey test).

Figure 4.4. Neuronal regeneration of the CA3 pyramidal cell field is enhanced in Cx32KO mice following kainate injury. Animal numbers and abbreviations are as defined in Figure 4.1. *A*) Neurons were identified by NeuN immunolabelling (red). Scale bars, 200 μm. *B, C*) The number of $NeuN^+$ cells per 0.1 mm^2 was quantified in the dentate gyrus (*B*) and in the CA3a/b pyramidal cell field (*C*; area indicated by arrows in *A*). Note that the control number of neurons is comparable across genotype, with the most important neuronal loss observed 2 weeks following injury. Neuronal regeneration is observed in both genotypes by 4.5 weeks after seizure but only Cx32KOs exhibit a complete restoration of neuronal number (*$p<0.05$, **$p<0.01$, MANOVA, *post hoc* Tukey).

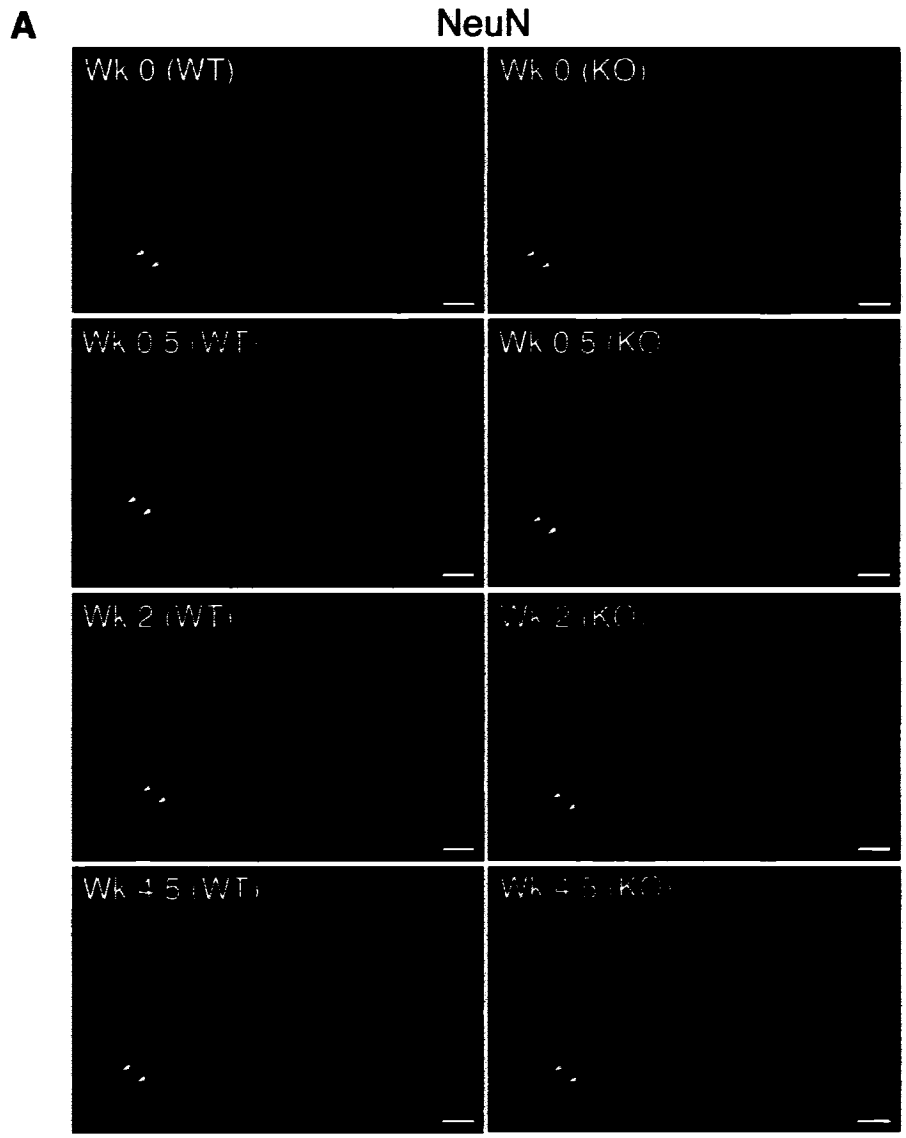
A
NeuN
Wk 0 (WT)
Wk 0 (KO)
Wk 0.5 (WT)
Wk 0.5 (KO)
Wk 2 (WT)
Wk 2 (KO)
Wk 4.5 (WT)
Wk 4.5 (KO)
B
WT
KO
NeuN+ Cells / 0.1mm2 in DG
900
800
700
600
500
400
300
200
100
0
0
0.5
1
2
4.5
Weeks After KA Induced Seizure
C
WT
KO
NeuN+ Cells / 0.1mm2 in CA3a/b
300
250
200
150
100
50
0
*
**
*
0
0.5
1
2
4.5
Weeks After KA Induced Seizure

Figure 4.4

Conversely, in Cx32KO mice, the number of $NeuN^+$ cells in the CA3 pyramidal cell field was restored to control levels 4.5 weeks after seizure induction (Figure 4.4 *A,C*).

4.6.5 Cells found in the CA3 pyramidal cell field following kainate injury are not ectopic granule neurons

Previous studies have shown that new granule neurons are generated in the dentate gyrus following seizure and that some of these cells migrate and abnormally integrate into damaged pyramidal cell fields (Scharfman et al., 2000). To identify regenerated neurons, sections were double-labelled with NeuN and calbindin, a calcium-binding protein found primarily in granule cell neurons as well as in some gamma-aminobutyric acid (GABA)ergic interneurons of the pyramidal cell fields (Baimbridge, 1992; Sik et al., 1997). Both Cx32KO and WT mice exhibited the expected $calbindin^+$ mossy fibre projections from dentate gyrus granule neurons to CA3 pyramidal neurons at 0 and 4.5 weeks after kainate injection (Figure 4.5). $Calbindin^+$ neurons were identified in the granule cell layer of the dentate gyrus as well as in the stratum lucidum of both WT and Cx32KO mice 4.5 weeks post-seizure (Figure 4.5 *C,D*). Staining was found to be equivalent in localization and intensity to control animals (Figure 4.5, *A,B*). No ectopic calbindin staining was observed in the CA3 pyramidal cell field of either genotype 4.5 weeks following injury (Figure 4.5 *C,D*). Together, these data indicate that neuronal repopulation observed at this time point is not due to ectopic granule cell migration or to an aberrant increase in GABAergic interneurons. Instead, neurons observed in the CA3 region at this time point exhibited the characteristic morphology of pyramidal neurons, with nuclear size and localization comparable to control animals.

Figure 4.5. Cells found in the CA3a/b pyramidal cell field following kainate injury are not ectopic granule neurons. Abbreviations CA3 and DG are as defined in Figure 4.1; S.Rad., stratum radiatum; S.Lu., stratum lucidum. *A-D*) Control WT (*A*), Control Cx32KO (*B*), Wk 4.5 WT (*C*), and Wk 4.5 Cx32KO (*D*) hippocampal sections from different bregmas were labelled with NeuN (green) and calbindin (red). Photomicrographs depict sections from WT and Cx32KO animals exhibiting maximal regeneration 4.5 weeks post seizure. The frequency and distribution of calbindin$^+$ cells (red) is comparable between genotypes and across the kainic acid time course, indicating that the CA3a/b pyramidal cell field is not repopulated by ectopic granule neurons. Scale bars, 50 μm.

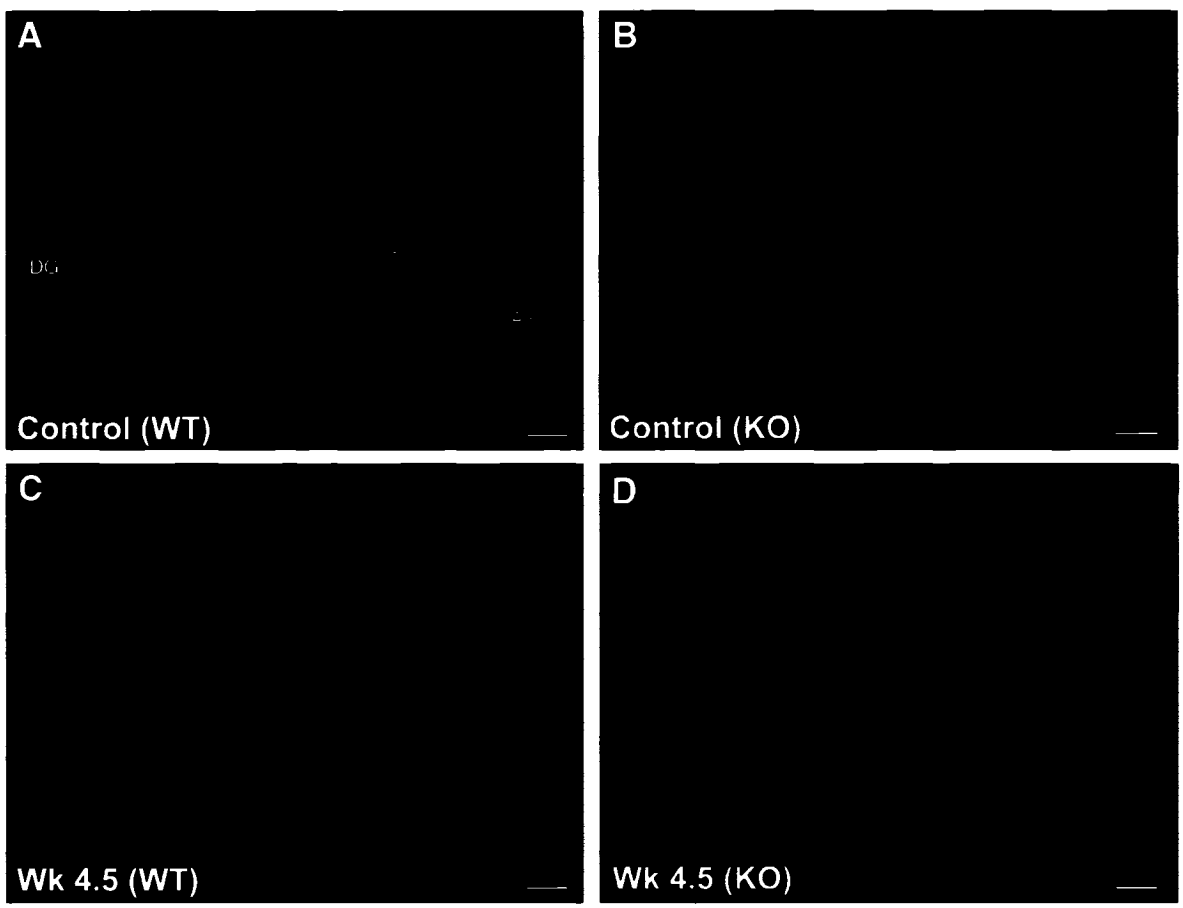
Calbindin (Cy3) / NeuN (FITC)
A
B
Control (WT)
Control (KO)
C
D
Wk 4.5 (WT)
Wk 4.5 (KO)

Figure 4.5

4.6.6 Parvalbumin-positive neurons are regenerated more effectively in Cx32KO than WT mice

To further determine the identity of the newly born neurons, sections from animals sacrificed 4-5 weeks post-seizure were labelled with parvalbumin, a calcium-binding protein found in basket and chandelier interneurons (Matyas et al., 2004; Figure 4.6). Previous literature has suggested that parvalbumin levels are greatly downregulated following kainic acid-induced seizure (Best et al., 1993). In control animals of both genotypes, an equivalent number of parvalbumin$^+$ interneurons was identified in the stratum lucidum and CA3 pyramidal layer (Figure 4.6 *A,B*). In injured WT mice, the number of parvalbumin$^+$ neurons as well as the overall intensity of the staining was greatly reduced (Figure 4.6 *C*). Conversely, in Cx32KO mice, the number of interneurons detected in the pyramidal layer was equivalent to controls (Figure 4.6 *D*). Furthermore, double-labelling for parvalbumin and NeuN revealed that the CA3 region of Cx32KO mice was more effectively repopulated than WT by both parvalbumin$^+$ interneurons as well as parvalbumin$^-$/NeuN$^+$ pyramidal neurons (Figure 4.6 *E,F*). These results demonstrate that both pyramidal neurons and interneurons of the CA3a/b pyramidal layer and stratum lucidum are regenerated to a greater extent in Cx32KO than WT animals following kainic acid-induced seizure.

4.6.7 Cx32-null mutation does not enhance kainic acid-induced progenitor cell proliferation

To determine whether the increase in NeuN$^+$ neurons in Cx32KO mice reflected increased neurogenesis or enhanced survival of newly born neurons relative to WT, we compared viable cell number, cell proliferation, cell specification, and survival of newly

Figure 4.6. Parvalbumin-positive interneurons are regenerated more effectively in Cx32KO than WT mice. Abbreviations are as defined in Figure 4.5. *A-D*) Control WT (*A*), Control Cx32KO (*B*), Wk 4.5 WT (*C*), and Wk 4.5 Cx32KO (*D*) hippocampal sections were labelled with parvalbumin for qualitative assessment. The number of parvalbumin$^+$ cells is comparable between control WT, control KO and Wk 4.5 KO animals, while it appears to be decreased in WT animals 4.5 weeks following injury (arrows). *E, F*) Adjacent Wk 4.5 WT (*E*) and Wk 4.5 Cx32KO (*F*) hippocampal sections were double-labelled with parvalbumin (red) and NeuN (green). Note that the Cx32KO CA3 region exhibits more parvalbumin$^+$ cells as well as more parvalbumin$^-$/NeuN$^+$ neurons than WT CA3 at the same time point. Scale bars, 50 μm,

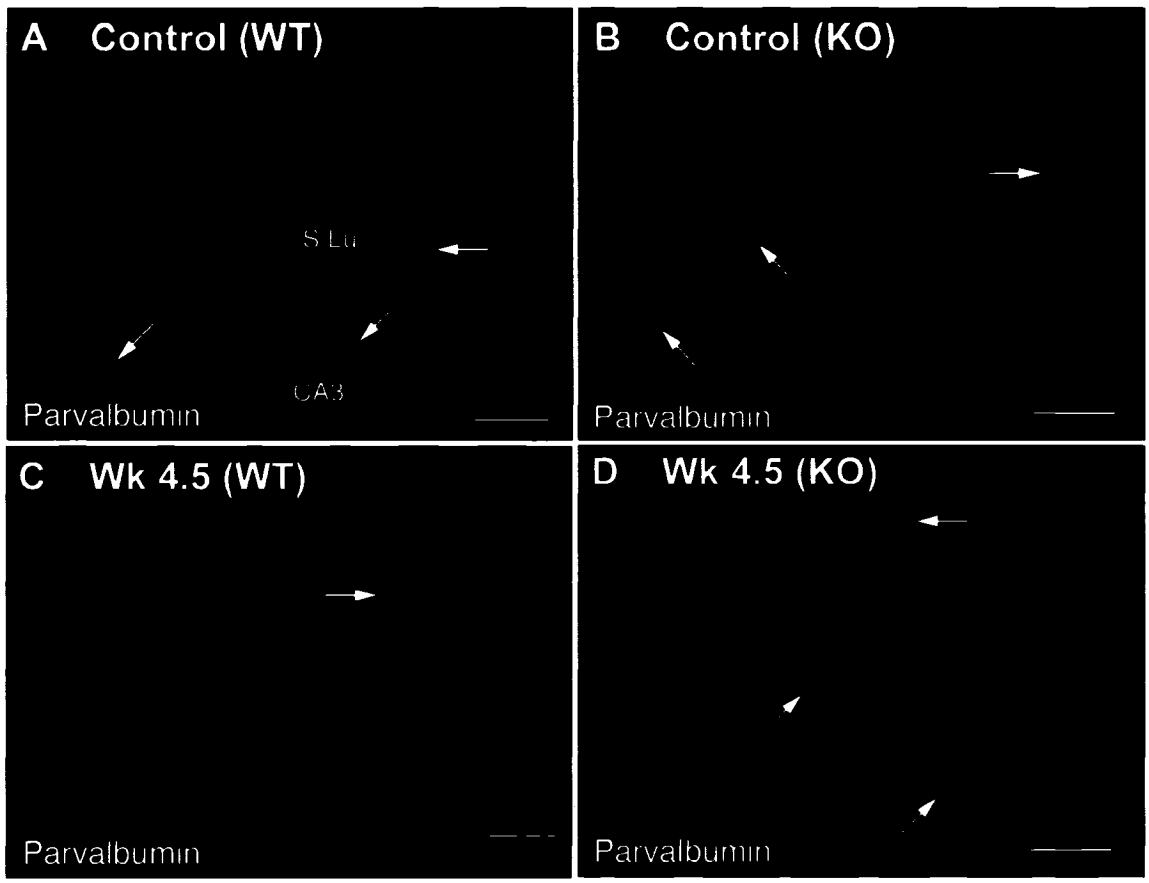

Parvalbumin (Cy3) / NeuN (FITC)

Figure 4.6

born cells in the dentate gyrus and the CA3 pyramidal cell field for up to 35 days following kainic acid-induced seizure. We first assessed whether the increase in neuronal number in Cx32-null mutant mice was due to enhanced expansion of endogenous progenitor cell populations following seizure, thereby providing more cells capable of neuronal specification and/or migration to the CA3a/b layer. To test this hypothesis, mice received 5 injections of BrdU over 3 days and were sacrificed 24 hours after the last injection at 0 (uninjured), 0.5, 1, 2, and 4 weeks following kainic acid administration. As described in Chapter 2, more proliferating cells were identified in the dentate gyrus of control (Wk 0) Cx32KO than WT mice (Figure 4.7 *A,B,E*; *$p<0.05$, MANOVA, *post hoc* Tukey test). In both WT and Cx32KO animals, cell proliferation in the dentate gyrus increased 0.5 and 1 week after the seizure, reaching statistical significance in WT but not Cx32KO mice at this later time point (Figure 4.7 *C-E*; **$p<0.01$, MANOVA, *post hoc* Tukey test). The number of proliferating cells decreased 2 and 4 weeks following the seizure in both genotypes, at which point it was comparable to uninjured WT animals (Figure 4.7 *E*). $BrdU^+$ cells localized to the SGZ and were NeuN, GFAP and F4/80 negative (Figure 4.7 *C, inset and data not shown*), indicating that they were not neurons undergoing DNA repair, proliferating astrocytes, or proliferating microglia. Thus, the increase in new neurons in Cx32KO mice cannot be attributed to enhanced expansion of activated cells in the SGZ. Instead, proliferating cells in Cx32KO animals may be less responsive to activation stimuli. These data are consistent with other unpublished findings from our laboratory that progenitors in SGZ of Cx32KO mice do not respond to voluntary wheel running or estrogen-induced proliferation (unpublished data).

Figure 4.7. Progenitor proliferation is increased in the dentate gyrus of WT and Cx32KO mice following kainic acid-induced seizure. Animals received 5 injections of BrdU at various time points following seizure and were sacrificed 3 to 24 hours following the last BrdU injection. Animal numbers are as defined in Figure 4.1. *A-D*) $BrdU^+$ proliferating cells (green) were detected by immunolabelling in the DG of WT and Cx32KO animals 0 (*A, B*) and 1 (*C, D*) week following seizure. The granule cell layer of the DG was stained with anti-NeuN (red). Scale bars, 50 μm. Inset demonstrates that the majority of $BrdU^+$ cells were GFAP- (red) and NeuN- (blue) negative. *E*) $BrdU^+$ cells were quantitated in dentate gyrus sections from WT and Cx32KO mice sacrificed 0, 0.5, 1, 2, or 4 weeks following injury and expressed as the number of $BrdU^+$ cells in the DG ± SEM per $0.1mm^2$. Note that the number of $BrdU^+$ cells peaks in both genotypes 1 week post seizure, although this increase is only statistically significant for WT mice (**$p<0.01$, MANOVA, *post hoc* Tukey).

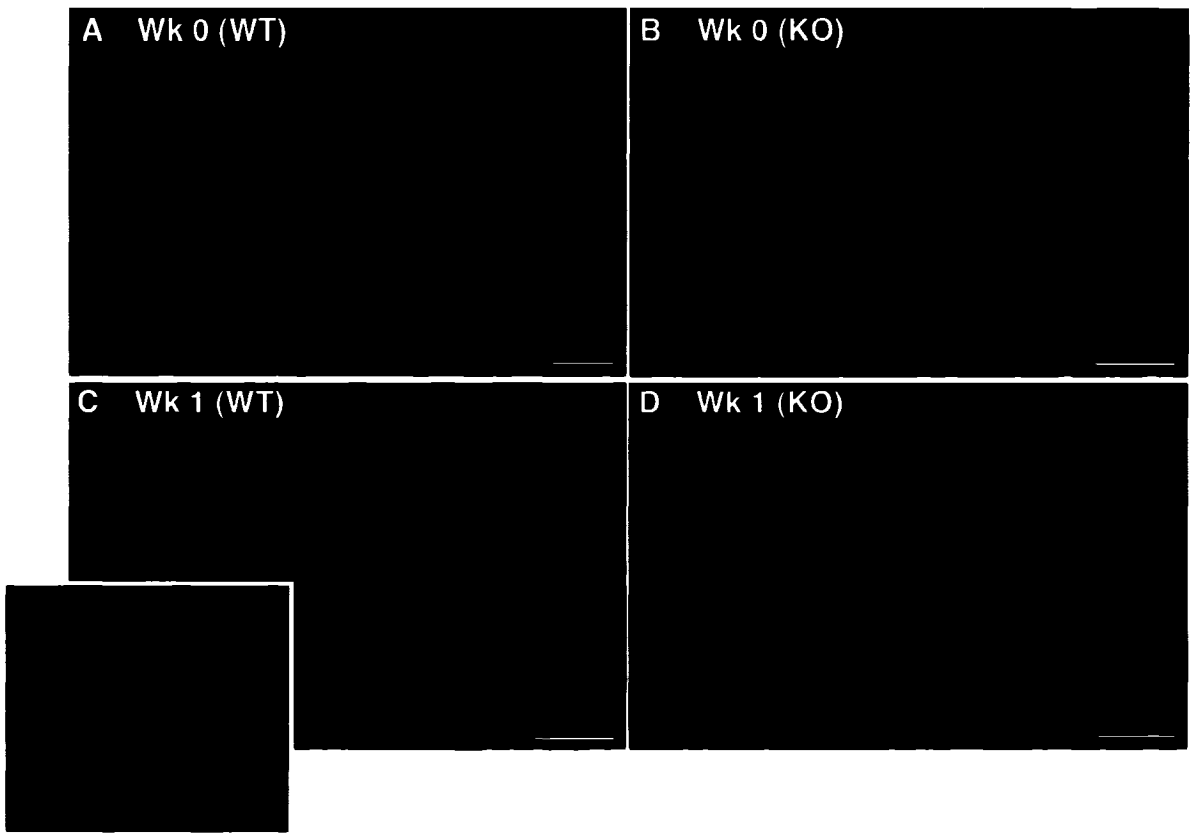
A Wk 0 (WT)
B Wk 0 (KO)
C Wk 1 (WT)
D Wk 1 (KO)

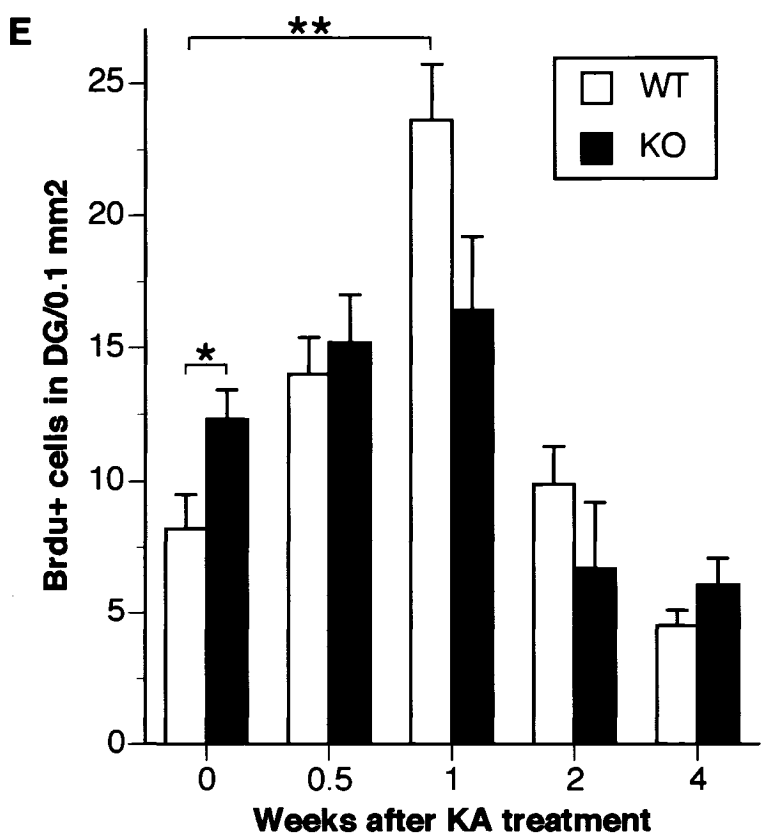
E
**
*
WT
KO
Brdu+ cells in DG/0.1 mm2
0
5
10
15
20
25
0
0.5
1
2
4
Weeks after KA treatment

Figure 4.7

4.6.8 Neurogenesis and gliogenesis in the dentate gyrus of WT and Cx32KO mice

Alternatively, neuronal replacement observed in Cx32KO mice 4.5 weeks after seizure could be due to improved long-term survival and/or specification of progenitor cells activated 1 week post-seizure. In previous reports, some $BrdU^+$ cells labelled 1 week post-seizure were found to become $NeuN^+$ neurons, 5 weeks after hippocampal injury (Yoshimura et al., 2001). To identify changes in progenitor cell fate in WT and Cx32KO mice, we followed the survival and specification of cells labelled with BrdU at the peak proliferative period 1 week after seizure induction (Figure 4.8 *A*). A small proportion of cells labelled 1 week after seizure induction were found to survive 4 weeks later (5 weeks after the seizure) in the dentate gyrus of both WT and Cx32KO mice (Figure 4.8 *C, 14-32% survival*). Lineage analysis was performed by double-labelling to determine whether the BrdU-labelled progenitors had differentiated to mature neurons ($NeuN^{+}$), astrocytes ($GFAP^+$), or oligodendrocytes ($CNPase^+$) (Figure 4.8 *D*). As a control, immunofluorescence was also performed on uninjured mice, as well as WT and Cx32KO animals sacrificed 24 h after the last BrdU injection (Figure 4.8 *B, Wk 1*). This control allowed us to confirm that BrdU double-labelled cells were the differentiated progeny of progenitor cells and not terminally differentiated cells undergoing DNA repair. Low levels of oligodendrogenesis and astrogliosis were observed in the dentate gyrus of WT and Cx32KO mice 5 weeks post-seizure (Figure 4.8 *D*). However, these levels were comparable to uninjured controls (data not shown). Conversely, 50% of all surviving BrdU-labelled progenitors were found to differentiate to a neuronal phenotype 5 weeks after seizure induction in both genotypes (Figure 4.8 *D*). We did not detect significant BrdU incorporation in terminally differentiated neurons or glia when animals were sacrificed 24 h after the last injection 1 wk after seizure.

Figure 4.8. Progenitor specification in the dentate gyrus of WT and Cx32KO mice is comparable 5 weeks following kainic acid-induced seizure. Animal numbers are as defined in Figure 4.1. *A*) Diagram showing methodology for the following experiments. Progenitors were labelled with BrdU on days 6, 7, and 8 following seizure and WT and Cx32KO mice were sacrificed 24 hours or 28 days after the last BrdU injection (week 1 or week 5 post-seizure*). B*) $BrdU^+$ cells were detected in dentate gyrus sections from WT and Cx32KO animals sacrificed 1 week post-seizure (24 hours after BrdU labelling). The identity of the proliferating cells was determined by co-immunolabelling with BrdU (green) and GFAP (astrocytes), CNPase (oligodendrocytes), or NeuN (neurons; red). Scale bars, 50 μm. *C*) To assess the survival of BrdU-labelled proliferating cells, the number of $BrdU^+$ cells was counted 5 weeks post-seizure (28 days after BrdU labelling). Survival of $BrdU^+$ cells is equivalent between genotypes. *D*) Specification of surviving $BrdU^+$ was established by quantitation of cells immunoreactive for BrdU and a marker of terminal differentiation (GFAP, CNPase, or NeuN). Data are expressed as percentage of BrdU double-positive cells in the dentate gyrus ± SEM. In both genotypes, 50% of BrdU-labelled progenitors differentiate to a neuronal phenotype 5 weeks after seizure induction.

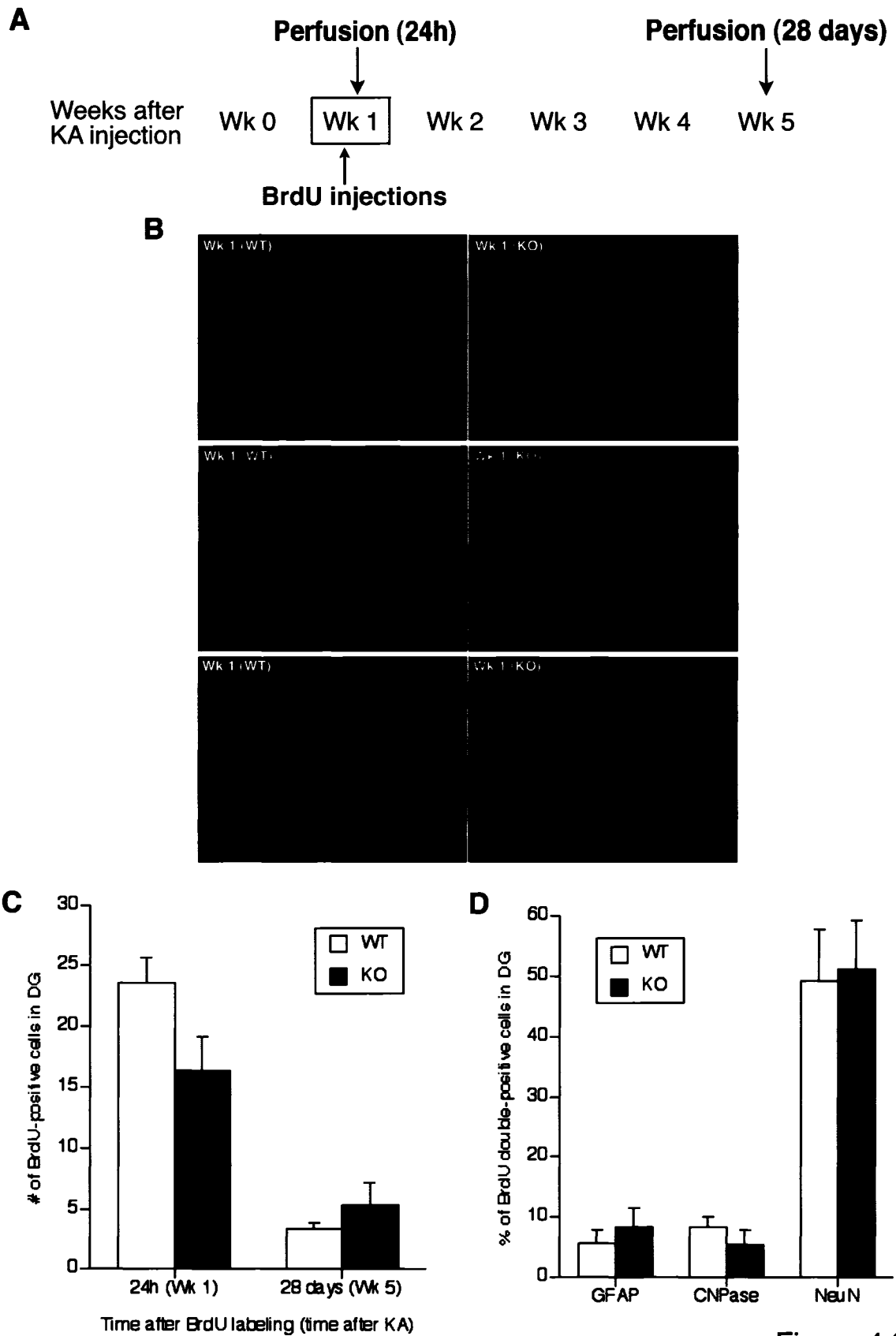
A
Perfusion (24h)
Perfusion (28 days)
Weeks after KA injection
Wk 0
Wk 1
Wk 2
Wk 3
Wk 4
Wk 5
BrdU injections
B
C
# of BrdU-positive cells in DG
WT
KO
24h (Wk 1)
28 days (Wk 5)
Time after BrdU labeling (time after KA)
D
% of BrdU double-positive cells in DG
GFAP
CNPase
NeuN

Figure 4.8

Thus, although neurogenesis was observed in the dentate gyrus of both WT and Cx32KO mice 5 weeks after kainate injection, there was no difference between genotypes in the degree of specification of progenitors labelled 1 week post-seizure.

4.6.9 Progenitor proliferation and gliogenesis in the CA3 region of WT and Cx32KO mice

In addition to mobilizing SGZ progenitor populations, seizure activity has also been shown to activate putatively dormant progenitor cells in the pyramidal cell layers of the hippocampus (Dong et al 2003). To identify these cells, we labelled proliferating cells with BrdU at 0.5, 1, 2, and 4 weeks after kainic acid administration (Figure 4.9). Some sections were double-labelled with GFAP or F4/80 to detect activated astroyctes and microglia. Quantification revealed consistently low levels of $BrdU^+$ cells in the CA3 region of both WT and Cx32KO mice, with the exception of 0.5 week after the seizure, when a significant and transient increase in BrdU labelling was detected (Figure 4.9 *A*; $^{**}p<0.01$, MANOVA, *post hoc* Tukey test). Double-labelling revealed high levels of astrogliosis throughout the hippocampus, notably in the stratum lucidum and stratum radiatum of WT and Cx32KO animals, 0.5 week following injury (Figure 4.9 *B, arrows*; 4.10 *A*). However, most of the $BrdU^+$ cells found in the damaged CA3a/b pyramidal layer were GFAP and F4/80 negative (Figure 4.9 *B,C*; 4.10 *A,B*). Adjacent sections were further labelled with NG2 to identify proliferating glial progenitors. High levels of proliferating glial progenitors were observed in the stratum oriens, stratum lucidum, and stratum radiatum of WT and Cx32KO mice (Figure 4.9 *D,E*; 4.10 *C*). Furthermore, the majority of $BrdU^+$ cells in the CA3a/b pyramidal cell layer were $NG2^+$ progenitor cells indicating that a large part of the transient

Figure 4.9. Progenitor proliferation in the CA3 pyramidal cell field of WT and Cx32KO mice is increased 0.5 week following kainate injury. Animal numbers are as defined in Figure 4.1. Abbreviations are as defined in Figure 4.5 and S.O., stratum oriens. *A*) BrdU was administered at various time points following seizure and WT and Cx32KO animals were sacrificed 3 to 24 hours following the last BrdU injection. *A*) $BrdU^+$ cells were quantitated in the CA3a/b pyramidal cell field of WT and Cx32KO animals sacrificed 0, 0.5, 1, 2, or 4 weeks following injury. Note that the number of $BrdU^+$ cells peaks in both WT and Cx32KO mice 0.5 week after seizure (**$p<0.01$, MANOVA, *post hoc* Tukey). *B-E*) To establish the identity of the $BrdU^+$ cells observed 0.5 week post seizure, sections were double-labelled with NeuN (neurons; blue) and GFAP (astrocytes; red; *B, C*), or NG2 (glial progenitors; red; *D, E*). Note that $BrdU^+$ astrocytes are detected in both genotypes (arrows) in the stratum oriens, stratum radiatum, and molecular layer of the hippocampus, but that no $BrdU^+$ neurons are found in either genotype (*B, C*). Proliferating $NG2^+$ progenitors are detected in both genotypes throughout the CA3 pyramidal cell field, stratum oriens and stratum radiatum (arrows; *D, E*). Scale bars, 50 μm.

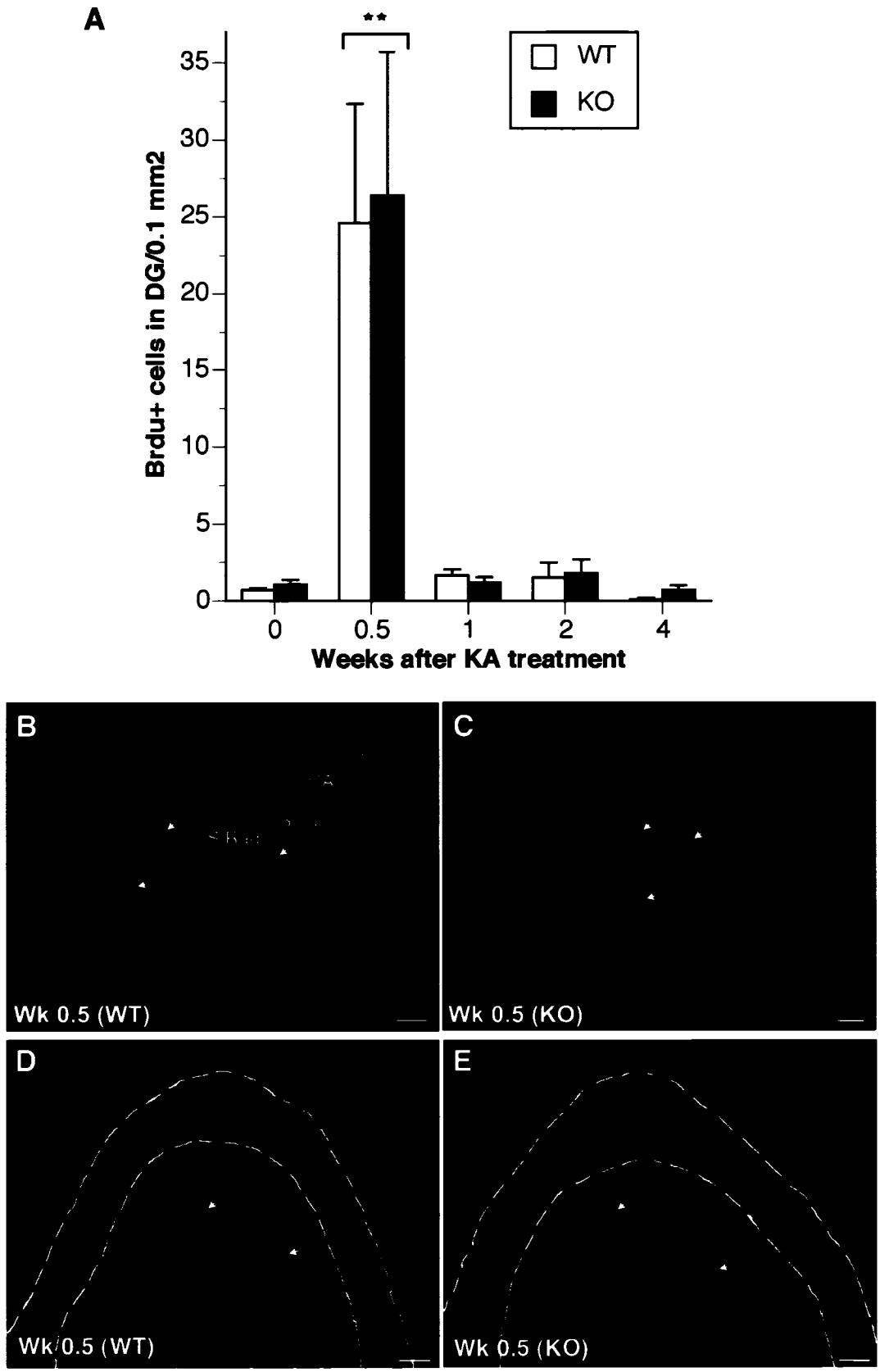
A
**
WT
KO
Brdu+ cells in DG/0.1 mm2
35
30
25
20
15
10
5
0
0
0.5
1
2
4
Weeks after KA treatment
B
Wk 0.5 (WT)
C
Wk 0.5 (KO)
D
Wk 0.5 (WT)
E
Wk 0.5 (KO)

Figure 4.9

Figure 4.10. $NG2^+$ progenitors are mobilized in both WT and Cx32KO CA3a/b pyramidal layer 0.5 week following kainic acid-induced seizure. Abbreviations CA1, 2, 3a, 3b, 3c pyramidal cell field; GrDG, granule cell layer of the dentate gyrus; SGZ, subgranular zone; Sr, stratum radiatum; slu, stratum lucidum; so, stratum oriens. Location of digital micrographs is indicated by the box in the each schematic. A) Triple immunodetection of BrdU (green), NeuN (blue), and GFAP (red) in WT (*A1*) and Cx32 KO (*A2*) mice injected with BrdU 0.5 week after seizure. Arrowheads point to representative $BrdU^+/GFAP^+$ astrocytes. Arrows point to representative injured neurons exhibiting nuclear vacuolization and localization of NeuN to the periphery of damaged nuclei. Note that BrdU-labelled nuclei do not colocalize with damaged $NeuN^+$ neuronal nuclei in both WT and Cx32KO mice (*Insets A1' and A2'*). *B*) Triple immunodetection of BrdU (blue), NeuN (green), and F4/80 (red) in WT (*B1*) and Cx32KO (*B2*) 0.5 week after seizure. Red arrows point to representative $F4/80^+$ microglia. White arrows point to representative injured neurons exhibiting nuclear vacuolization and localization of NeuN to the periphery of damaged nuclei. Note numerous $F4/80^+$ microglia in close proximity to damaged neurons but only a minority of $BrdU^+$ cells in the CA3a/b pyramidal layer identified as proliferating $F4/80^+$ microglia (*Insets B1'* and *B2'*). *C*) Double immunolabelling for BrdU (green) and NG2 (red) 0.5 week after seizure in WT (*C1*) and Cx32KO (*C2*) mice. White dotted lines indicate the boundary of the CA3a/b pyramidal layer. Yellow arrowheads indicate representative $BrdU^+/NG2^+$ progenitor cells. A substantial increase in proliferating $NG2^+$ progenitors was detected in the stratum oriens, CA3 pyramidal cell fields, stratum lucidum, and stratum radiatum. Scale bars in *A, B*, 100 μm; Insets *A, B*, 50 μm; *C*, 50 μm.

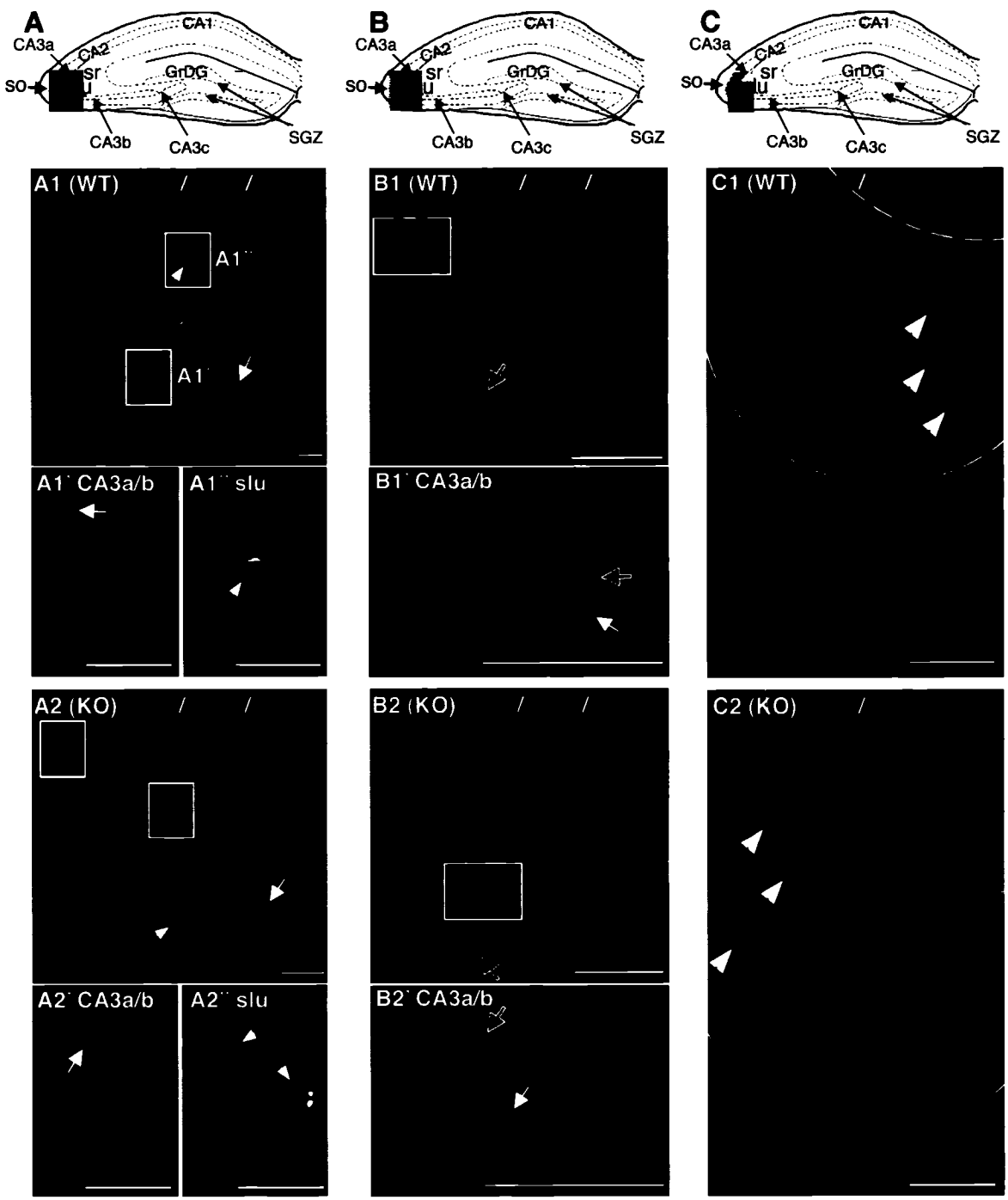
A
CA3a
CA2
CA1
SO
Sr
u
GrDG
CA3b
CA3c
SGZ
B
CA3a
CA2
CA1
SO
Sr
u
GrDG
CA3b
CA3c
SGZ
C
CA3a
CA2
CA1
SO
Sr
u
GrDG
CA3b
CA3c
SGZ
A1 (WT)
A1''
A1'
A1' CA3a/b
A1'' slu
B1 (WT)
B1' CA3a/b
C1 (WT)
A2 (KO)
A2' CA3a/b
A2'' slu
B2 (KO)
B2' CA3a/b
C2 (KO)

Figure 4.10

increase of actively dividing cells observed at this time point can be attributed to glial/early oligodendrocyte progenitor proliferation (Figure 4.9 *D,E*; 4.10 *C*). Taken together, these results demonstrate that kainic acid-induced seizures induce *de novo* proliferation of $NG2^+$ progenitors in the CA3 pyramidal cell field.

These data suggest that progenitors activated 1 week post-seizure in the SGZ do not contribute significantly to neuronal replacement in the CA3a/b pyramidal cell field. However, in the absence of Cx32, $NG2^+$ progenitors activated 0.5 week after kainate injury appear to be more responsive to neurogenic stimuli and are likely responsible for the enhanced neuronal replacement observed in Cx32KO mice. Data generated by my colleagues in the Bennett laboratory further supporting this hypothesis are discussed briefly in the discussion portion of this chapter.

4.7 Discussion

4.7.1 Strain differences in kainic acid sensitivity are abrogated in congenic WT and Cx32KO mice

In this study, we show that, following hippocampal damage, the CA3a/b pyramidal layer is regenerated more efficiently in the absence of Cx32. We first established that Cx32KO and WT mice exhibit the same seizure susceptibility and intensity following kainic acid administration. Previous studies have suggested that, although C57BL/6 mice exhibit a high seizure severity score and a low behavioural sensitivity (lower dose required to trigger seizure), they are less susceptible to cell loss than BALB/c, 129/Ola, and DBA/2J strains (Ferraro et al., 1995; McKhann et al., 2003; Royle et al., 1999) and do not develop mossy fiber sprouting following a seizure as observed in rats and 129/SvEMS mice (Cantallops

and Routtenberg, 2000; Schauwecker et al., 2000). However, a recent study by Benkovic *et al.* reported that, when using more sensitive indicators of injury such as fluorojade B and cupric-Silver, significant neuronal damage and reactive astrogliosis were observed throughout the hippocampus of adult C57BL/6J animals (Benkovic et al., 2004). In that study, marked cellular loss was consistently observed in the CA3 pyramidal cell field of all C57BL/6 mice. Pyknosis and loss of cell viability were accompanied by the presence of vacuoles. Our study is consistent with these findings and previous reports that maximal damage was observed in the CA3a/b > CA3c > CA1 > CA2 > dentate gyrus regions (Benkovic et al., 2004; Pollard et al., 1994). Here, we show that by backbreeding mixed strain null mutant mice into a 99.95% C57BL/6 background we can recapitulate this injury in our congenic WT and Cx32KO animals.

4.7.2 Neuroregeneration is more effective in the absence of Cx32

Following kainic acid-induced seizure, the most extensive damage has consistently been observed in the hippocampal formation (Strain and Tasker, 1991). In the present study, TUNEL assay, fluorojade staining, and NeuN immunodetection revealed that, up until 4.5 weeks following seizure, no cell loss is observed in the dentate gyrus of mice from either genotype. Conversely, the CA3 pyramidal layer exhibited significant damage, with a 50% reduction in viable cell number measured 0.5 week after the injury. WT and Cx32KO mice exhibited similar kinetics of excitotoxic cell death, as determined by fluorojade, cresyl violet, H&E, and MGPY stainings, as well as TUNEL assays. However, 4.5 weeks following the seizure, MGPY staining revealed a significant difference between genotypes.

While the number of viable cells remained significantly reduced in WT mice, it was restored to control levels in Cx32KO animals.

Immunodetection of mature neurons using the NeuN marker confirmed that neuronal regeneration was more effective in Cx32-null mutant mice. Consistent with other studies, mature neurons were partially regenerated in the WT CA3 region 4.5 weeks post-seizure, although this number remained significantly lower than the neuronal population observed in WT control animals (Dong et al., 2003; Parent et al., 1997). By contrast, in Cx32KO mice, near complete regeneration of neuronal numbers was observed in the CA3 pyramidal layer. Scharfman *et al.* had previously suggested that the partial repopulation observed in the CA3c region was due to aberrantly expressed granule neurons rather than pyramidal cells generated from activated SGZ progenitor cells (Scharfman et al., 2000). Immunodetection of the granule cell marker calbindin confirmed that few ectopic granule cells were introduced in the CA3c pyramidal layer of both WT and Cx32KO mice 4.5 weeks post-seizure. Cells detected in the CA3 pyramidal layer at this time point were similar in size and location to those observed in control animals, including parvalbumin$^+$ interneurons. Taken together, these results strongly suggest that both interneurons and pyramidal neurons are regenerated more efficiently in the absence of Cx32 following kainate-induced seizure.

The precise mechanisms by which a Cx32-null mutation alters neuronal regeneration remain to be elucidated. Cx32 is an oligodendrocyte connexin expressed early in the oligodendrocyte lineage and, as such, is likely to influence terminally differentiated "instructive" oligodendrocyte populations and/or NG2$^+$ progenitor cells (Belliveau et al., 1991; Melanson-Drapeau et al., 2003; Scherer et al., 1995). My colleague in the Bennett laboratory, Mario Morin, has shown as part of his M.Sc. thesis that Cx32 levels increase in

the CA3a/b layer 0.5 week after seizure, localizing to $NG2^+$ progenitors. Thus, it is likely that Cx32 expression directly impacts on the fate of these progenitors. Although unlikely, we cannot definitively discount a minority of reports that Cx32 may be expressed by rare neuronal subtypes within the hippocampus. While Cx32 is found in GABAergic striatal neurons and all reports agree that it is not found in pyramidal neurons, it has been suggested by some to be expressed by GABAergic interneurons of the hippocampus (Oguro et al., 2001; Venance et al., 2004). $Parvalbumin^+$ interneurons are more sensitive to injury such as kainic acid lesion than $calbindin^+$ interneurons (Sanon et al., 2005; Strain and Tasker, 1991; Waldvogel et al., 1991), with losses of 71 to 97% of parvalbumin-immunopositive neurons within 4 weeks following kainate administration (Best et al., 1993; Best et al., 1994; Dong et al., 2003). This loss was qualitatively observed in the present study in WT mice. Cx32 expression by interneurons could therefore be detrimental and lead to cell loss as described below. However, since both interneurons and pyramidal cells appear to be regenerated to the same extent in the Cx32KO mice and Cx32 is generally accepted not to be expressed by pyramidal neurons, it is unlikely that the effects of Cx32 are mediated by its putative neuronal expression.

Instead, we propose two possible mechanisms of Cx32-mediated control of neural progenitor fate and/or of the survival of newly born neurons. First, neuronal regeneration and/or survival could be an indirect effect of Cx32 expression by oligodendrocytes. This possibility will be discussed further in "4.7.4 Connexins and cell death." Alternatively, enhanced neuronal specification of hippocampal progenitors in the absence of Cx32 could also account for the more efficient neuronal repopulation observed in these mice as discussed in "4.7.3 Origin of newly born cells".

4.7.3 Origin of newly born cells

Pilocarpine- and kainic acid-induced seizures both result in a dramatic increase in levels of proliferating $BrdU^+$ cells, followed by specification to the neuronal lineage and insertion into the granule cell layer (Gray and Sundstrom, 1998; Parent et al., 1997; Yoshimura et al., 2001). $Calbindin^+$ granule cells were shown to repopulate the hilus, migrating as far as the CA3c cell layer and developing synchronous activity with neighboring pyramidal neurons, while retaining similar granule cell morphological, neurochemical, and electrophysiological properties (Parent et al., 1997; Scharfman et al., 2000; Wang et al., 2004). More recently, increased neurogenesis was also demonstrated in the CA3b region of neonatal rats, resulting in the partial regeneration of the damaged CA3 pyramidal cell field (Dong et al., 2003). It was further shown that hippocampal neurodegeneration is not necessary to stimulate progenitor proliferation (Nakagawa et al., 2000) and that aged rodents retain the same capacity for seizure-induced neurogenesis than younger animals (Gray et al., 2002). Although progenitor proliferation has been well characterized, the precise mechanisms by which cells are instructed to follow a specific fate remain to be elucidated. In this study, BrdU labelling of proliferating progenitors revealed an increased proliferation in the dentate gyrus of WT animals 1 week post-seizure that correlates with previous observations documented in the literature (Gray and Sundstrom, 1998; Yoshimura et al., 2001). In Cx32KO animals however, the increase in progenitor proliferation was not significant at any time point following injury.

Cx32 may be expressed by committed oligodendrocyte progenitors that cannot be induced to a different cell lineage. As such, there would be no difference in neuronal regeneration between Cx32KO and WT mice. However, in the CA3 pyramidal cell field,

analysis of $NeuN^+$ cells revealed that neuronal number is increased in Cx32KO mice relative to WT, 4.5 weeks after seizure. Further results demonstrated that this enhanced regenerative capacity is not the result of a) enhanced proliferative responsiveness to kainate seizure in the absence of Cx32KO (Figure 4.7 & 4.9) or b) enhanced specification to a neuronal lineage in cells activated 1 week after seizure in the Cx32KO (Figure 4.8). Thus, we suggest that 1) $NG2^+$ progenitors in the CA3 specify to a greater extent to neurons in the absence of Cx32 and/or 2) newly born neurons survive to a greater extent in the absence of Cx32.

$NG2^+$ progenitors are typically characterized as glial progenitors destined to specify to an oligodendrocyte phenotype (Levine et al., 1993; Yang et al., 2005). However, experiments published by Kondo and Raff first demonstrated that, when cultured *in vitro*, putative oligodendrocyte progenitors could be differentiated towards a neuronal lineage if exposed to neurogenic stimuli (Kondo and Raff, 2000). Furthermore, when transplanted into mouse lateral ventricule, $NG2^+$ progenitors were found to migrate to the olfactory bulb and give rise to populations of oligodendrocytes as well as interneurons (Aguirre and Gallo, 2004). More recently, Belachew *et al.* demonstrated that postnatal $NG2^+$ progenitors are, in fact, multipotent, with a subset of hippocampal $NG2^+$ progenitors giving rise to functional GABAergic interneurons (Belachew et al., 2003). Oligodendrocyte progenitors were also shown to survive and retain the ability to proliferate following neurotoxic treatment (Dzwonek, 2005). In our model, high levels of proliferating $NG2^+/BrdU^+$ progenitors were observed in the WT and Cx32KO CA3 region 0.5 week post-seizure (Figure 4.9). In order to provide further mechanistic insight into the enhanced neuroregeneration observed in Cx32KO mice, experiments were undertaken by our laboratory in which BrdU was

administered 0.5 week post-seizure (instead of 1 week after seizure) to label the peak of proliferating cells observed in the CA3 region at this time point. Neurogenesis and gliogenesis were then assessed 28 days later. Results from these experiments confirmed that a higher percentage of $NG2^+$ cells labelled 0.5 week after seizure survive 28 days later in the Cx32KO CA3 pyramidal cell field. Moreover, these cells specify more efficiently to neurons in the absence of Cx32, at the expense of oligodendrogenesis, resulting in the complete neuronal repopulation observed in the Cx32KO mouse.

4.7.4 Connexins and cell death

An alternative explanation is that, in the absence of Cx32, neurogenesis may not be altered, but rather survival of newly born neurons may be enhanced. TUNEL assays and fluorojade stainings revealed a difference between genotypes in the levels of cell death observed in the CA3 region 4.5 weeks post-seizure (Figure 4.3). Elevated levels of cell death were seen in the WT CA3 region, whereas the apoptotic index remained low in Cx32KO mice. This finding implies that Cx32 might play a role in cell death yet are discongruent with the repeated observation that Cx32 is not expressed by newly born or mature neurons.

Gap junctions can mediate cell death by spreading stress signals and/or toxic metabolites. Direct evidence for the propagation of damage through gap junctions was provided using alpha-particle radiation, implicating Cx43 in the transmission of damage signals to nonirradiated cells (Azzam et al., 2001). Following cerebral infarct, surrounding tissue is progressively recruited into the infarct. This propagation of injury termed 'bystander death' occurs through apoptotic cell death. For example, when cells engineered

to resist injury by Bcl2 overexpression were co-cultured with other Cx43-expressing C6 glioma cells, they became vulnerable to oxidative stress, calcium overload, and metabolic inhibition (Lin et al., 1998). Furthermore, bystander cell death was shown to be directly related to the extent of connexin expression and intercellular coupling (Lin et al., 1998). Various gap junction blockers such as octanol, heptanol, and halothane were shown to reduce infarct volume and to limit necrosis in myocardial cells following myocardial ischemia (Garcia-Dorado et al., 1997; Rawanduzy et al., 1997; Saito et al., 1997). This transmission of toxicity to neighbouring cells was further observed in cells treated with ganciclovir, a drug currently used in cancer treatment. The extent of apoptotic cell death in adjacent cells was found to depend on the identity of the connexin and its degree of expression in transfectants.

Since Cx32 is predominantly expressed by oligodendrocytes and a subset of $NG2^+$ progenitor cells in the hippocampus, its role in mediating neuronal cell death would be indirect. Glia such as astrocytes and oligodendrocytes have recently been suggested to form a glial network whose primary function would be to maintain tissue homeostasis during axonal activity (Theis et al., 2005). According to this hypothesis, potassium ions as well as glutamate secreted by neurons would be taken up by oligodendrocytes and would then diffuse to neighboring astrocytes through gap junctions, thereby maintaining ionic levels and protecting surrounding neurons. This function is referred to as "spatial buffering" (Sohl et al., 2004). Heterocellular glial junctions have been extensively demonstrated, with astrocytic Cx26 and oligodendroglial Cx32 forming a key pair (Altevogt and Paul, 2004). Furthermore, as reviewed in Chapter 1, a subset of connexins has been demonstrated to form hemichannels, connexons linking the cell's cytoplasm to the extracellular milieu. For

example, astrocytic hemichannels have been shown to mediate ATP and glutamate release (Ye et al., 2003). Since Cx32 is the preponderant connexin expressed by oligodendrocytes and Cx32 hemichannels have been shown to be functional *in vitro* (Boucher and Bennett, 2003), it is reasonable to assume that they could occur *in vivo*, in rodent hippocampus. An enhanced number of hemichannels or an increase in the proportion of these channels found in the open state could potentially lead to the loss of crucial molecules such as sodium or calcium ions, inositol 1,4,5-trisphosphate (IP_3), glucose, and ATP, resulting in cell death (reviewed in De Maio et al., 2002). Such an increase in open channels is known to occur in metabolically inhibited cells (Saez et al., 2003). Therefore, following seizure, an increased number of open Cx32 hemichannels might lead to altered spatial buffering, causing elevated extracellular ion levels and resulting in neuronal toxicity and death.

Chapter 5: Connexin32 ectopic expression reduces hippocampal progenitor cell specification towards a neuronal lineage *in vitro*

5.1 Objectives

In chapter 2, I established that Cx32 is expressed when a subset of $NG2^+$ progenitor cells commit to an early oligodendroctye lineage in uninjured mice. In chapter 4, I showed that Cx32-null mutation promotes more effective neurogenesis from $NG2^+$ progenitor cells activated in the CA3a/b pyramidal zone following excitoxoic injury. This increase in neuronal specification from $NG2^+$ progenitor cells in the absence of Cx32 could be due to cell-autonomous effects of Cx32 on neural progenitor fate and/or altered capacity of $NG2^+$ cells to communicate through gap junctional intercellular communication with neighbouring instructive cells. This chapter involves two specific objectives aimed at providing mechanistic insight into whether Cx32 elicits cell-autonomous control on the fate of hippocampal progenitors: **(1)** establish the specification potential of primary progenitor cells isolated from neonatal WT and Cx32KO hippocampal formation and **(2)** determine whether Cx32 gain of function (ectoptic expression) alters specification of these neurosphere-forming cells.

5.2 Statement of collaborator contributions

I performed all of the studies reported in this chapter with the exception of the immunocytochemistry, reverse transcription-polymerase chain reaction (RT-PCR), and Western analysis of Cx32 expression in neurospheres (Figure 5.1). These analyses were performed by Lianne Gauvin as part of her M.Sc. studies. I confirmed lack of Cx32 expression in WT neurospheres following plating by immunocytochemistry.

5.3 Abstract

Primary cultures of progenitor cells obtained from both WT and Cx32KO postnatal day 2 (P2) hippocampi were expanded for 8 days as neurospheres to assess proliferative indices. Neurospheres were then plated on an adhesive substrate and the spontaneous specification potential of these progenitor cells was determined by antigenic lineage analysis. Consistent with the *in vivo* Cx32 expression pattern, P2 WT neurospheres did not express Cx32. Some progenitors expanded as neurospheres were infected at the time of plating with a Cx32 and green fluorescent protein (GFP)-containing adenovirus or an adenovirus containing GFP alone, as a control. The percentage of specification to each lineage (neuron, astrocyte, and oligodendrocyte) of these infected cells was assessed. Ectopic expression of Cx32 enhanced the number of $NG2^+$ progenitors and reduced the number of $TuJ1^+$ immature neurons observed over the course of spontaneous specification. These results further implicate Cx32-mediated signaling in promoting oligodendrocyte specification.

5.4 Introduction

Gap junctional coupling has been implicated in epidermis, keratinocyte, as well as pulmonary alveolar cell differentiation (Brissette et al., 1994; Isakson et al., 2001a; Isakson et al., 2001b; Risek et al., 1994). Recent evidence has also implicated cell-autonomous connexin-mediated communication in regulating neural progenitor specification to neuronal or glial lineages in the absence of instructive cell partners. For example, terminal differentiation of neural precursor cells into neurons or glia is reduced by pharmacological inhibitors of gap junctions and hemichannels, suggesting an important role for intercellular communication between neural precursors themselves and/or functional hemichannel activitiy (Bani-Yaghoub et al., 1999; Boucher and Bennett, 2003). Found in early progenitor populations committed to an oligodendrocyte lineage (Melanson-Drapeau et al., 2003), the kinetics of Cx32 expression correspond to differentiation of myelinating glial cells (Parnavelas et al., 1983). In previous experiments (Chapter 2), we observed a block in progenitor specification towards the oligodendrocytic lineage, in the absence of Cx32. However the molecular mechanisms underlying the role of Cx32 in oligodendrocyte differentiation have yet to be investigated

During embryogenesis, gap junctions have been suggested to provide intercellular pathways for the diffusion of mitogens, morphogens, and other developmentally relevant factors such as calcium (Caveney, 1985). Recent literature has demonstrated that environment dictates stem cell fate and the resulting proportion of neurogenesis and gliogenesis (Lim and Alvarez-Buylla, 1999; Song et al., 2002). Furthermore, channels formed by different connexons may possess different biophysical properties, favouring the passage of different molecules. Cx32 has been shown to form functional hemichannels

(Boucher and Bennett, 2003; Gomez-Hernandez et al., 2003). Signals exchanged between cells and the extracellular milieu could therefore dictate cell specification. Conversely, direct contact between progenitor cells was also shown to influence their specification (Caldwell et al., 2001), suggesting a possible role for progenitor-progenitor gap junctional communication. The goal of these experiments was to provide mechanistic insight into the regulatory mechanisms of Cx32-mediated communication.

5.5 Materials and methods

5.5.1 Tissue dissociation and neurosphere assay

P2 mice were euthanized with sodium pentobarbital, in accordance with procedures approved by the University of Ottawa Animal Care department. Brains were removed and placed in ice-cold artificial cerebrospinal fluid (aCSF). Using a vibratome (Leica), 500 μm sections were cut and every section from Bregma – 0.9 mm to Bregma –3.0 mm was collected. Under a dissecting microscope, hippocampi were dissected using surgical instruments and placed in clean aCSF. Tissue was dissociated by incubation at 37°C with a mixture of papain (0.01%), DNAse (0.01%) and neutral protease (0.1%) in Dissociation Media for 45 minutes. Enzymes were inactivated by adding 5 mL PBS, followed by centrifugation at 1500 rpm for 5 minutes. Cells were then washed in 10 mL PBS, dissociated by trituration, centrifuged, and resuspended in Dulbecco's modified Eagle medium (DMEM/F12) containing B27 supplement (2%), L-glutamine (2mM), penicillin (100U/mL), and streptomycin (100 μg/mL). Cells were plated in 6 cm Ultra low attachment polystyrene dishes (Fisher), at a concentration of 5×10^5 to 1×10^6 cells per plate. The growth factors human epidermal growth factor (hEGF) (20 ng/mL) and bFGF (10 ng/mL)

were added to the media every other day. On day 4, growing spheres were passed 1:3 and fresh media was added. Cells were grown following this protocol for 8 days. An earlier optimization protocol of this technique was published as (Bennett and Melanson-Drapeau, 2003). In some cases, neurospheres were embedded in 20% sucrose in 10 mM PBS, flash-frozen in CO_2, and cryostat-sectioned (10 μm).

5.5.2 Cell differentiation and immunodetection

On day 8, neurospheres were plated in laminin-coated 10 cm tissue culture dishes each containing 7 glass coverslips. Cells were grown in the same supplemented DMEM/F12 media, but without any growth factors. For gain of function expression studies, Cx32/GFP- or GFP alone-containing adenovirus was added at the time of plating in a minimal volume (3 mL) of media, at a multiplicity of infection (MOI) of 100. Plates were incubated at 37°C and gently rocked every 10 minutes to ensure equal distribution of the virus. Media (7mL) was added after 45 minutes to dilute the remaining adenovirus. All plated neurospheres were subsequently cultured for 6 days. On day 14, coverslips were removed and immunocytochemistry was performed as previously described (see Chapter 2, Material and methods). The primary antibodies used were anti-nestin, anti-NG2, anti-GFAP, anti-TuJ1 (1:250; Research Diagnostics Inc, Concord MA), and anti-Rip (Chemicon; 1:2000), followed by anti-mouse- or anti-Rb- conjugated to Cy3. Cell nuclei were visualized by Hoechst 33258 staining.

5.5.3 RT-PCR

Total RNA was isolated from neurospheres cultured in the presence of mitogens for

8 days as described above using Trizol reagent (Invitrogen) according to the manufacturer's recommendations. RNA template was treated with DNaseI (Promega) to eliminate residual genomic DNA. First-strand cDNA synthesis was performed using random hexamers (Promega) and Superscript II RT (Invitrogen) according to the manufacturer's recommendations. cDNA templates were amplified with 1 ug/ml forward primer (Cx32: 5'-GTGGCGTGAATCGGCACTCTAC-3' or GAPDH: 5'-TGGTGCTGAGTATGTCGTG GAGT-3') and reverse (Cx32: 5'-CTCCGCCACGTTGAGGATAATG-3' or GAPDH: 5'-AGTCTTCTGAGTGGCAGTGATGG-3'), PCR buffer (Applied BioScience), and 10 mM deoxynucleoside triphosphates (dNTPs; Promega) according to the following protocol: 94°C for 5 min, 35 cycles of 94°C for 25 sec, 59°C for 50 sec, and 72°C for 1 min, and a final incubation at 72°C for 7 min.

5.5.4 Western analysis

Proteins were isolated from neurospheres cultured for 8 days in mitogens using RIPA buffer (PBS, 1% Nonidet P-40, 0.1% SDS, 0.5% sodium deoxycholate, 50 μg/ml aprotinin, 1 mM sodium orthovanadate, 1 mg/ml phenylmethylsulfonyl fluoride, 1 mM sodium fluoride). Immumoblotting was performed as in Chapter 2. Briefly, proteins (30 μg) were separated by 12.5% SDS-PAGE under reducing conditions. Antibodies used were monoclonal anti-Cx32 (1:250, Zymed) and peroxidase-conjugated anti-mouse IgG (1:2000, Jackson Immunoresearch), diluted in PBS containing 1% casein. All other details are as described in Chapter 2.5.3.

5.5.5 Statistical analyses

Data are presented as the mean ± SEM. Data were analyzed by (a) ANOVA followed by *post hoc* Tukey tests to identify conditions that differed significantly from WT or (b) Student's *t* tests as applicable.

5.6 Results

5.6.1 Cx32 protein is not expressed in WT P2 hippocampus

Cx32 expression was assessed by immunocytochemistry in both proliferating neurospheres and following plating in cells dissociated from WT hippocampi and Cx32KO hippocampi as a negative control (Figure 5.1 *A*). Proliferating neurospheres do not express Cx32 protein (Figure 5.1 *C*), but do express mRNA (Figure 5.1 *B*). Cx32 protein is not induced following plating (Figure 5.1 *A*).

5.6.2 Progenitors derived from WT and Cx32KO neurospheres differentiate towards neuronal and glial lineages to the same extent

Since Cx32 protein is not detected in these early postnatal neurospheres (Figure 5.1), we did not expect to see a difference in spontaneous progenitor cell specification. To test this hypothesis, we compared the basal differentiation rates of WT and Cx32KO progenitors isolated from P2 hippocampi. On day 6 after plating, the percentage of neurogenesis and gliogenesis was assessed by immunodetection of multiple progenitor and terminally differentiated cell markers (Figure 5.2 *A-E*). The number of marker-positive cells was counted and expressed as a percentage of total cells per field (determined by Hoechst staining). Following this protocol, percentages of nestin$^+$ neural progenitors, NG2$^+$

Figure 5.1. Mouse P2 hippocampal progenitors express Cx32 mRNA but not protein. *A*) Hippocampal progenitor cells were extracted from P2 WT mice and expanded as neurospheres (left panel) before cryostat sectioning. After 8 days of neurosphere culture, cells were plated on laminin-coated coverslips and cultured for 6 days (right panel). Immunocytochemistry was performed to detect Cx32 protein (red). Cell nuclei were stained with Hoescht. Scale bars, 50 μm. *B*) RT-PCR was performed to detect Cx32, using RNA isolated from WT and Cx32KO adult brain (negative control) as well as WT neurospheres. Primers for GAPDH were used to verify template integrity. Negative controls included reactions processed in the absence of template. *C*) Western blotting for Cx32 was performed on protein extracted from WT adult brain, WT neurospheres and Cx32KO adult brain. Actin assessment was used as a loading control. Note that Cx32 mRNA is expressed in WT neurospheres, but that Cx32 protein is not detected by western blotting or immunocytochemistry.

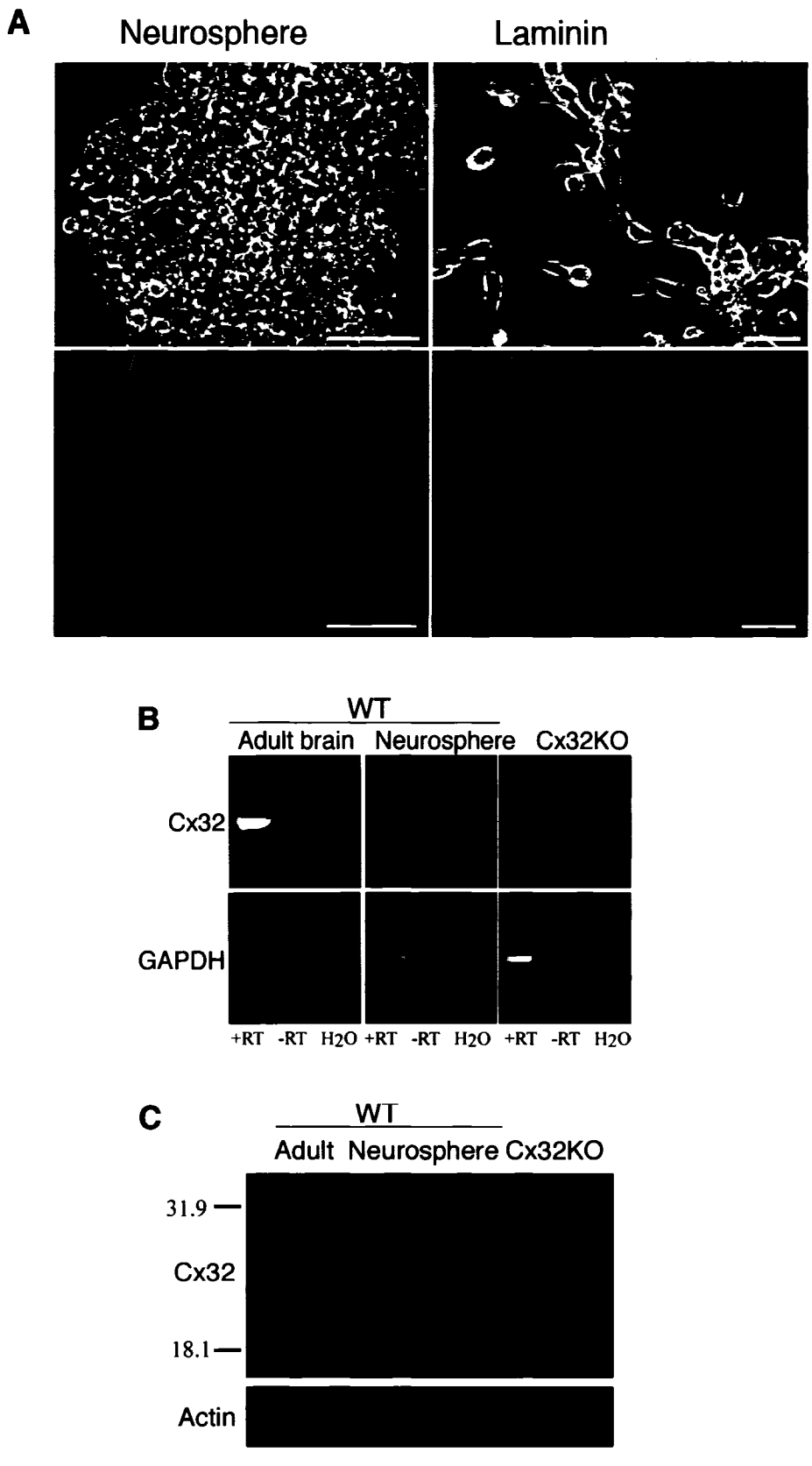
A
Neurosphere
Laminin
B
WT
Adult brain
Neurosphere
Cx32KO
Cx32
GAPDH
+RT -RT H2O +RT -RT H2O +RT -RT H2O
C
WT
Adult
Neurosphere
Cx32KO
31.9
Cx32
18.1
Actin

Figure 5.1

Figure 5.2. Specification rates towards glial and neuronal lineages are comparable between WT and Cx32KO hippocampal progenitors. *A-E*) Spontaneous differentiation of hippocampal WT and Cx32KO neurosphere-derived progenitor cells was induced by plating on laminin-coated coverslips and withdrawal of growth factors. Immunocytochemistry (red) was performed to detect nestin$^+$ neural progenitors (*A*), NG2$^+$ glial/early oligodendrocyte progenitors (*B*), Rip$^+$ mature oligodendrocytes (*C*), GFAP$^+$ astrocytes (*D*), and TuJ1$^+$ immature neurons (*E*). Nuclei were visualized by Hoescht staining (blue). Scale bars, 100 μm. *F*) Specification rates were assessed by counting Hoescht-labelled cells double-positive for the specific lineage markers. Data are expressed as % Lineage marker/Hoescht double-positive ± SEM. Note that specification rates between WT and Cx32KO cultures are similar as expected given that both cultures do not express Cx32 protein at this developmental time point.

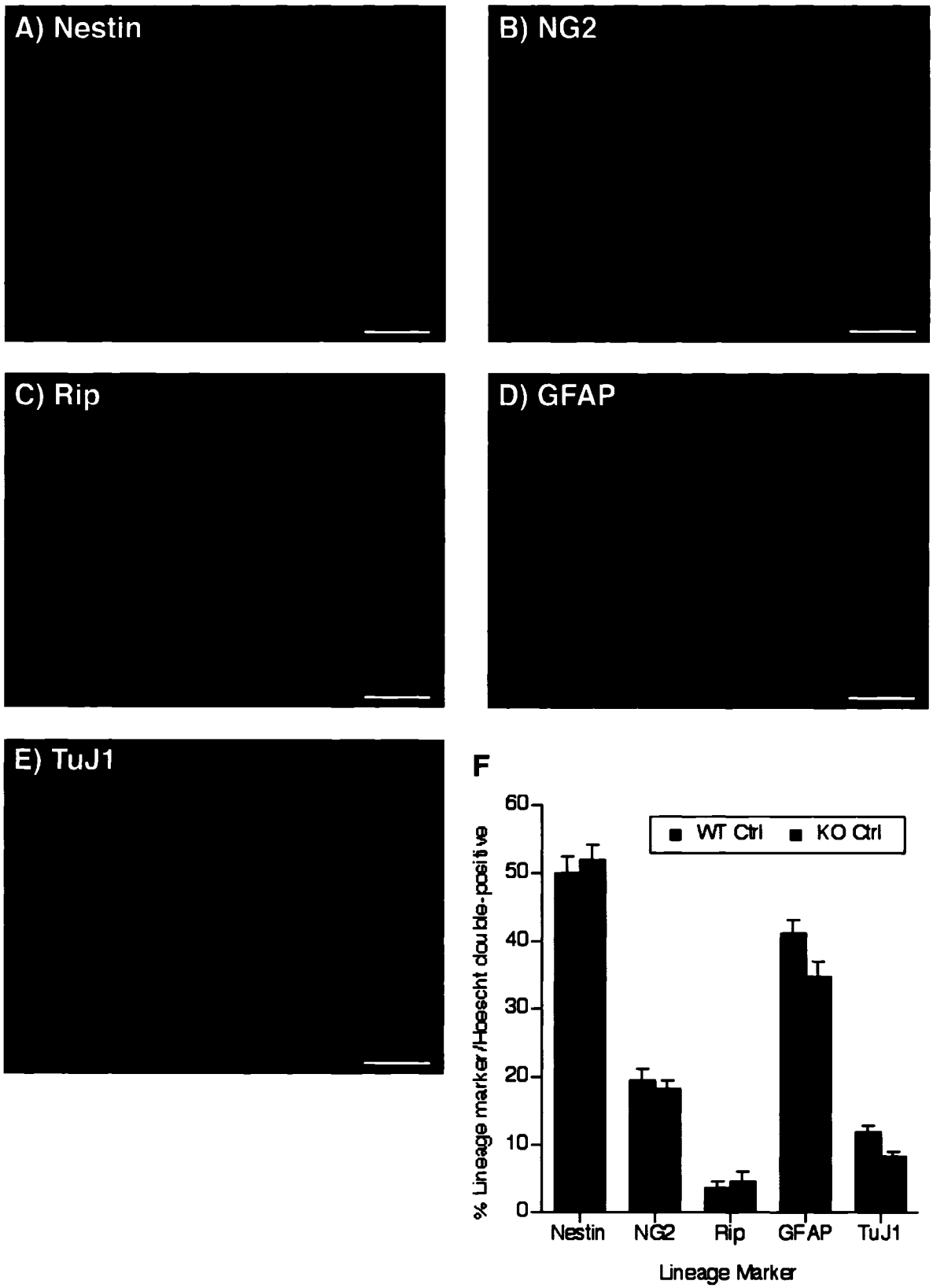
A) Nestin
B) NG2
C) Rip
D) GFAP
E) TuJ1
F
WT Ctrl
KO Ctrl
% Lineage marker/Hoescht double-positive
60
50
40
30
20
10
0
Nestin
NG2
Rip
GFAP
TuJ1
Lineage Marker

Figure 5.2

glial/oligodendrocyte progenitors, Rip^+ mature oligodendrocytes, $GFAP^+$ astrocytes, and $TuJ1^+$ immature neurons were determined (Figure 5.2 *F*). The majority of cells (~ 50%) still exhibited a neural precursor phenotype ($nestin^+$) 6 days after neurosphere plating. Of these precursors, 18% were committed towards a glial lineage ($NG2^+$). A high percentage of cells (~ 40%) were GFAP-positive. Spontaneous neurogenesis was favoured over oligodendrogenesis, with approximately 10% of all cells committed to an early neuronal lineage ($TuJ1^+$) but only a small percentage (~ 4%) identified as post-mitotic oligodendrocytes (Rip^+). Markers of mature neurons (i.e., NeuN) or oligodendrocytes (i.e., MBP) were not detected, indicating that cells did not adopt a terminally differentiated neuronal or oligodendrocytic phenotype within 6 days of differentiation (data not shown). Overall, neurospheres obtained from WT and Cx32KO hippocampi gave rise to similar populations of progenitors as well as differentiated progeny consistent with the fact that both populations do not express Cx32 protein at this developmental time point. The genetic manipulations associated with generating our Cx32KO or with embryogenesis in the absence of the Cx32 gene do not, therefore, alter P2 neural progenitor cell specification.

5.6.3 Neurosphere morphology is not altered following Cx32/GFP adenoviral infection

To establish the functional consequences of Cx32 expression, neurospheres were plated on laminin-coated coverslips and cultured for 6 days to induce spontaneous differentiation. As early as 24 hours following plating, neurospheres adhered to the coverslips and the cells at the neurosphere periphery could be seen migrating away from the core in a radial pattern (Figure 5.3, *A*). Over the course of migration, cells at the periphery

began to adopt a differentiated morphology, characterized mainly by the presence of developing extensions. Infection with either GFP- or Cx32/GFP–containing adenovirus did not alter cell morphology. Infection efficiency was comparable between groups, as assessed by GFP immunofluorescence. In both groups, GFP levels were undetected on day 1, increasing progressively to reach maximal expression by day 3. These high levels of GFP expression were maintained until 6 days following infection (Figure 5.3 *B,C*).

5.6.4 Oligodendroglial specification of Cx32KO hippocampal progenitors is enhanced following infection with Cx32-containing adenovirus

The differentiation rate of Cx32KO progenitors isolated from P2 hippocampi was compared following infection with either Cx32/GFP- or GFP alone–containing adenovirus. Cells were infected at the time of plating and the percentage of neurogenesis and gliogenesis was assessed by immunodetection of antigenic lineage markers as described above (Figure 5.4 *A*). Only marker-positive/GFP-positive cells were counted and data are expressed as a percentage of GFP double-positive cells (Figure 5.4 *B*). Similar to control non-infected cells, approximately 45% of GFP-expressing cells exhibited a neural precursor phenotype (nestin$^+$) 6 days after neurosphere plating. Approximately 35% of cells were GFAP$^+$ astrocytes, while only 2% of adenovirus-infected cells expressed a marker of mature oligodendrocytes (Rip$^+$). As observed in control groups, no markers of mature neurons or oligodendrocytes could be detected, indicating that cells did not adopt a terminally

Figure 5.3. Adenoviral infection of neurospheres does not alter cell morphology. *A-C*) WT neurospheres were plated on laminin-coated coverslips and infected with an adenovirus containing GFP alone (*B*), or GFP and Cx32 (*C*). The control group was not infected (*A*). Neurosphere-derived cells were cultured for 6 days and GFP fluorescence was assessed daily by microscopy (green). *D*) The pAdTrack vector used to generate the adenovirus is shown in the bottom panel. Note that GFP expression is similar between the GFP only and the Cx32/GFP groups and that infection did not alter cell morphology, when compared to the control group. Scale bars, 25 μm.

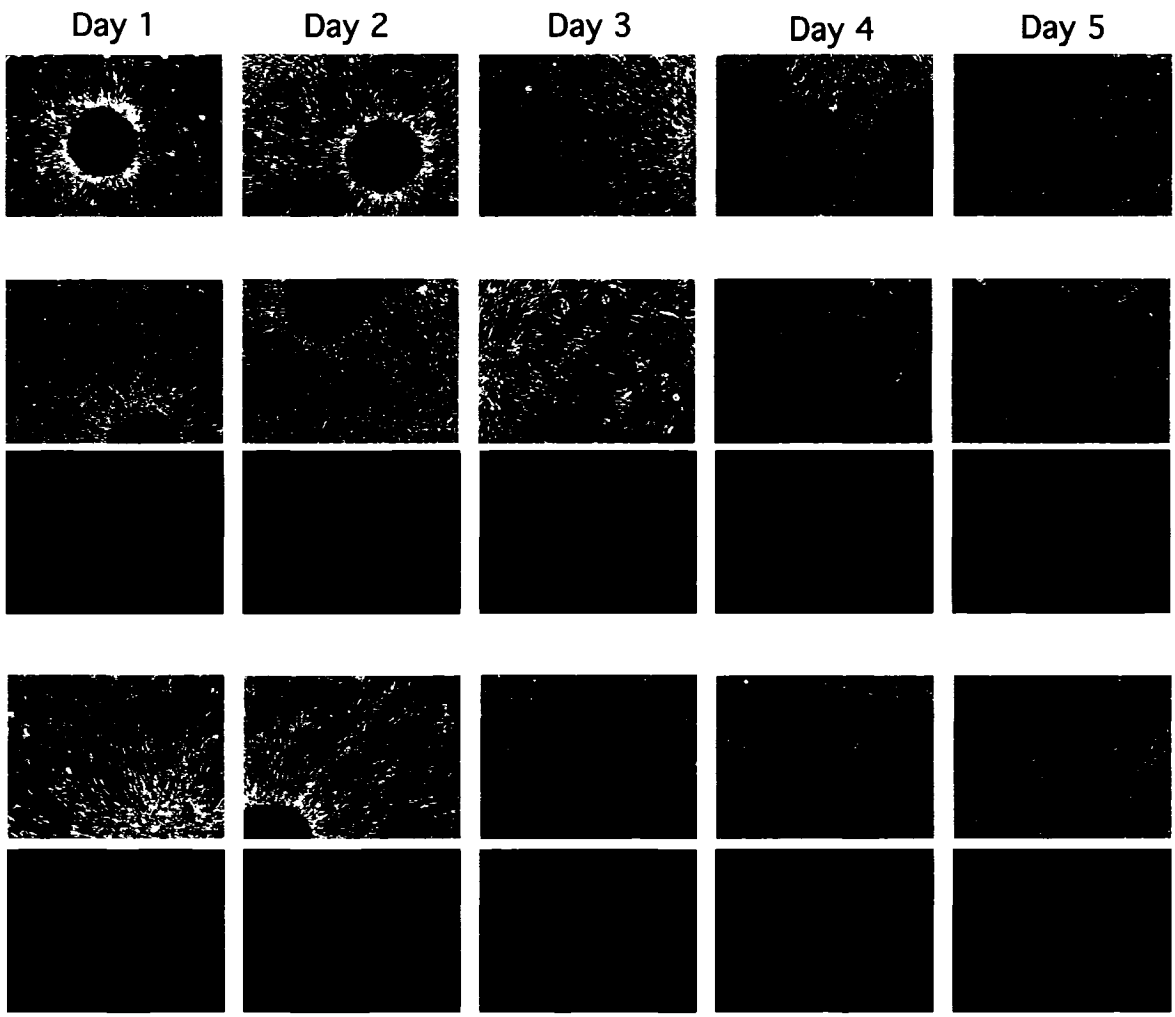
Day 1
Day 2
Day 3
Day 4
Day 5

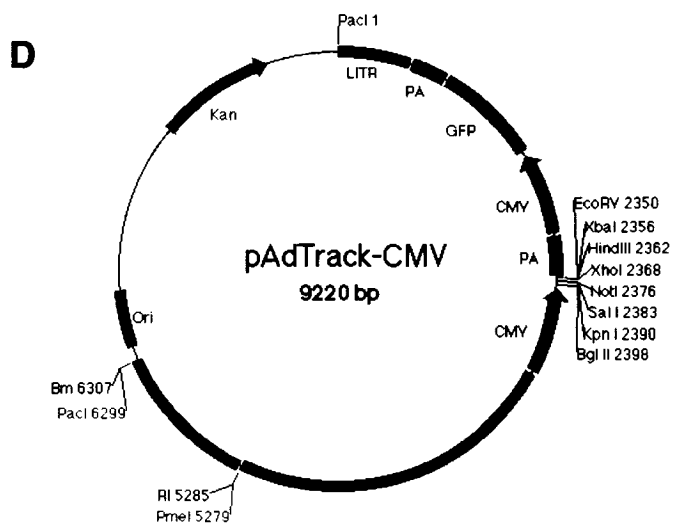
D
PacI 1
LITR
PA
GFP
CMV
PA
CMV
Kan
Ori
pAdTrack-CMV
9220 bp
EcoRV 2350
XbaI 2356
HindIII 2362
XhoI 2368
NotI 2376
SalI 2383
KpnI 2390
BglII 2398
Bm 6307
PacI 6299
RI 5285
PmeI 5279

Figure 5.3

Figure 5.4. Ectopic expression of Cx32 alters specification rates of hippocampal progenitors. *A*) Cx32KO neurospheres were infected at the time of plating with an adenovirus containing GFP alone, or Cx32 and GFP. Cells were immunoreacted for the cell lineage markers nestin, NG2, Rip, GFAP, and TuJ1 (red). *B*) The percentage of GFP-positive cells (green) expressing each lineage marker was calculated. Ectopic Cx32 expression had no effect on the percentages of nestin$^+$ progenitors, GFAP$^+$ astrocytes, or Rip$^+$ oligodendrocytes. More cells committed to an NG2$^+$ glial lineage and fewer cells committed to a TuJ1$^+$ neuronal lineage in the presence of Cx32 (*$p<0.05$, **$p<0.01$, Student's *t* test).

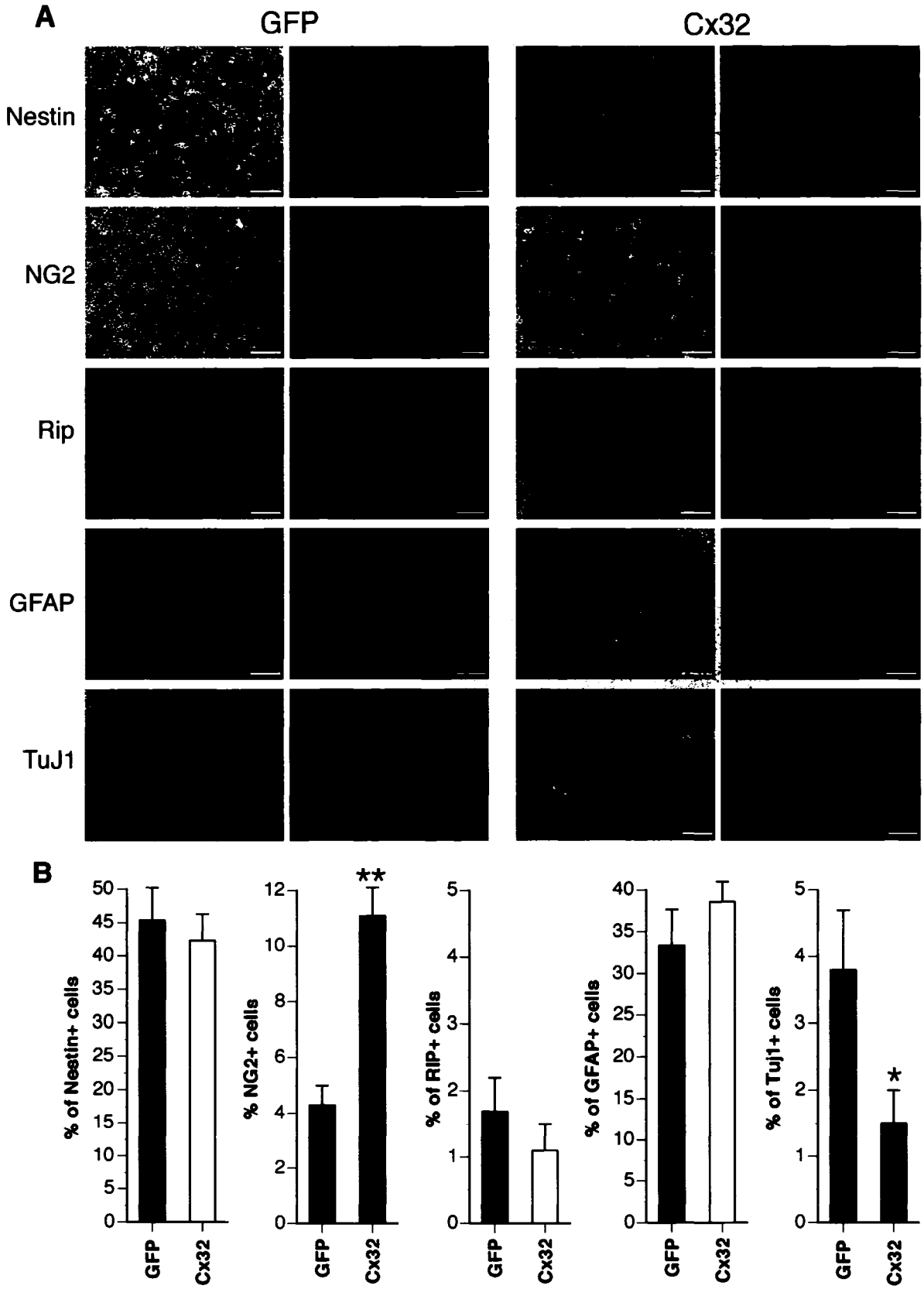
A
GFP
Cx32
Nestin
NG2
Rip
GFAP
TuJ1
B
% of Nestin+ cells
% NG2+ cells
% of RIP+ cells
% of GFAP+ cells
% of Tuj1+ cells
**
*
GFP
Cx32

Figure 5.4

differentiated neuronal or oligodendrocytic phenotype within 6 days of differentiation, in the presence or absence of Cx32.

Surprisingly, a statistically significant difference was observed in the percentage of progenitors committed towards a glial lineage ($NG2^+$ cells). While only about 4% of cells infected with the GFP-only adenovirus expressed NG2, 11% of cells infected with the Cx32/GFP-containing adenovirus were identified as $NG2^+$ progenitors (Figure 5.4 *B*; $^{**}p<0.01$, Student's *t* test). Furthermore, the percentage of cells differentiating to a neuronal lineage ($TuJ1^+$) was significantly decreased following Cx32 expression as compared to GFP expression alone (Figure 5.4 *B*; $^{*}p<0.05$, Student's *t* test). These data suggest that ectopic Cx32 expression promotes commitment to an $NG2^+$ lineage at the expense of neurogenesis, while self-renewal ($nestin^+/GFP^+$) and astrocytic differentiation ($GFAP^+/GFP^+$) are not altered.

5.7 Discussion

In these experiments, we expanded postnatal hippocampal progenitor cells using a neurosphere assay and determined their differentiation potential. Cx32 mRNA is first detected between P1-5 in rodent brain, with protein levels peaking around P14 (Nadarajah et al., 1997). We therefore did not expect the WT and Cx32KO hippocampal progenitors isolated on P2 to show any phenotypic difference. However, the effects of genetic manipulation on embryonic development and progenitor potential should not be underestimated. To confirm the comparable morphology of WT and Cx32KO P2 progenitors, hippocampal cells from both genotypes were cultured and expanded in a

neurosphere assay, resulting in the formation of floating cell clusters, first described by (Reynolds and Weiss, 1992). Our data demonstrate that proliferating neural progenitor cells isolated from the hippocampus on P2 do not express Cx32 protein, but do express mRNA, consistent with reports that Cx32 transcript can be detected between P1-5 (Nadarajah et al., 1997; Sohl et al., 2001b). Interestingly, we did not detect Cx32 expression over the course of spontaneous differentiation. Moreover, we show that progenitor cell specification is comparable between WT and Cx32KO neurospheres. Together, these data argue that the genetic alterations associated with constitutive Cx32-null mutation do not impact upon early postnatal progenitor cell specification through developmental molecular mechanisms other than Cx32 loss of function.

Neurosphere-maintaining media was supplemented with the mitogens bFGF and hEGF, both known to enhance neural precursor cell proliferation and to be sufficient for their sustained and continous expansion in culture (Cameron et al., 1998; Conti et al., 2005; Gritti et al., 1996; Laskowski et al., 2005). In this study, approximately half the cells, regardless of genotype, retained their stem cell-like phenotype, as evidenced by nestin immunodetection. Low levels of neurogenesis and oligodendrogenesis were detected in cultures from both genotypes, while a considerable portion of plated cells expressed GFAP (40%). This is consistent with current literature, according to which approximately half of neurosphere-derived progenitors assume an astrocytic phenotype following plating, especially in the absence of any growth factors or neurotrophins such as BDNF, NT3, and NT4, known to induce neuronal differentiation (Caldwell et al., 2001; Morshead et al., 2002). Furthermore, in the adult hippocampus, neurogenesis can be derived from $GFAP^+$ precursors with astrocytic properties (Seri et al., 2001; Steiner et al., 2004). Although the

majority of $GFAP^+$ cells in our cultures exhibited an astrocytic morphology, a small portion of these cells could be $nestin^+/GFAP^+$ Type B progenitors described by Doetsch (2003).

We next performed gain of function studies to provide mechanistic insight into our loss of function *in vivo* analyses of Cx32-null mutant mice. The impact of ectopic Cx32 expression on differentiation rate of Cx32KO progenitors was determined following infection with an adenovirus containing either a Cx32/GFP construct, or the GFP construct alone. Adenoviral infection did not alter progenitor cell specification indices. Percentages of GFP/lineage marker double-positive cells were first determined and, overall, were found to be equivalent to the percentages of lineage markers observed in the control cell population. While levels of neuronal and astrocytic markers were comparable following infection with Cx32, a difference was observed in the number of NG2-positive cells. The number of $NG2^+$ glial/early oligodendrocyte progenitors observed in the Cx32-infected group was almost three times higher than that observed in the GFP only-infected group (11% vs 4%). In Chapter 2, we showed that Cx32 protein is first expressed at the cell membrane of $NG2^+$ hippocampal progenitors, committed to an oligodendrocytic lineage. We speculated that Cx32 expression determines the fate of this subset of $NG2^+$ progenitor cells. In the absence of Cx32 *in vivo*, this unique $NG2^+$ subpopulation of progenitors transiently accumulates, as progeny are unable to commit to an oligodendrocyte lineage, and defective cells are deleted by apoptosis. The data presented in this chapter support a direct role for Cx32 in dictating progenitor cell specification and afford some insight into this regional control of progenitor fate by Cx32 in the adult brain. In the presence of Cx32, more progenitors are driven towards an oligodendroglial lineage at the expense of neurogenesis,

resulting in a higher percentage of committed $NG2^+$ oligodendrocyte progenitors and a lower percentage of $TuJ1^+$ neurons. Future experiments should assess differentiation rates at later time points in order to determine whether these higher levels of oligodendrocyte progenitors give rise to a bigger population of mature oligodendrocytes. Levels of mature neurons could also be determined more accurately, since neural progenitors destined to a neuronal fate usually only become NeuN-positive 4 weeks after the start of their differentiation process (Steiner et al., 2004).

Taken together, these data confirm the capacity of Cx32 to act in a cell-autonomous fashion. By gain of function analysis, we showed that Cx32 expression in neural progenitor cells, in the absence of any other terminally differentiated cell type, is sufficient to direct their fate.

Chapter 6: General discussion

6.1 The role of Cx32 in dictating progenitor cell fate

Several lines of evidence have implicated connexin- and/or gap junction-mediated communication in embryonic progenitor cell regulation, proliferation, and specification, as reviewed in "Chapter 1: General introduction". The overarching goal of my research was to establish the role of connexin-mediated communication in the determination of the plasticity, commitment, and/or fate of adult progenitor populations. The results presented in this thesis suggest a role for Cx32 in dictating adult hippocampal progenitor cell fate, by promoting oligodendrogenesis over neurogenesis (Figure 6.1).

I first investigated the cellular localization of Cx32 in the dentate gyrus of adult WT mice, and found that Cx32 protein is expressed not only in mature oligodendroglia, but also in $NG2^+$ glial/early oligodendrocyte progenitors, as well as $PDGF\alpha R^+$ late oligodendrocyte progenitors. In the dentate gyrus of Cx32KO mice, I showed that the constitutive turnover of $NG2^+$ progenitors is enhanced, but that the progeny of these cells fail to terminally differentiate and are instead rapidly deleted through an apoptotic-like mechanism. These observations led me to ask whether hippocampal function was affected by the enhanced turnover of these $NG2^+$ progenitors. Mice from both genotypes were therefore tested in the radial arm maze, a standard maze designed to assess behavioural indices of learning and memory. Using this paradigm, working and reference memory were evaluated. Cx32KO mice exhibit an obvious impairment in the acquisition portion of the maze linked to hippocampal activity, suggesting that unscheduled progenitor activation is sufficient to impact upon hippocampal associated cognitive function.

Figure 6.1. Putative role of Cx32 in dictating progenitor cell fate. Results described in Chapters 2–5 led us to conclude that Cx32 plays a role in the regulation of hippocampal progenitors, *in vivo* as well as *in vitro*. In Chapter 2, we determined that Cx32 is expressed by $NG2^+$ progenitors and hypothesized that it plays a role in promoting the differentiation of these progenitors towards an oligodendrocytic lineage. In Chapter 3, we found that the dynamic defect in progenitor turnover observed in Cx32KO mice had a negative effect on their performance in a learning and memory task. In Chapter 4, we found that, following brain injury, neurogenesis derived from $NG2^+$ hippocampal progenitors was more efficient in the absence of Cx32. We confirmed the dictating role of Cx32 in Chapter 5, by showing that Cx32 promotes oligodendrogenesis over neuronal differentiation *in vitro*. These major findings are recapitulated in this model figure.

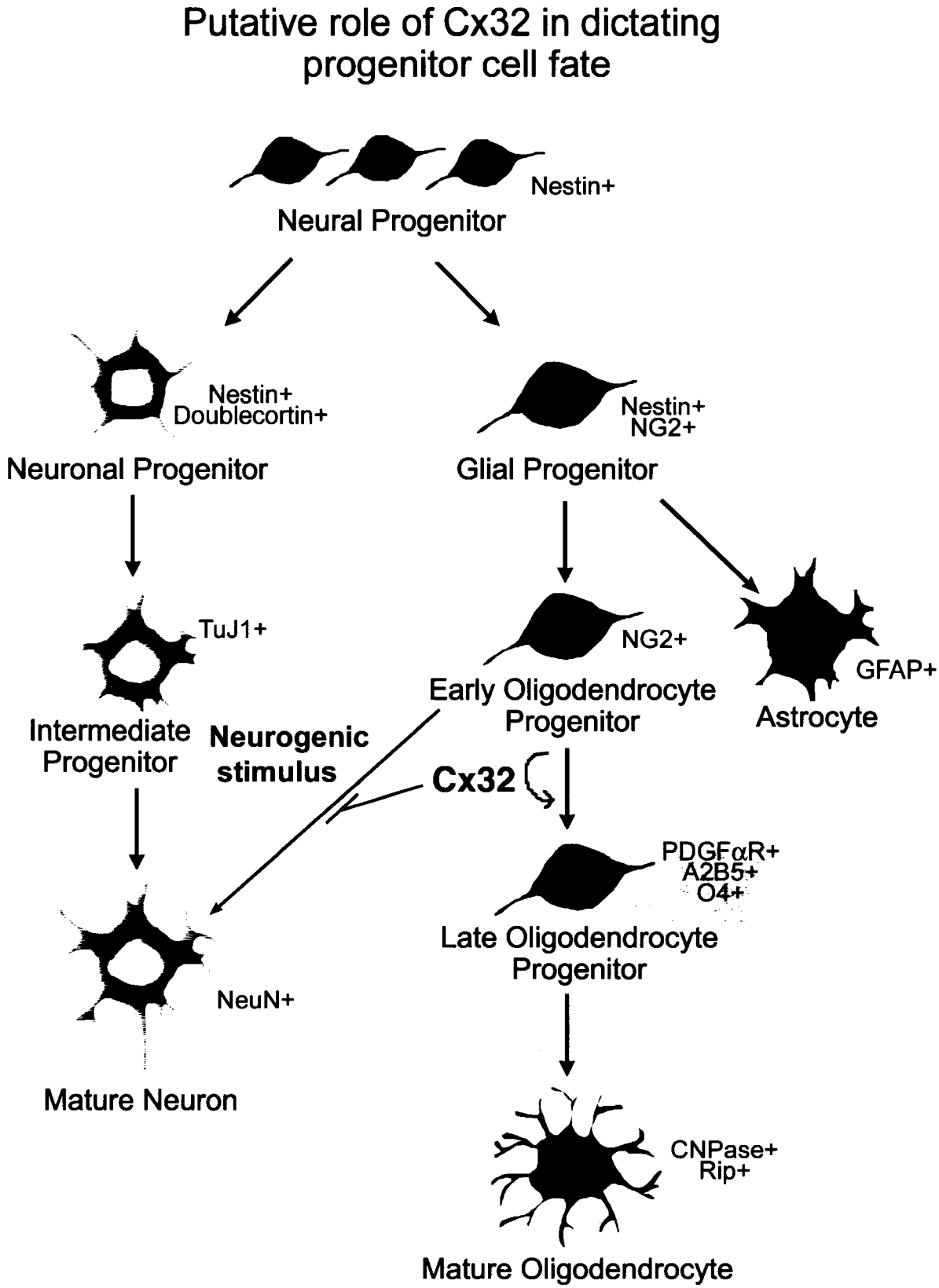
Putative role of Cx32 in dictating progenitor cell fate
Nestin+
Neural Progenitor
Nestin+
Doublecortin+
Neuronal Progenitor
Nestin+
NG2+
Glial Progenitor
TuJ1+
Intermediate Progenitor
Neurogenic stimulus
NG2+
Early Oligodendrocyte Progenitor
GFAP+
Astrocyte
Cx32
PDGFαR+
A2B5+
O4+
Late Oligodendrocyte Progenitor
NeuN+
Mature Neuron
CNPase+
Rip+
Mature Oligodendrocyte

Figure 6.1

Using an *in vitro* clonogenic assay, I showed that more proliferating progenitor cells can be cultured from adult Cx32KO hippocampus than WT. Significantly, these progenitors specify to neurons when treated with a neurogenic stimulus, to a greater extent than progenitors cultured from adult WT mice. This finding prompted me to ask whether $NG2^+$ progenitor cells could specify to neurons when subjected to a neurogenic stimulus *in vivo*, and whether neurogenesis would be more or less efficient in the absence of Cx32. Kainic acid-induced seizures were used as an *in vivo* neurogenic stimulus. Known to produce a well-defined pattern of seizure activity resulting in hippocampal neuronal loss, this injury model had previously been shown to cause the activation of endogenous granule progenitor cells, resulting in the partial regeneration of hippocampal tissue (Gray and Sundstrom, 1998; Nakagawa et al., 2000; Parent et al., 1997; Wang et al., 2004). I found that neuronal regeneration of the CA3a/b pyramidal cell field is enhanced in Cx32KO as compared to WT mice. Moreover, data suggests that the increase in neuroregeneration is due to an enhanced specification of $NG2^+$ progenitors towards a neuronal phenotype, in the absence of Cx32. To determine more precisely the mechanism by which Cx32-mediated intercellular communication directs the fate of hippocampal progenitors, I performed gain of function studies and assessed whether Cx32 expression directs specification of hippocampal progenitors cultured *in vitro*. I found that, in the presence of Cx32, more progenitor cells specify to an oligodendrocytic lineage ($NG2^+$), at the expense of neurogenesis ($TuJ1^+$). In the absence of Cx32, spontaneous differentiation to neurons is more effective.

While these data provide strong evidence that Cx32 expression by putative multipotential progenitors promotes oligodendroglial commitment over neurogenesis, we have yet to establish how Cx32 expression directly influences progenitor fate. Four

possibilities can be postulated. First, gap junctions may enable coupled progenitor cells to coordinate their responses to extrinsic stimuli, with the repertoire of connexins expressed dictating which second messengers can be shared between progenitor populations. Second, progenitor cells may interact directly with adjacent "instructive cells" through gap junctional intercellular communication. Third, connexin oligomers have been shown to form gated hemichannels in non-junctional membranes, allowing progenitor cells to share signalling molecules with the extracellular environment. Fourth, channel-autonomous signalling may be achieved through protein-protein interaction at the connexin C-terminal tail. These possibilities will be addressed in the following summary.

6.2 Gap junctional-mediated communication between progenitor cells

Several molecules such as ions (i.e., Na^+, K^+, Ca^{2+}, Cl^-), amino acids, cyclic nucleotides, ATP, IP_3, and vitamins can pass through gap junctions (Alexander and Goldberg, 2003; Goldberg et al., 2004; Krysko et al., 2005). ATP, 3', 5' – cyclic adenosine monophosphate (cAMP), IP_3, and calcium are important cell fate modulators, with intracellular levels of each molecule varying greatly during events such as cellular differentiation and apoptosis (reviewed in Krysko et al., 2005). For example, increases in intracellular levels of adenosine diphosphate (ADP) and ATP promote oligodendrocyte differentiation of progenitor cells (reviewed in Agresti et al., 2005). Since connexin expression patterns and intercellular coupling seem to correlate with key neuronal differentiation events, gap junctions are suggested to play a role in the synchronous diffusion of signaling molecules promoting these events (Lee et al., 1987; Rozental et al., 1998; Warner et al., 1984; Wong et al., 1998). For example, in the early postnatal

neocortex, IP_3 propagation and intercellular calcium waves are mediated by dendritic gap junctions. This process is thought to form the basis of the immature neocortex partition, dividing it into columnar patches of coordinated activity (Kandler and Katz, 1998; Peinado et al., 1993a; Yuste et al., 1995; Yuste et al., 1992). Furthermore, gap junctions have been suggested to coordinate the release of calcium from intracellular stores observed in mitotic precursor cells (Owens and Kriegstein, 1998). Thus, it is possible that coordination of ATP and ADP exchange between cells could facilitate population-based progenitor specification.

Alternatively, Cx32-mediated gap junctional communication between progenitors may actively inhibit neurogenesis. As previously mentioned, the connexin composition of each channel confers different biochemical properties, allowing the preferential passage of certain molecules. Gap junctions composed of Cx32 have been shown to be 12-fold more permeable to adenosine then gap junctions composed of Cx43 (Goldberg et al., 2002). Homomeric Cx32 gap junctions have been further shown to pass cAMP more readily than heteromeric Cx32/Cx26 gap junctions (Bevans et al., 1998). Altering Cx32 expression could influence the intercellular concentration of these key molecules, thereby altering progenitor cell fate. Salient to this argument, adenosine has been shown to stimulate neuronal differentiation of neural crest cells, specifically catecholinergic differentiation (Bilodeau et al., 2005), while cAMP-responsive elements promote differentiation of neurons in the olfactory bulb and ensure their subsequent survival (Giachino et al., 2005). Thus, it is possible that passage of adenosine between cells could alter the concentration gradient of second messengers required to ensure successful neuronal specification.

6.3 Instructive cells: Cell-cell contact and differentiation

Recent literature has demonstrated that environment dictates stem cell proliferation and the resulting proportions of neurogenesis and gliogenesis (Lim and Alvarez-Buylla, 1999; Song et al., 2002). In experiments published by Song *et al.*, astrocytes were shown to promote the neuronal differentiation of precursor cells isolated from adult hippocampus (2002). Furthermore, when cultured on top of mature neurons, the same precursor cells were shown to differentiate to an oligodendrocyte phenotype (Song et al., 2002). Interestingly, although exposure to conditioned media containing astrocyte-derived factors alone could promote low levels of neuronal specification, it did not provide the same supportive environment. Direct contact was therefore proposed to play a crucial role in stem cell fate determination. While these authors have pursued the Wnt juxtracrine pathway in mediating this phenotype (Lie et al., 2005), gap junctional communication between progenitor cells and neighbouring "instructive" populations may also be influential. The absence of Cx32 in junctions between progenitor and "instructive" cells could therefore influence the fate of these unspecified cells.

Although it remains ambiguous whether mature oligodendrocytes can communicate between each other through gap junctions, heterocellular junctional plaques have been extensively described (Rash, 2001), mainly associated with oligodendrocyte somata (Nagy et al., 2003a). Cx32 is capable of forming junctions with astrocytic Cx43, Cx26, and Cx30 (Rash et al., 1998). In Cx32KO mice, Cx26 and Cx30 expression at astrocyte-oligodendrocyte junctions is drastically reduced, suggesting that these connexins are the main coupling partners of Cx32 and that their presence in those junctions is dependent on the Cx32 protein (Nagy et al., 2003b). Future experiments investigating the coupling

capacity of oligodendrocyte progenitor cells with terminally differentiated cells are required to provide insight into the extent of this instructive control in the hippocampus of adult rodents.

6.4 Impact of Cx32 hemichannels

Alternatively, hemichannels allowing the exchange of signals between progenitor cells and the extracellular milieu could dictate their fate. Permeable to small physiologically significant molecules such as ATP, nicotinamide adenine dinucleotide (NAD^+), and glutamate, Cx43 hemichannels have been suggested to mediate paracrine as well as autocrine signaling (reviewed in Stout et al., 2004). The regulation of hemichannels as well as their impact on cell fate has been extensively studied in CNS glia. For example, as briefly discussed in Chapter 1, astrocytes respond to a variety of stimuli and are capable of widespread intercellular communication through the propagation of increases in intracellular calcium concentration, either in individual cells or as waves directly transmitted to surrounding cells. Astrocytic calcium waves are involved in diverse processes such as long-range signaling (Cornell-Bell et al., 1990), the modulation of synaptic signaling between neurons (Araque et al., 1998; Kang et al., 1998; Parpura and Haydon, 2000), the regulation of blood-brain barrier permeability (Zonta et al., 2003), and, salient to our discussion, the regulation of neural precursor cell proliferation and migration (Weissman et al., 2004). First thought to be a property of gap junctions between astrocytes (Charles, 1998; Charles et al., 1992; Nedergaard, 1994), propagation of these calcium waves is more likely mediated by the release of ATP through Cx43 hemichannels (Stout et al., 2002) and the subsequent activation of purinergic receptors capable of evoking a calcium response in astrocytes

(Guthrie et al., 1999). Hemichannels also directly impact upon neighbouring cell fate by altering regional ionic conductance as described in the feedback modulation of glutamate release from cone photoreceptors by horizontal cells in mammalian retina. Located on the dendrites of horizontal cells (DeVries and Schwartz, 1992; Kamermans et al., 2001), Cx26 hemichannels are proposed to act as a current sink rendering neighbouring photoreceptors more sensitive to changing membrane potential. With the opening of dendritic hemichannels on horizontal cells in the immediate vicinity of photoreceptors, the extracellular potential becomes negative as a result of the ionic conductance into the horizontal cells. The voltage-gated calcium channels located on presynaptic cones thereby detect a more positive membrane potential and release glutamate (Kamermans et al., 2001). Cx32 is also known to form functional hemichannels and the significance of these channels has been discussed in the previous chapters.

In Chapter 5, I focused on determining whether Cx32 could act in a cell-autonomous fashion or whether the *in vivo* impact of Cx32-null mutation on cell fate described in Chapters 2-4 reflected the loss of Cx32 function in instructive cell populations. By gain of function analysis, I demonstrated that Cx32 expression in hippocampal progenitor cells is sufficient to direct their fate, in the absence of any other terminally differentiated cell type. The specificity of connexin expression by various progenitor cell populations would thereby represent a cell fate control mechanism, limiting their intrinsic capacity to communicate and respond to changes within their environment.

6.5 Connexin protein-protein interactions

As briefly discussed in Chapter 4, some connexin effects may be mediated

independently of gap junction channel or hemichannel function. In various models of cell injury, ectopic expression of Cx32, Cx40, and Cx43 was suggested to protect C6 glioma cells by inducing phenotypic transformations such as cellular flattening and actin organization into parallel arrays of stress fibers (Lin et al., 2003). Connexin contribution to the cytoskeletal organization and cell geometry could thereby influence cellular resistance (Chen et al., 1997; Cotrina et al., 1998). Binding partners for Cx43 such as the tight junction-associated proteins zona occludens-1 (ZO-1) and ZO-2 have been identified (Guerrier et al., 1995; Singh et al., 2005; Toyofuku et al., 1998). The Src homology 2 (SH2) and SH3 domains of the Rous sarcoma virus transforming protein (v-SRC) were also found to bind the C-terminal tail of Cx43 (Kanemitsu et al., 1997). The role of Cx43 as a tumor suppressor was further suggested to be mediated independently of gap junctions (Qin et al., 2002). Free carboxy-tail was indeed found to localize to the nucleus and to bind DNA (Dang et al., 2003), suggesting that Cx43 growth inhibition effects could be mediated by its binding to the promoter region of the regulated genes (reviewed in Krysko et al., 2005). In future experiments, identifying possible Cx32 protein binding partners by immunoprecipitation and mass spectrometry would determine whether some Cx32-mediated effects are exerted through a channel-independent mechanism.

6.6 Significance of research

Neurodegenerative diseases such as Alzheimer's and Parkinson's disease are of increasing prevalence in our aging population. Current therapies temporarily reduce symptoms thereby transiently improving quality of life, but do little to halt disease progression. The recent recognition that the brain is capable of regeneration, albeit limited,

has provided new hopes, introducing stem cell therapy as a potential approach to brain repair. While exogenous stem cell transplants is one potential strategy, it carries certain disadvantages such as graft rejection as well as the possible formation of brain tumors (Singh et al., 2004a; Singh et al., 2003; Singh et al., 2004b). Harnessing the regenerative potential of adult endogenous stem and progenitor cells therefore constitutes an invaluable alternative approach for the treatment of neurodegenerative diseases, but requires rigorous validation.

Achieving a better understanding of the precise molecular mechanisms regulating adult progenitor cell fate is of critical importance if we are to explore the potential of cell replacement strategies. In this thesis, I focused on elucidating how Cx32-mediated communication controls progenitor cell survival, proliferation, and differentiation in injured and uninjured rodent brain. I found that Cx32 dictates adult hippocampal progenitor fate by promoting oligodendrogenesis and/or inhibiting neurogenesis (Figure 6.1). These data represent the first time that connexin-mediated signalling has been implicated in the control of neural progenitor fate in the uninjured and injured adult mammalian brain. I argue that this research provides a strong basis for focussing on connexin-mediated communication in directing neural progenitor specification. A thorough understanding of this signalling is essential if we are to validate the promise of stem cell therapy in neurodegenerative diseases, and this thesis represents a step in this direction. Based on the studies described, I argue that a new area of stem cell research should focus on designing specific connexin inhibitors which, when administered locally, could potentially promote endogenous neurogenesis following brain injury by modulating Cx32 expression.

References

Agresti, C., Meomartini, M. E., Amadio, S., Ambrosini, E., Volonte, C., Aloisi, F., and Visentin, S. (2005). ATP regulates oligodendrocyte progenitor migration, proliferation, and differentiation: involvement of metabotropic P2 receptors. Brain Res Brain Res Rev *48*, 157-165.

Aguirre, A., and Gallo, V. (2004). Postnatal neurogenesis and gliogenesis in the olfactory bulb from NG2-expressing progenitors of the subventricular zone. J Neurosci *24*, 10530-10541.

Al-Hazzaa, A. A., and Bowen, I. D. (1998). Improved cytochemical methods for demonstrating cell death using LR White as an embedding medium. Histochem J *30*, 897-902.

Alexander, D. B., and Goldberg, G. S. (2003). Transfer of biologically important molecules between cells through gap junction channels. Curr Med Chem *10*, 2045-2058.

Altevogt, B. M., Kleopa, K. A., Postma, F. R., Scherer, S. S., and Paul, D. L. (2002). Connexin29 is uniquely distributed within myelinating glial cells of the central and peripheral nervous systems. J Neurosci *22*, 6458-6470.

Altevogt, B. M., and Paul, D. L. (2004). Four classes of intercellular channels between glial cells in the CNS. J Neurosci *24*, 4313-4323.

Altman, J. (1969). Autoradiographic and histological studies of postnatal neurogenesis. IV. Cell proliferation and migration in the anterior forebrain, with special reference to persisting neurogenesis in the olfactory bulb. J Comp Neurol *137*, 433-457.

Altman, J., and Das, G. D. (1965). Autoradiographic and histological evidence of postnatal hippocampal neurogenesis in rats. J Comp Neurol *124*, 319-335.

Anzini, P., Neuberg, D. H., Schachner, M., Nelles, E., K., W., Zielasek, J., Toyka, K. V., Suter, B., and Martini, R. (1997). Structural abnormalities and deficient maintenance of peripheral nerve myelin in mice lacking gap junction protein connexin 32. J Neurosci *17*, 4545-4551.

Araque, A., Parpura, V., Sanzgiri, R. P., and Haydon, P. G. (1998). Glutamate-dependent astrocyte modulation of synaptic transmission between cultured hippocampal neurons. Eur J Neurosci *10*, 2129-2142.

Ayetey, H. (2002). Neuronal stem cells: the past, present and future (Guys, Kings & St. Thomas' Hospitals School of Medicine, Dentistry and Biomedical Sciences, London, UK,).

Azzam, E. I., de Toledo, S. M., and Little, J. B. (2001). Direct evidence for the participation of gap junction-mediated intercellular communication in the transmission of damage signals from alpha-particle irradiated to nonirradiated cells. Proc Natl Acad Sci USA *98*, 473-478.

Bahr, M., Andres, F., Timmerman, V., Nelis, M. E., Van Broeckhoven, C., and Dichgans, J. (1999). Central visual, acoustic, and motor pathway involvement in a Charcot-Marie-Tooth family with an Asn205Ser mutation in the connexin 32 gene. J Neurol Neurosurg Psychiatry *66*, 202-206.

Baimbridge, K. G. (1992). Calcium-binding proteins in the dentate gyrus. Epilepsy Res Suppl *7*, 211-220.

Bani-Yaghoub, M., Bechberger, J. F., and Naus, C. C. (1997). Reduction of connexin43 expression and dye-coupling during neuronal differentiation of human NTera2/clone D1 cells. J Neurosci Res *49*, 19-31.

Bani-Yaghoub, M., Felker, J. M., Sans, C., and Naus, C. C. (2000). The effects of bone morphogenetic protein 2 and 4 (BMP2 and BMP4) on gap junctions during neurodevelopment. Exp Neurol *162*, 13-26.

Bani-Yaghoub, M., Underhill, T. M., and Naus, C. C. (1999). Gap junction blockage interferes with neuronal and astroglial differentiation of mouse P19 embryonal carcinoma cells. Dev Genet *24*, 69-81.

Bao, X., Reuss, L., and Altenberg, G. A. (2004). Regulation of purified and reconstituted connexin43 hemichannels by protein kinase C-mediated phosphorylation of Serine 368. J Biol Chem *279*, 20058-20066.

Barr, L., Dewey, M. M., and Berger, W. (1965). Propagation of action potentials and the structure of the nexus in cardiac muscle. J Gen Physiol *48*, 797-823.

Becq, H., Jorquera, I., Ben-Ari, Y., Weiss, S., and Represa, A. (2005). Differential properties of dentate gyrus and CA1 neural precursors. J Neurobiol *62*, 243-261.

Belachew, S., Chittajallu, R., Aguirre, A. A., Yuan, X., Kirby, M., Anderson, S., and Gallo, V. (2003). Postnatal NG2 proteoglycan-expressing progenitor cells are intrinsically multipotent and generate functional neurons. J Cell Biol *161*, 169-186.

Belliveau, D. J., Bechberger, J. F., Rogers, K. A., and Naus, C. C. (1997). Differential expression of gap junctions in neurons and astrocytes derived from P19 embryonal carcinoma cells. Dev Genet *21*, 187-200.

Belliveau, D. J., and Naus, C. C. (1995). Cellular localization of gap junction mRNAs in developing rat brain. Dev Neurosci *17*, 81-96.

Belliveau, D. J., Kidder, G. M., and Naus, C. C. G. (1991). Expression of gap junction genes during postnatal neural development. Dev Genet *12*, 308-317.

Ben-Ari, Y. (1985). Limbic seizure and brain damage produced by kainic acid: mechanisms and relevance to human temporal lobe epilepsy. Neuroscience *14*, 375-403.

Benkovic, S. A., O'Callaghan, J. P., and Miller, D. B. (2004). Sensitive indicators of injury reveal hippocampal damage in C57BL/6J mice treated with kainic acid in the absence of tonic-clonic seizures. Brain Res *1024*, 59-76.

Bennett, M. V., Contreras, J. E., Bukauskas, F. F., and Saez, J. C. (2003). New roles for astrocytes: gap junction hemichannels have something to communicate. Trends Neurosci *26*, 610-617.

Bennett, S. A., and Melanson-Drapeau, L. (2003). Primary culture of adult neural progenitors. Methods Mol Med *79*, 397-404.

Bennett, S. A., Chen, J., Pappas, B. A., Roberts, D. C. S., and Tenniswood, M. (1998a). Alterations in platelet activating factor receptor expression associated with neuronal apoptosis in an in vivo model of excitotoxicity. Cell Death Differ *5*, 867-875.

Bennett, S. A., Pappas, B. A., Stevens, W. D., Davidson, C. M., Fortin, T., and Chen, J. (2000). Cleavage of amyloid precursor protein elicited by chronic cerebral hypoperfusion. Neurobiol Aging *21*, 207-214.

Bennett, S. A., Stevenson, B., Staines, W. A., and Roberts, D. C. S. (1995). Periodic acid-Schiff (PAS)-positive deposits in brain following kainic acid-induced seizures: relationships to fos induction, neuronal necrosis, reactive gliosis, and blood-brain barrier breakdown. Acta Neuropathol *89*, 126-138.

Bennett, S. A., Tenniswood, M., Chen, J. H., Davidson, C. M., Keyes, M. T., Fortin, T., and Pappas, B. A. (1998b). Chronic cerebral hypoperfusion elicits neuronal apoptosis and behavioral impairment. Neuroreport *9*, 161-166.

Bergoffen, J., Schere, S. S., Wang, S., Oronzi Scott, M., Bone, L. J., Paul, D. L., Chen, K., Lensch, M. W., Chance, P. F., and Fischbeck, K. H. (1993). Connexin mutations in X-linked Charcot-Marie-Tooth disease. Science *262*, 2039-2042.

Best, N., Mitchell, J., Baimbridge, K. G., and Wheal, H. V. (1993). Changes in parvalbumin-immunoreactive neurons in the rat hippocampus following a kainic acid lesion. Neurosci Lett *155*, 1-6.

Best, N., Mitchell, J., and Wheal, H. V. (1994). Ultrastructure of parvalbumin-immunoreactive neurons in the CA1 area of the rat hippocampus following a kainic acid injection. Acta Neuropathol *87*, 187-195.

Bevans, C. G., Kordel, M., Rhee, S. K., and Harris, A. L. (1998). Isoform composition of connexin channels determines selectivity among second messengers and uncharged molecules. J Biol Chem *273*, 2808-2816.
Beyer, E. C., Paul, D. L., and Goodenough, D. A. (1987). Connexin43: a protein from rat heart homologous to a gap junction protein. J Cell Biol *105*, 2621-2629.

Bilodeau, M. L., Ji, M., Paris, M., and Andrisani, O. M. (2005). Adenosine signaling promotes neuronal, catecholaminergic differentiation of primary neural crest cells and CNS-derived CAD cells. Mol Cell Neurosci *29*, 394-404.

Bittman, K., Owens, D. F., Kriegstein, A. R., and LoTurco, J. J. (1997). Cell coupling and uncoupling in the ventricular zone of the developing neocortex. J Neurosci *17*, 7037-7044.

Bittman, K. S., and LoTurco, J. J. (1999). Differential regulation of connexin 26 and 43 in murine neocortical precursors. Cereb Cortex *9*, 188-195.

Blanc, E. M., Bruce-Keller, A. J., and Mattson, M. P. (1998). Astrocytic gap junctional communication decreases neuronal vulnerability to oxidative stress-induced disruption of Ca2+ homeostasis and cell death. J Neurochem *70*, 958-970.

Bockamp, E., Maringer, M., Spangenberg, C., Fees, S., Fraser, S., Eshkind, L., Oesch, F., and Zabel, B. (2002). Of mice and models: improved animal models for biomedical research. Physiol Genomics *11*, 115-132.

Boucher, S., and Bennett, S. A. (2003). Differential connexin expression, gap junction intercellular coupling, and hemichannel formation in NT2/D1 human neural progenitors and terminally differentiated hNT neurons. J Neurosci Res *72*, 393-404.

Brezun, J. M., and Daszuta, A. (1999). Depletion in serotonin decreases neurogenesis in the dentate gyrus and the subventricular zone of adult rats. Neuroscience *89*, 999-1002.

Brissette, J. L., Kumar, N. M., Gilula, N. B., Hall, J. E., and Paolo Dotto, G. (1994). Switch in gap junction protein expression is associated with selective changes in junctional permeability during keratinocyte differentiation. Proc Natl Acad Sci USA *91*, 6453-6457.

Bruzzone, R. (2001). Learning the language of cell-cell communication through connexin channels. Genome Biol *2*, 4027.4021-4027.4025.

Bruzzone, R., White, T. W., and Paul, D. L. (1996). Connections with connexins: the molecular basis of direct intercellular signaling. Eur J Biochem *238*, 1-27.

Bruzzone, R., White, T. W., Scherer, S. S., Fischbeck, K. H., and Paul, D. L. (1994). Null mutations of connexin32 in patients with X-linked Charcot-Marie-Tooth disease. Neuron *13*, 1253-1260.

Buniello, A., Montanaro, D., Volinia, S., Gasparini, P., and Marigo, V. (2004). An expression atlas of connexin genes in the mouse. Genomics *83*, 812-820.

Burghaus, L., Schutz, U., Krempel, U., Lindstrom, J., and Schroder, H. (2003). Loss of nicotinic acetylcholine receptor subunits alpha4 and alpha7 in the cerebral cortex of Parkinson patients. Parkinsonism Relat Disord *9*, 243-246.

Caldwell, M. A., He, X., Wilkie, N., Pollack, S., Marshall, G., Wafford, K. A., and Svendsen, C. N. (2001). Growth factors regulate the survival and fate of cells derived from human neurospheres. Nat Biotechnol *19*, 475-479.

Cameron, H. A., and Gould, E. (1994). Adult neurogenesis is regulated by adrenal steroids in the dentate gyrus. Neuroscience *61*, 203-209.

Cameron, H. A., Hazel, T. G., and McKay, R. D. G. (1998). Regulation of neurogenesis by growth factors and neurotransmitters. J Neurobiol *36*, 287-306.

Cameron, H. A., McEwen, B. S., and Gould, E. (1995). Regulation of adult neurogenesis by excitatory input and NMDA receptor activation in the dentate gyrus. J Neurosci *15*, 4687-4692.

Cantallops, I., and Routtenberg, A. (2000). Kainic acid induction of mossy fiber sprouting: dependence on mouse strain. Hippocampus *10*, 269-273.

Castro, C., Gomez-Hernandez, J. M., Silander, K., and Barrio, L. C. (1999). Altered formation of hemichannels and gap junction channels caused by C-terminal connexin-32 mutations. J Neurosci *19*, 3752-3760.

Caveney, S. (1985). The role of gap junctions in development. Ann Rev Physiol *47*, 319-335.

Chang, M., Werner, R., and Dahl, G. (1996). A role for an inhibitory connexin in testis? Dev Biol *175*, 50-56.

Charles, A. (1998). Intercellular calcium waves in glia. Glia *24*, 39-49.

Charles, A. C., Naus, C. C., Zhu, D., Kidder, G. M., Dirksen, E. R., and Sanderson, M. J. (1992). Intercellular calcium signaling via gap junctions in glioma cells. J Cell Biol *118*, 195-201.

Chen, C. S., Mrksich, M., Huang, S., Whitesides, G. M., and Ingber, D. E. (1997). Geometric control of cell life and death. Science *276*, 1425-1428.

Cheung, E. C., Melanson-Drapeau, L., Cregan, S. P., Vanderluit, J. L., Ferguson, K. L., McIntosh, W. C., Park, D. S., Bennett, S. A., and Slack, R. S. (2005). Apoptosis-inducing

factor is a key factor in neuronal cell death propagated by BAX-dependent and BAX-independent mechanisms. J Neurosci *25*, 1324-1334.

Chiba, S., Iwasaki, Y., Sekino, H., and Suzuki, N. (2003). Transplantation of motoneuron-enriched neural cells derived from mouse embryonic stem cells improves motor function of hemiplegic mice. Cell Transplant *12*, 457-468.

Christie, M. J., and Jelinek, H. F. (1993). Dye-coupling among neurons of the rat locus coeruleus during postnatal development. Neuroscience *56*, 129-137.

Condorelli, D. F., Trovato-Salinaro, A., Mudo, G., Mirone, M. B., and Belluardo, N. (2003). Cellular expression of connexins in the rat brain: neuronal localization, effects of kainate-induced seizures and expression in apoptotic neuronal cells. Eur J Neurosci *18*, 1807-1827.

Connors, B. W., Benardo, L. S., and Prince, D. A. (1983). Coupling between neurons of the developing rat neocortex. J Neurosci *3*, 773-782.

Conti, L., Pollard, S. M., Gorba, T., Reitano, E., Toselli, M., Biella, G., Sun, Y., Sanzone, S., Ying, Q. L., Cattaneo, E., and Smith, A. (2005). Niche-independent symmetrical self-renewal of a mammalian tissue stem cell. PLoS Biol *3*, e283.

Contreras, J. E., Saez, J. C., Bukauskas, F. F., and Bennett, M. V. (2003a). Functioning of cx43 hemichannels demonstrated by single channel properties. Cell Commun Adhes *10*, 245-249.

Contreras, J. E., Saez, J. C., Bukauskas, F. F., and Bennett, M. V. L. (2003b). Gating and regulating of connexin 43 (Cx43) hemichannels. Proc Natl Acad Sci USA *100*, 11388-11393.

Contreras, J. E., Sanchez, H. A., Veliz, L. P., Bukauskas, F. F., Bennett, M. V., and Saez, J. C. (2004). Role of connexin-based gap junction channels and hemichannels in ischemia-induced cell death in nervous tissue. Brain Res Brain Res Rev *47*, 290-303.

Cooper-Kuhn, C. M., and Khun, H. G. (2002). Is it all DNA repair? Methodological considerations for detecting neurogenesis in the adult brain. Dev Brain Res *134*, 13-21.

Cornell-Bell, A. H., Finkbeiner, S. M., Cooper, M. S., and Smith, S. J. (1990). Glutamate induces calcium waves in cultured astrocytes: long-range glial signaling. Science *247*, 470-473.

Cotrina, M. L., Lin, J. H., and Nedergaard, M. (1998). Cytoskeletal assembly and ATP release regulate astrocytic calcium signaling. J Neurosci *18*, 8794-8804.

Dahl, G., Nonner, W., and Werner, R. (1994). Attempts to define functional domains of gap junction proteins with synthetic peptides. Biophys J *67*, 1816-1822.

Dang, X., Doble, B. W., and Kardami, E. (2003). The carboxy-tail of connexin-43 localizes to the nucleus and inhibits cell growth. Mol Cell Biochem *242*, 35-38.

Dawson, M. R., Levine J.M., Reynolds,R. (2000). NG2-expressing cells in the central nervous system: Are they oligodendroglial progenitors? J Neurosci Res *61*, 479.

De Maio, A., Vega, V. L., and Contreras, J. E. (2002). Gap junctions, homeostasis, and injury. J Cell Physiol *191*, 269-282.

De Mello, W. C. (1987). Cell-to-cell coupling assayed by means of electrical measurements. Experientia *43*, 1075-1079.

Dere, E., De Souza-Silva, M. A., Frisch, C., Teubner, B., Sohl, G., Willecke, K., and Huston, J. P. (2003). Connexin30-deficient mice show increased emotionality and decreased rearing activity in the open-field along with neurochemical changes. Eur J Neurosci *18*, 629-638.

Dermietzel, R., Farooq, M., Kessler, J. A., Althaus, H., Hertzberg, E. L., and Spray, D. C. (1997). Oligodendrocytes express gap junction protein connexin32 and connexin45. Glia *20*, 101-114.

Dermietzel, R., Gao, Y., Scemes, E., Vieira, D., Urban, M., Kremer, M., Bennett, M. V., and Spray, D. C. (2000). Connexin43 null mice reveal that astrocytes express multiple connexins. Brain Res Brain Res Rev *32*, 45-56.

Dermietzel, R., Hertberg, E. L., Kessler, J. A., and Spray, D. C. (1991). Gap junctions between cultured astrocytes immunocytochemical, molecular, and electrophysiological analysis. J Neurosci *11*, 1421-1432.

Dermietzel, R., and Spray, D. C. (1993). Gap junctions in the brain: where, what type, how many and why? Trends Neurosci *16*, 186-192.

Dermietzel, R., Traub, O., Hwang, T. K., Beyer, E., Bennett, M. V. L., and Spray, D. C. (1989). Differential expression of three gap junction proteins in developing and mature brain tissues. Proc Natl Acad Sci USA *86*, 10148-10152.

DeVries, S. H., and Schwartz, E. A. (1992). Hemi-gap-junction channels in solitary horizontal cells of the catfish retina. J Physiol *445*, 201-230.

Di Matteo, V., and Esposito, E. (2003). Biochemical and therapeutic effects of antioxidants in the treatment of Alzheimer's disease, Parkinson's disease and amyotrophic lateral sclerosis. Curr Drug Target CNS Neurol Disord *2*, 95-107.

Doetsch, F. (2003). The glial identity of neural stem cells. Nat Neurosci *6*, 1127-1134.

Dong, H., Csernansky, C. A., Goico, B., and Csernansky, J. G. (2003). Hippocampal neurogenesis follows kainic acid-induced apoptosis in neonatal rats. J Neurosci *23*, 1742-1749.

Dowling-Warriner, C. V., and Trosko, J. E. (2000). Induction of gap junctional intercellular communication, connexin43 expression, and subsequent differentiation in human fetal neuronal cells by stimulation of the cyclic AMP pathway. Neuroscience *95*, 859-868.
Duval, N., Gomes, D., Calaora, V., Calabrese, A., Meda, P., and Bruzzone, R. (2002). Cell coupling and Cx43 expression in embryonic mouse neural progenitor cells. J Cell Sci *115*, 3241-3251.

Dzwonek, K. (2005). NG2 expressing cells in hippocampal cultures survive neurotoxic insult and retain the ability to divide. Acta Neurobiol Exp *65*, 173-176.

Ebihara, L., Berthoud, V. M., and Beyer, E. C. (1995). Distinct behavior of connexin56 and connexin46 gap junctional channels can be predicted from the behavior of their hemi-gap-juncitonal channels. Biophys J *68*, 1796-1803.

Elfgang, C., Eckert, R., Lichtenberg-Frate, H., Butterweck, A., Traub, O., Klein, R. A., Hulser, D. F., and Willecke, K. (1995). Specific permeability and selective formation of gap junction channels in connexin-transfected HeLa cells. J Cell Biol *129*, 805-817.

Englund, U., Bjorklund, A., and Wictorin, K. (2002) Migration patterns and phenotypic differentiation of long-term expanded human neural progenitor cells after transplantation into the adult rat brain. Dev Brain Res *134*, 123-141.

Ferraro, T. N., Golden, G. T., Smith, G. G., and Berrettini, W. H. (1995). Differential susceptibility to seizures induced by systemic kainic acid treatment in mature DBA/2J and C57BL/6J mice. Epilepsia *36*, 301-307.

Frantseva, M. V., Kokarovtseva, L., Naus, C. G., Carlen, P. L., MacFabe, D., and Perez Velazquez, J. L. (2002a). Specific gap junctions enhance the neuronal vulnerability to brain traumatic injury. J Neurosci *22*, 644-653.

Frantseva, M. V., Kokarovtseva, L., and Perez Velazquez, J. L. (2002b). Ischemia-induced brain damage depends on specific gap-junctional coupling. J Cereb Blood Flow Metab *22*, 453-462.

Fraser, S. E., and Bryant, P. J. (1985). Patterns of dye coupling in the imaginal wing disk of Drosophila melanogaster. Nature *317*, 533-536.

Fraser, S. E., Green, C. R., Bode, H. R., and Gilula, N. B. (1987). Selective disruption of gap junctional communication interferes with a patterning process in hydra. Science *237*, 49-55.

Frisch, C., Theis, M., De Souza Silva, M. A., Dere, E., Sohl, G., Teubner, B., Namestkova, K., Willecke, K., and Huston, J. P. (2003). Mice with astrocyte-directed inactivation of

connexin43 exhibit increased exploratory behaviour, impaired motor capacities, and changes in brain acetylcholine levels. Eur J Neurosci *18*, 2313-2318.

Froes, M. M., Correia, A. H. P., Garcia-Abreu, J., Spray, D. C., De Carvalho, A. C. C., and Moura Neto, V. (1999). Gap-junctional coupling between neurons and astrocytes in primary central nervous system cultures. Proc Natl Acad Sci USA *96*, 7541-7546.

Froes, M. M., and de Carvalho, A. C. (1998). Gap junction-mediated loops of neuronal-glial interactions. Glia *24*, 97-107.

Fulton, B. P. (1995). Gap junctions in the developing nervous system. Perspect Dev Neurobiol *12*, 327-334.

Furshpan, E. J., and Potter, D. D. (1959). Transmission at the giant motor synapses of the crayfish. J Physiol *145*, 289-325.

Furshpan, E. J., and Potter, D. D. (1968). Low-resistance junctions between cells in embryos and tissue culture. Curr Top Dev Biol *3*, 95-127.

Gage, F. H. (2000). Mammalian neural stem cells. Science *267*, 1433-1438.

Gage, F. H., Kempermann, G., Palmer, T. D., Peterson, D. A., and Ray, J. (1998). Mulipotent progenitor cells in the adult dentate gyrus. J Neurobiol *36*, 249-266.

Gangemi, R. M. R., Perera, M., and Corte, G. (2004) Regulatory genes controlling cell fate choice in embryonic and adult neural stem cells. J Neurochem *89*, 286-306.

Garcia-Dorado, D., Inserte, J., Ruiz-Meana, M., Gonzalez, M. A., Solares, J., Julia, M., Barrabes, J. A., and Soler-Soler, J. (1997). Gap junction uncoupler heptanol prevents cell-to-cell progression of hypercontracture and limits necrosis during myocardial reperfusion. Circulation *96*, 3579-3586.

Garry, D. J., Masino, A. M., Meeson, A. P., and Martin, C. M. (2003). Stem cell biology and therapeutic applications. Curr Opin Nephrol Hypertens *12*, 447-454.

Giachino, C., De Marchis, S., Giampietro, C., Parlato, R., Perroteau, I., Schutz, G., Fasolo, A., and Peretto, P. (2005). cAMP response element-binding protein regulates differentiation and survival of newborn neurons in the olfactory bulb. J Neurosci *25*, 10105-10118.

Giaume, C., Fromaget, C., Elaoumari, A., Cordier, J., Glowinski, J., and Gros, D. (1991). Gap junctions in cultured astrocytes single channel currents and characterization of channel forming protein. Neuron *6*, 133-143.

Giaume, C., and Mccarthy, K. D. (1996). Control of gap-junctional communication in astrocytic networks. Trends Neurosci *19*, 319-325.

Giaume, C., and Venance, L. (1998). Intercellular calcium signaling and gap junctional communication in astrocytes. Glia *24*, 50-64.

Goldberg, G. S., Moreno, A. P., and Lampe, P. D. (2002). Gap junctions between cells expressing connexin 43 or 32 show inverse permselectivity to adenosine and ATP. J Biol Chem *277*, 36725-36730.

Goldberg, G. S., Valiunas, V., and Brink, P. R. (2004). Selective permeability of gap junction channels. Biochim Biophys Acta *1662*, 96-101.

Gomez-Hernandez, J. M., de Miguel, M., Larrosa, B., Gonzalez, D., and Barrio, L. C. (2003). Molecular basis of calcium regulation in connexin-32 hemichannels. Proc Natl Acad Sci USA *100*, 16030-16035.
Goodenough, D. A., Goliger, J. A., and Paul, D. L. (1996). Connexins, connexons, and intercellular communication. Annu Rev Biochem *65*, 475-502.

Goodenough, D. A., and Paul, D. L. (2003). Beyond the gap: functions of unpaired connexon channels. Nat Rev Mol Cell Biol *4*, 285-294.

Gould, E., Beylin, A., Tanapat, P., Reeves, A., and Shors, T. J. (1999). Learning enhances adult neurogenesis in the hippocampal formation. Nat Neurosci *2*, 260-265.

Gould, E., and Tanapat, P. (1999). Stress and hippocampal neurogenesis. Biol Psychiatry *46*, 1472-1479.

Gray, W. P., May, K., and Sundstrom, L. E. (2002). Seizure induced dentate neurogenesis does not diminish with age in rats. Neurosci Lett *330*, 235-238.

Gray, W. P., and Sundstrom, L. E. (1998). Kainic acid increases the proliferation of granule cell progenitors in the dentate gyrus of the adult rat. Brain Res *790*, 52-59.

Gritti, A., Bonfanti, L., Doetsch, F., Caille, I., Alvarez-Buylla, A., Lim, D. A., Galli, R., Verdugo, J. M., Herrera, D. G., and Vescovi, A. L. (2002). Multipotent neural stem cells reside into the rostral extension and olfactory bulb of adult rodents. J Neurosci *22*, 437-445.

Gritti, A., Parati, E. A., Cova, L., Frolichsthal, P., Galli, R., Wanke, E., Faravelli, L., Morassutti, D. J., Roisen, F., Nickel, D. D., and Vescovi, A. L. (1996). Multipotential stem cells from the adult mouse brain proliferate and self-renew in response to basic fibroblast growth factor. J Neurosci *16*, 1091-1100.

Guerrier, A., Fonlupt, P., Morand, I., Rabilloud, R., Audebet, C., Krutovskikh, V., Gros, D., Rousset, B., and Munari-Silem, Y. (1995). Gap junctions and cell polarity: connexin32 and connexin43 expressed in polarized thyroid epithelial cells assemble into separate gap junctions, which are located in distinct regions of the lateral plasma membrane domain. J Cell Sci *108 (Pt 7)*, 2609-2617.

Gulisano, M., Parenti, R., Spinella, F., and Cicirata, F. (2000). Cx36 is dynamically expressed during early development of mouse brain and nervous system. Neuroreport *11*, 3823-3828.

Guthrie, P. B., Knappenberger, J., Segal, M., Bennett, M. V., Charles, A. C., and Kater, S. B. (1999). ATP released from astrocytes mediates glial calcium waves. J Neurosci *19*, 520-528.

Guthrie, S. C., and Gilula, N. B. (1989). Gap junctional communication and develoment. Trends Neurosci *12*, 12-16.

Haefliger, J. A., Bruzzone, R., Jenkins, N. A., Gilbert, D. J., Copeland, N. G., and Paul, D. L. (1992). Four novel members of the connexin family of gap junction proteins: molecular cloning, expression and chromosome mapping. J Biol Chem *267*, 2057-2064.

Hahnlein, I., and Schuster, T. (1994). Decrease of gap junction number in the rat neural tube between ED 11 and ED 15. J Hirnforsch *35*, 549-557.

Hastings, N. B., and Gould, E. (1999). Rapid extension of axons into the CA3 region by adult-generated granule cells. J Comp Neurol *413*, 146-154.

Hofer, A., and Dermietzel, R. (1998). Visualization and functional blocking of gap junction hemichannels (connexons) with antibodies against external loop domains in astrocytes. Glia *24*, 141-154.

Holopainen, I. E., Järvelä, J., Lopez-Picon, F. R., Pelliniemi, L. J., and Kukko-Lukjanov, T. K. (2004). Mechanisms of kainate-induced region-specific neuronal death in immature organotypic hippocampal slice cultures. Neurochem Int *45*, 1-10.

Holthoff, K., and Witte, O. W. (2000). Directed spatial potassium redistribution in rat neocortex. Glia *29*, 288-292.

Hombach, S., Janssen-Bienhold, U., Sohl, G., Schubert, T., Bussow, H., Ott, T., Weiler, R., and Willecke, K. (2004). Functional expression of connexin57 in horizontal cells of the mouse retina. Eur J Neurosci *19*, 2633-2640.

Humphrey, W. M., Dong, H., Csernansky, C. A., and Csernansky, J. G. (2002). Immediate and delayed hippocampal neuronal loss induced by kainic acid during early postnatal development in the rat. Dev Brain Res *137*, 1-12.

Isakson, B. E., Evans, W. H., and Boitano, S. (2001a). Intercellular Ca2+ signaling in alveolar epithelial cells through gap junctions and by extracellular ATP. Am J Physiol Lung Cell Mol Physiol *280*, L221-L228.

Isakson, B. E., Lubman, R. L., Seedorf, G. J., and Boitano, S. (2001b). Modulation of pulmonary alveolar type II cell phenotype and communication by extracellular matrix and KGF. Am J Physiol Cell Physiol *281*, C1291-C1299.

John, S. A., Kondo, R., Wang, S.-Y., Goldhaber, J. I., and Weiss, J. N. (1999). Connexin-43 hemichannels opened by metabolic inhibition. J Biol Chem *274*, 236-240.

Jones, R. S. (1993). Entorhinal-hippocampal connections: a speculative view of their function. Trends Neurosci *16*, 58-64.

Kamermans, M., Fahrenfort, I., Schultz, K., Janssen-Bienhold, U., Sjoerdsma, T., and Weiler, R. (2001). Hemichannel-mediated inhibition in the outer retina. Science *292*, 1178-1180.
Kammermans, M., Fahrenfort, I., Schultz, K., Janssen-Bienhold, U., Sjoerdsma, T., and Weiler, R. (2001). Hemichannel-mediated inhibition in the outer retina. Science *292*, 1178-1180.

Kandler, K. (1997). Coordination of neuronal activity by gap junctions in the developing neocortex. Semin Cell Dev Biol *8*, 43-51.

Kandler, K., and Katz, L. C. (1995). Neuronal coupling and uncoupling in the developing nervous system. Curr Opin Neurobiol *5*, 98-105.

Kandler, K., and Katz, L. C. (1998). Coordination of neuronal activity in developing visual cortex by gap junction-mediated biochemical communication. J Neurosci *18*, 1419-1427.

Kanemitsu, M. Y., Loo, L. W., Simon, S., Lau, A. F., and Eckhart, W. (1997). Tyrosine phosphorylation of connexin 43 by v-Src is mediated by SH2 and SH3 domain interactions. J Biol Chem *272*, 22824-22831.

Kang, J., Jiang, L., Goldman, S. A., and Nedergaard, M. (1998). Astrocyte-mediated potentiation of inhibitory synaptic transmission. Nat Neurosci *1*, 683-692.

Kempermann, G., Kuhn, H. G., and Gage, F. H. (1997a). Genetic influence on neurogenesis in the dentate gyrus of adult mice. Proc Natl Acad Sci USA *94*, 10409-10414.

Kempermann, G., Kuhn, H. G., and Gage, F. H. (1997b). More hippocampal neurons in adult mice living in an enriched environment. Nature *386*, 493-495.

Kettenmann, H., and Ransom, B. R. (1988). Electrical coupling between astrocytes and between oligodendrocytes studied in mammalian cell cultures. Glia *1*, 64-73.

Kim, D. Y., Kam, Y., Koo, S. K., and Joe, C. O. (1999). Gating connexin 43 channels reconstituted in lipid vesicles by mitogen-activated protein kinase phosphorylation. J Biol Chem *274*, 5581-5587.

Kizer, J. S., Nemeroff, C. B., and Youngblood, W. W. (1977). Neurotoxic amino acids and structurally related analogs. Pharmacol Rev *29*, 301-318.

Kleopa, K. A., Orthmann, J. L., Enriquez, A., Paul, D. L., and Scherer, S. S. (2004). Unique distributions of the gap junction proteins connexin29, connexin32, and connexin47 in oligodendrocytes. Glia *47*, 346-357.

Komjati, K., Besson, V. C., and Szabo, C. (2005). Poly (adp-ribose) polymerase inhibitors as potential therapeutic agents in stroke and neurotrauma. Curr Drug Target CNS Neurol Disord *4*, 179-194.

Kondo, T., and Raff, M. (2000). Oligodendrocyte precursor cells reprogrammed to become multipotential stem cells. Science *289*, 1754-1757.
Kondziolka, D., Wechsler, L., Goldstein, S., Meltzer, C., Thulborn, K. R., Gebel, J., Jannetta, P., DeCesare, S., Elder, E. M., McGrogan, M., *et al.* (2000). Transplantation of cultured human neuronal cells for patients with stroke. Neurology *55*, 565-569.

Krysko, D. V., Leybaert, L., Vandenabeele, P., and D'Herde, K. (2005). Gap junctions and the propagation of cell survival and cell death signals. Apoptosis *10*, 459-469.

Kuhn, G., Dickinson-Anson, H., and Gage, F. H. (1996). Neurogenesis in the dentate gyrus of the adult rat: age-related decrease of neuronal progenitor proliferation. J Neurosci *16*, 2027-2033.

Kumar, N., M., and Gilula, N. B. (1996). The gap junction communication channel. Cell *84*, 381-388.

Kunzelmann, P., Blumcke, I., Traub, O., Dermietzel, R., and Willecke, K. (1997). Coexpression of connexin45 and -32 in oligodendrocytes of rat brain. J Neurocytol *26*, 17-22.

Laskowski, A., Schmidt, W., Dinkel, K., Martinez-Sanchez, M., and Reymann, K. G. (2005). bFGF and EGF modulate trauma-induced proliferation and neurogenesis in juvenile organotypic hippocampal slice cultures. Brain Res *1037*, 78-89.

Lassalle, J. M., Bataille, T., and Halley, H. (2000). Reversible inactivation of the hippocampal mossy fiber synapses in mice impairs spatial learning, but neither consolidation nor memory retrieval, in the Morris navigation task. Neurobiol Learn Mem *73*, 243-257.

Ledbetter, M. L., and Lubin, M. (1979). Transfer of potassium. A new measure of cell-cell coupling. J Cell Biol *80*, 150-165.

Lee, I., and Kesner, R. P. (2002). Differential contribution of NMDA receptors in hippocampal subregions to spatial working memory. Nat Neurosci *5*, 162-168.

Lee, S., Gilula, N. B., and Warner, A. E. (1987). Gap junctional communication and compaction during preimplantation stages of mouse development. Cell *51*, 851-860.

Lendahl, U., Zimmerman, L. B., and McKay, R. D. (1990). CNS stem cells express a new class of intermediate filament protein. Cell *60*, 585-595.

Levine, J. M., Stincone, F., and Lee, Y. S. (1993). Development and differentiation of glial precursor cells in the rat cerebellum. Glia *7*, 307-321.

Li, H., Liu, T. F., Lazrak, A., Peracchia, C., Goldberg, G. S., Lampe, P. D., and Johnson, R. G. (1996). Properties and regulation of gap junctional hemichannels in the plasma membranes of cultured cells. J Cell Biol *134*, 1019-1030.

Li, J., Hertzberg, E. L., and Nagy, J. I. (1997). Connexin32 in oliogdendrocytes and association with myelinated fibers in mouse and rat brain. J Comp Neurol *379*, 571-591.

Lie, D. C., Colamarino, S. A., Song, H. J., Desire, L., Mira, H., Consiglio, A., Lein, E. S., Jessberger, S., Lansford, H., Dearie, A. R., and Gage, F. H. (2005). Wnt signalling regulates adult hippocampal neurogenesis. Nature *437*, 1370-1375.

Lim, D. A., and Alvarez-Buylla, A. (1999). Interaction between astrocytes and adult subventricular zone precursors stimulates neurogenesis. Proc Natl Acad Sci USA *96*, 7526-7531.

Lin, J. H., Weigel, H., Cotrin, M. L., Liu, S., Bueno, E., Hansen, A. J., Hansen, T. W., Goldman, S., and Nedergaard, M. (1998). Gap-junction-mediated propagation and amplification of cell injury. Nat Neurosci *1*, 432.

Lin, J. H. C., Yang, J., Liu, S., Takano, T., Wang, X., Gao, Q., Willecke, K., and Nedergaard, M. (2003). Connexin mediates gap junction-independent resistance to cellular injury. J Neurosci *23*, 430-441.

Liu, T. F., Li, H. Y., Atkinson, M. M., and Johnson, R. G. (1995). Intracellular lucifer yellow leakage from Novikoff cells in the presence of ATP or low extracellular Ca: evidence for hemi-gap junction channels. Methods Find Exp Clin Pharmacol *17*, 23-28.

Lo Turco, J. J., and Kriegstein, A. R. (1991). Clusters of coupled neuroblasts in embryonic neocortex. Science *252*, 563-566.

Lopez, O. L., and Becker, J. T. (2002). Treatment of Alzheimer's disease. Rev Neurol *35*, 850-859.

Luskin, M. B. (1998). Neuroblasts of the postnatal mammalian forebrain: their phenotype and fate. J Neurobiol *36*, 221-233.

Macklis, J. D. (2001). Neurobiology: New memories from new neurons. Nature *410*, 314-315, 317.

MacVicar, B. A., and Dudek, F. E. (1981). Electrotonic coupling between pyramidal cells: a direct demonstration in rat hippocampal slices. Science *213*, 782-785.

Magavi, S. S., Leavitt, B. R., and Macklis, J. D. (2000). Induction of neurogenesis in the neocortex of adult mice. Nature *405*, 951-955.

Magavi, S. S., and Macklis, J. D. (2002). Induction of neuronal type-specific neurogenesis in the cerebral cortex of adult mice: manipulation of neural precursors in situ. Brain Res Dev Brain Res *134*, 57-76.

Maric, D., and Barker, J. L. (2004). Neural stem cells redefined: a FACS perspective. Mol Neurobiol *30*, 49-76.

Markakis, E. A., and Gage, F. H. (1999). Adult-generated neurons in the dentate gyrus send axonal projections to field CA3 and are surrounded by synaptic vesicles. J Comp Neurol *406*, 449-460.

Massa, P. T., and Mugnaini, E. (1982). Cell junctions and intramembrane particles of astrocytes and oligodendrocytes: a freeze-fracture study. Neuroscience *7*, 523-538.

Matsumoto, A., Arai, Y., Urano, A., and Hyodo, S. (1991). Cellular localization of gap junction messenger RNA in the neonatal rat brain. Neurosci Lett *124*, 225-228.

Matyas, F., Freund, T. F., and Gulyas, A. I. (2004). Immunocytochemically defined interneuron populations in the hippocampus of mouse strains used in transgenic technology. Hippocampus *14*, 460-481.

McBride, J. L., Behrstock, S. P., Chen, E. Y., Jakel, R. J., Siegel, I., Svendsen, C. N., and Kordower, J. H. (2004). Human neural stem cell transplants improve motor function in a rat model of Huntington's disease. J Comp Neurol *475*, 211-219.

Mckhann, G. M. 2nd, Wenzel, H. J., Robbins, C. A., Sosunov, A. A., and Schwartzroin, P. A. (2003). Mouse strain differences in kainic acid sensitivity, seizure behavior, mortality, and hippocampal pathology. Neuroscience *122*, 551-561.

Melanson-Drapeau, L., Beyko, S., Davé, S., Hebb, A. L. O., Franks, D. J., Sellito, C., Paul, D. L., and Bennett, S. A. (2003). Oligodendrocyte progenitor enrichment in the connexin32 null-mutant mouse. J Neurosci *23*, 1759-1768.

Meltzer, C. C., Kondziolka, D., Villemagne, V. L., Wechsler, L., Goldstein, S., Thulborn, K. R., Gebel, J., Elder, E. M., DeCesare, S., and Jacobs, A. (2001). Serial [18F] fluorodeoxyglucose positron emission tomography after human neuronal implantation for stroke. Neurosurgery *49*, 586-591; discussion 591-582.

Mercier, F., and Hatton, G. L. (2001). Connexin 26 and basic fibroblast growth factor are expressed primarily in the suppial and subependymal layers in adult brain parenchyma: roles in stem cell proliferation and morphological plasticity? J Comp Neurol *431*, 88-104.

Mergenthaler, P., Dirnagi, U., and Meisel, A. (2004). Pathophysiology of stroke: lessons from animal models. Metab Brain Dis *19*, 151-167.

Milks, L. C., Kumar, N. M., Houghten, R., Unwin, N., and Gilula, N. B. (1988). Topology of the 32-kd liver gap junction protein determined by site-directed antibody localizations. EMBO J *7*, 2967-2975.

Moffitt, P. (1994). A methyl green-pyronin technique for demonstrating cell death in the murine tumour S180. Cell Biol Int *18*, 677-679.

Mollgard, K., and Moller, M. (1975). Dendrodendritic gap junctions: a developmental approach. Adv Neurol *12*, 79-89.

Morshead, C. M., Benveniste, P., Iscove, N. N., and van der Kooy, D. (2002). Hematopoietic competence is a rare property of neural stem cells that may depend on genetic and epigenetic alterations. Nat Med *8*, 268-273.

Morshead, C. M., Reynolds, B. A., Craig, C. G., McBurney, M. W., Staines, W. A., Morassutti, D., Weiss, S., and Van der Kooy, D. (1994). Neural stem cells in the adult mammalian forebrain: a relatively quiescent subpopulation of subependymal cells. Neuron *13*, 1071-1082.

Nadarajah, B., Jones, A. M., Evans, W. H., and Parnavelas, J. G. (1997). Differential expression of connexins during neocortical development and neuronal circuit formation. J Neurosci *17*, 3096-3111.

Nadarajah, B., Makarenkova, H., Becker, D. L., Evans, W. H., and Parnavelas, J. G. (1998). Basic FGF increases communication between cells of the developin neocortex. J Neurosci *18*, 7881-7890.

Nadel, L., and Moscovitch, M. (1998). Hippocampal contributions to cortical plasticity. Neuropharmacology *37*, 431-439.

Nadler, J. V. (1981). Minireview. Kainic acid as a tool for the study of temporal lobe epilepsy. Life Sci *29*, 2031-2042.

Nadler, J. V., Perry, B. W., Gentry, C., and Cotman, C. W. (1980). Degeneration of hippocampal CA3 pyramidal cells induced by intraventricular kainic acid. J Comp Neurol *192*, 333-359.

Nagy, J. I., Ionescu, A. V., Lynn, B. D., and Rash, J. E. (2003a). Connexin29 and connexin32 at oligodendrocyte and astrocyte gap junctions and in myelin of the mouse central nervous system. J Comp Neurol *464*, 356-370.

Nagy, J. I., Ionescu, A. V., Lynn, B. D., and Rash, J. E. (2003b). Coupling of astrocyte connexins Cx26, Cx30, Cx43 to oligodendrocyte Cx29, Cx32, Cx47: Implications from normal and connexin32 knockout mice. Glia *44*, 205-218.

Nagy, J. I., and Rash, J. E. (2000). Connexins and gap junctions of astrocytes and oligodendrocytes in the CNS. Brain Res Dev Brain Res Rev *32*, 29-44.

Nakagawa, E., Aimi, Y., Yasuhara, O., Tooyama, I., Shimada, M., McGeer, P. L., and Kimura, H. (2000). Enhancement of progenitor cell division in the dentate gyrus triggered by initial limbic seizures in rat models of epilepsy. Epilepsia *41*, 10-18.

Nakase, T., and Naus, C. C. (2004). Gap junctions and neurological disorders of the central nervous system. Biochim Biophys Acta *1662*, 149-158.

Nakatomi, H., Kuriu, T., Okabe, S., Yamamoto, S., Hatano, O., Kawahara, N., Tamura, A., Kirino, T., and Nakafuku, M. (2002). Regeneration of hippocampal pyramidal neurons after ischemic brain injury by recruitment of endogenous neural progenitors. Cell *110*, 429-441.

Naus, C. C., Belliveau, D. J., and Bechberger, J. F. (1990). Regional differences in connexin32 and connexin43 messenger RNAs in rat brain. Neurosci Lett *111*, 297-302.

Nedergaard, M. (1994). Direct signaling from astrocytes to neurons in cultures of mammalian brain cells. Science *263*, 1768-1771.

Nelles, E., Buetzler, C., Jung, D., Temme, A., Gabriel, H. D., Dahl, U., Traub, O., Stuempel, F., Jungermann, K., Zielasek, J., *et al.* (1996). Defective propagation of signals generated by sympathetic nerve stimulation in the liver of connexin32-deficient mice. Proc Natl Acad Sci USA *93*, 9565-9570.

Nelson, P. T., Kondziolka, D., Wechsler, L., Goldstein, S., Gebel, J., DeCesare, S., Elder, E. M., Zhang, P. J., Jacobs, A., McGrogan, M., *et al.* (2002). Clonal human (hNT) neuron grafts for stroke therapy: neuropathology in a patient 27 months after implantation. Am J Pathol *160*, 1201-1206.

Newhouse, P. A., Potter, A., Kelton, M., and Corwin, J. (2001). Nicotinic treatment of Alzheimer's disease. Biol Psychiatry *49*, 268-278.

Newman, E. A. (1986). High potassium conductance in astrocyte endfeet. Science *233*, 453-454.

Nicholson, B. J., Weber, P. A., Cao, F., Chang, H., Lampe, P., and Goldberg, G. (2000). The molecular basis of selective permeability of connexins is complex and includes both size and charge. Braz J Med Biol Res *33*, 369-378.

Nicholson, S. M., and Bruzzone, R. (1997). Gap junctions: getting the message through. Curr Biol *7*, R340-344.

Nicholson, S. M., Ressot, C., Gomes, D., D'Andrea, P., Perea, J., Duval, N., and Bruzzone, R. (1999). Connexin32 in the peripheral nervous system. Functional analysis of mutations associated with X-linked Charcot-Marie-Tooth syndrome and implications for the pathophysiology of the disease. Ann NY Acad Sci *883*, 168-185.

Nilsson, M., Perfilieva, E., Johansson, U., Orwar, O., and Eriksson, P. S. (1999). Enriched environment increases neurogenesis in the adult rat dentate gyrus and improves spatial memory. J Neurobiol *39*, 569-578.

Ochalski, P. A. Y., Frankenstein, U. N., Hertzberg, E. L., and Nagy, J. I. (1997). Connexin-43 in rat spinal cord: localization in astrocytes and identification of heterotypic astro-oligodendrocytic gap junctions. Neuroscience *76*, 931-945.

Odermatt, B., Wellershaus, K., Wallraff, A., Seifert, G., Degen, J., Euwens, C., Fuss, B., Bussow, H., Schilling, K., Steinhauser, C., and Willecke, K. (2003). Connexin 47 (Cx47)-deficient mice with enhanced green fluorescent protein reporter gene reveal predominant oligodendrocytic expression of Cx47 and display vacuolized myelin in the CNS. J Neurosci *23*, 4549-4559.

Oguro, K., Jover, T., Tanaka, H., Lin, Y., Kojima, T., Oguro, N., Grooms, S. Y., Bennett, M. V., and Zukin, R. S. (2001). Global ischemia-induced increases in the gap junctional proteins connexin 32 (Cx32) and Cx36 in hippocamapus and enhanced vulnerability of Cx32 knock-out mice. J Neurosci *21*, 7534-7542.

Owens, D. F., and Kriegstein, A. R. (1998). Patterns of intracellular calcium fluctuation in precursor cells of the neocortical ventricular zone. J Neurosci *18*, 5374-5388.

Palmer, T. D., Markakis, E. A., Willhoite, A. R., Safar, F., and Gage, F. H. (1999). Fibroblast growth factor-2 activates a latent neurogenic program in neural stem cells from diverse regions of the adult CNS. J Neurosci *19*, 8487-8497.

Parent, J. M., Yu, T. W., Leibowitz, R. T., Geschwind, D. H., Sloviter, R. S., and Lowenstein, D. H. (1997). Dentate granule cell neurogenesis is increased by seizures and contributes to aberrant network reorganization in the adult rat hippocampus. J Neurosci *17*, 3727-3738.

Parenti, R., Campisi, A., Vanella, A., and Cicirata, F. (2002). Immunocytochemical and RT-PCR analysis of connexin36 in cultures of mammalian glial cells. Arch Ital Biol *140*, 101-108.

Parnavelas, J. G., Luder, R., Pollard, S. G., Sullivan, K., and Lieberman, A. R. (1983). A qualitative and quantitative ultrastructural study of glial cells in the developing visual cortex. Philos Trans R Soc Lond B Biol Sci *10*, 103-114.

Parpura, V., and Haydon, P. G. (2000). Physiological astrocytic calcium levels stimulate glutamate release to modulate adjacent neurons. Proc Natl Acad Sci USA *97*, 8629-8634.
Pasti, L., Volterra, A., Pozzan, T., and Carmignoto, G. (1997). Intracellular calcium oscillations in astrocytes: a highly plastic, bidirectional form of communication between neurons and astrocytes in situ. J Neurosci *17*, 7817-7830.

Paul, D. L. (1995). New functions for gap junctions. Curr Opin Cell Biol *7*, 665-672.

Paul, D. L., Ebihara, L., Takemoto, L. J., Swenson, K. I., and Goodenough, D. A. (1991). Connexin46, a novel lens gap junction protein, induces voltage-gated currents in nonjunctional plasma membrane of Xenopus oocytes. J Cell Biol *115*, 1077-1089.

Peinado, A., Yuste, R., and Katz, L. C. (1993a). Extensive dye coupling between rat neocortical neurons during the period of circuit formation. Neuron *10*, 103-114.

Peinado, A., Yuste, R., and Katz, L. C. (1993b). Gap junctional communication and the development of local circuits in neocortex. Cereb Cortex *3*, 488-498.

Pollard, H., Cantagrel, S., Charriaut-Marlangue, C., Moreau, J., and Ben-Ari, Y. (1994). Apoptosis associated DNA fragmentation in epileptic brain damage. Neuroreport *5*, 1053-1055.

Qin, H., Shao, Q., Curtis, H., Galipeau, J., Belliveau, D. J., Wang, T., Alaoui-Jamali, M. A., and Laird, D. W. (2002). Retroviral delivery of connexin genes to human breast tumor cells inhibits in vivo tumor growth by a mechanism that is independent of significant gap junctional intercellular communication. J Biol Chem *277*, 29132-29138.

Rami, A., Volkmann, T., and Winckler, J. (2001). Effective reduction of neuronal death by inhibiting gap junctional intercellular communication in a rodent model of global transient cerebral ischemia. Exp Neurol *170*, 297-304.

Ransom, B. R., and Kettenmann, H. (1990). Electrical coupling, without dye coupling, between mammalian astrocytes and oligodendrocytes in cell culture. Glia *3*, 258-266.

Rash, J. E., Duffy, H. S., Dudek, F. E., Bilhartz, B. L., Whalen, L. R., and Yasumura, T. (1997). Grid-mapped freeze-fracture analysis of gap junctions in gray and white matter of adult rat central nervous system, with evidence for a "panglial syncytium" that is not coupled to neurons. J Comp Neurol *388*, 265-292.

Rash, J. E., Staines, W. A., Yasumura, T., Patel, D., Furman, C. S., Stelmack, G. L., and Nagy, J. L. (2000). Immunogold evidence that neuronal gap junctions in adult rat brain and

spinal cord contain connexin-36 but not connexin-32 or connexin-43. Proc Natl Acad Sci USA *97*, 7573-7578.

Rash, J. E., Yasumura, T., and Dudek, F. E. (1998). Ultrastructure, histological distribution, and freeze-fracture immunocytochemistry of gap junctions in rat brain and spinal cord. Cell Biol Int *22*, 731-749.

Rash, J. E., Yasumura, T., Dudek, F. E., and Nagy, J. I. (2001). Cell-specific expression of connexins and evidence of restricted gap junctional coupling between glial cells and between neurons. J Neurosci *21*, 1983-2000.

Rawanduzy, A., Hansen, A., Hansen, T. W., and Nedergaard, M. (1997). Effective reduction of infarct volume by gap junction blockade in a rodent model of stroke. J Neurosurg *87*. 916-920.

Revel, J. P., and Karnosvsky, M. J. (1967). J Cell Biol *33*, C7-C12.

Reynolds, B. A., and Weiss, S. (1992). Generation of neurons and astrocytes from isolated cells of the adult mammalian central nervous system. Science *255*, 1707-1710.

Reynolds, R., Hardy, R. (1997). Oligodendroglial progenitors labeled with the O4 antibody persist in the adult rat cerebral cortex in vivo. J Neurosci Res *47*, 455-470.

Risek, B., Klier, F. G., and Gilula, N. B. (1994). Developmental regulation and structural organization of connexins in epidermal gap junctions. Dev Biol *164*, 183-196.

Ros, J., Pellerin, L., Magara, F., Dauguet, J., Schenk, F., and Magistretti, P. J. (2005). Metabolic activation pattern of distinct hippocampal subregions during spatial learning and memory retrieval. J Cereb Blood Flow Metab *Epub*.

Rouach, N., Avignone, E., Meme, W., Koulakoff, A., Venance, L., Blomstrand, F., and Giaume, C. (2002). Gap junctions and connexin expression in the normal and pathological central nervous system. Biol Cell *94*, 457-475.

Royle, S. J., Collins, F. C., Rupniak, H. T., Barnes, J. C., and Anderson, R. (1999). Behavioural analysis and susceptibility to CNS injury of four inbred strains of mice. Brain Res *816*, 337-349.

Rozental, R., Giaume, C., and Spray, D. C. (2000a). Gap junctions in the nervous system. Brain Res Dev Brain Res Rev *32*, 11-15.

Rozental, R., Morales, M., Mehler, M. F., Urban, M., Kremer, M., Dermeitzel, R., Kessler, J. A., and Spray, D. C. (1998). Changes in the properties of gap junctions during neuronal differentiation of hippocampal progenitor cells. J Neurosci *18*, 1753-1762.

Rozental, R., Srinivas, M., Gokhan, S., Urban, M., Dermietzel, R., Kessler, J. A., Spray, D. C., and Mehler, M. F. (2000b). Temporal expression of neuronal connexins during hippocampal ontogeny. Brain Res Brain Res Rev *32*, 57-71.

Saez, J. C., Contreras, J. E., Bukauskas, F. F., Retamal, M. A., and Bennett, M. V. L. (2003). Gap junction hemichannels in astrocytes of the CNS. Acta Physiol Scand *179*, 9-22.

Saito, R., Graf, R., Hubel, K., Fujita, T., Rosner, G., and Heiss, W. D. (1997). Reduction of infarct volume by halothane: effect on cerabral blood flow or perifocal spreading depression-like depolarizations. J Cereb Blood Flow Metab *17*, 857-864.

Sanon, N., Carmant, L., Emond, M., Congar, P., and Lacaille, J. C. (2005). Short-term effects of kainic acid on CA1 hippocampal interneurons differentially vulnerable to excitotoxicity. Epilepsia *46*, 837-848.

Scharfman, H. E., Goodman, J. H., and Sollas, A. L. (2000). Granule-like neurons at the hilar/CA3 border after status epilepticus and their synchrony with area CA3 pyramidal cells: functional implications of seizure-induced neurogenesis. J Neurosci *20*, 6144-6158.

Schauwecker, P. E., Ramirez, J. J., and Steward, O. (2000). Genetic dissection of the signals that induce synaptic reorganization. Exp Neurol *161*, 139-152.

Scherer, S. S., Deschenes, S. M., Xu, Y., Grinspan, J. B., Fischbeck, K. H., and Paul, D. L. (1995). Connexin32 is a myelin-related protein in the PNS and CNS. J Neurosci *15*, 8281-8294.

Scherer, S. S., Xu, Y. T., Nelles, E., Fischbeck, K., Willecke, K., and Bone, L. J. (1998). Connexin32-null mice develop demyelinating peripheral neuropathy. Glia *24*, 8-20.

Schmitt, W. B., Sprengel, R., Mack, V., Draft, R. W., Seeburg, P. H., Deacon, R. M., Rawlins, J. N., and Bannerman, D. M. (2005). Restoration of spatial working memory by genetic rescue of GluR-A-deficient mice. Nat Neurosci *8*, 270-272.

Seaberg, R. M., and van der Kooy, D. (2002). Adult rodent neurogenic regions: the ventricular subependyma contains neural stem cells, but the dentate gyrus contains restricted progenitors. J Neurosci *22*, 1784-1793.

Seaberg, R. M., and van der Kooy, D. (2003). Stem and progenitor cells: the premature desertion of rigorous definitions. Trends Neurosci *26*, 125-131.

Seri, B., Garcia-Verdugo, J. M., McEwen, B. S., and Alvarez-Buylla, A. (2001). Astrocytes give rise to new neurons in the adult mammalian hippocampus. J Neurosci *21*, 7153-7160.

Shihabuddin, L. S., Horner, P. J., Ray, J., and Gage, F. H. (2000). Adult spinal cord stem cells generate neurons after transplantation in the adult dentate gyrus. J Neurosci *20*, 8727-8735.

Sik, A., Penttonen, M., and Buzsaki, G. (1997). Interneurons in the hippocampal dentate gyrus: an in vivo intracellular study. Eur J Neurosci *9*, 573-588.

Singh, D., Solan, J. L., Taffet, S. M., Javier, R., and Lampe, P. D. (2005). Connexin 43 interacts with zona occludens-1 and -2 proteins in a cell cycle stage-specific manner. J Biol Chem *280*, 30416-30421.

Singh, S. K., Clarke, I. D., Hide, T., and Dirks, P. B. (2004a). Cancer stem cells in nervous system tumors. Oncogene *23*, 7267-7273.

Singh, S. K., Clarke, I. D., Terasaki, M., Bonn, V. E., Hawkins, C., Squire, J., and Dirks, P. B. (2003). Identification of a cancer stem cell in human brain tumors. Cancer Res *63*, 5821-5828.

Singh, S. K., Hawkins, C., Clarke, I. D., Squire, J. A., Bayani, J., Hide, T., Henkelman, R. M., Cusimano, M. D., and Dirks, P. B. (2004b). Identification of human brain tumour initiating cells. Nature *432*, 396-401.

Smith, C. M., and Luskin, M. B. (1998). Cell cycle length of olfactory bulb neuronal progenitors in the rostral migratory stream. Dev Dyn *213*, 220-227.

Sohl, G., Degen, J., Teubner, B., and Willecke, K. (1998). The murine gap junction gene connexin36 is highly expressed in mouse retina and regulated during brain development. FEBS Lett *428*, 27-31.

Sohl, G., Eiberger, J., Jung, Y. T., Kozak, C. A., and Willecke, K. (2001). The mouse gap junction gene connexin29 is highly expressed in sciatic nerve and regulated during brain development. Biol Chem *382*, 913-918.

Sohl, G., Odermatt, B., Maxeiner, S., Degen, J., and Willecke, K. (2004). New insights into the expression and function of neural connexins with transgenic mouse mutants. Brain Res Rev *47*, 245-259.

Sohl, G., Theis, M., Hallas, G., Brambach, S., Dahl, E., Kider, G., and Willecke, K. (2001b). A new alternatively spliced transcipt of the mouse connexin32 gene is expressed in embryonic stem cells, oocytes, and liver. Exp Cell Res *266*, 177-186.

Song, H., Stevens, C. F., and Gage, F. H. (2002). Astroglia induce neurogenesis from adult neural stem cells. Nature *417*, 39-44.

Spassky, N., Olivier, C., Cobos, I., LeBras, B., Goujet-Zalc, C., Martinez, S., Zalc, B., Thomas, J.L. (2001). The early steps of oligodendrogenesis: insights from the study of the plp lineage in the brain of chicks and rodents. Dev Neurosci *23*, 318-326.

Srinivas, M., Rozental, R., Kojima, T., Dermietzel, R., Mehler, M., Condorelli, D. F., Kessler, J. A., and Spray, D. C. (1999). Functional properties of channels formed by the neuronal gap junction protein connexin36. J Neurosci *19*, 9848-9855.

Stanfield, B. B., and Trice, J. E. (1988). Evidence that granule cells generated in the dentate gyrus of adult rats extend axonal projections. Exp Brain Res *72*, 399-406.

Steinberg, T. H., Civitelli, R., Geist, S. T., Robertson, A. J., Hick, E., Veenstra, R. D., Wang, H. Z., Warlow, P. M., Westphale, E. M., and Laing, J. G. (1994). Connexin43 and connexin45 form gap junctions with different molecular permeabilities in osteoblastic cells. EMBO J *13*, 744-750.

Steiner, B., Kronenberg, G., Jessberger, S., Brandt, M. D., Reuter, K., and Kempermann, G. (2004). Differential regulation of gliogenesis in the context of adult hippocampal neurogenesis in mice. Glia *46*, 41-52.

Stout, C., Goodenough, D. A., and Paul, D. L. (2004). Connexins: functions without junctions. Curr Opin Cell Biol *16*, 507-512.

Stout, C. E., Costantin, J. L., Naus, C. C., and Charles, A. C. (2002). Intercellular calcium signaling in astrocytes via ATP release through connexin hemichannels. J Biol Chem *277*, 10482-10488.

Strain, S. M., and Tasker, R. A. R. (1991). Hippocampal damage produced by systemic injections of domoic acid in mice. Neuroscience *44*, 343-352.

Suh, Y. H., and Checler, F. (2002). Amyloid precursor protein, presenilins, and alpha-synuclein: molecular pathogenesis and pharmacological applications in Alzheimer's disease. Pharmacol Rev *54*, 469-525.

Taguchi, A., Soma, T., Tanaka, H., Kanda, T., Nishimura, H., Yoshikawa, H., Tsukamoto, Y., Iso, H., Fujimori, Y., Stern, D. M., *et al.* (2004). Administration of CD34+ cells after stroke enhances neurogenesis via angiogenesis in a mouse model. J Clin Invest *114*, 330-338.

Tanapat, P., Galea, L. A., and Gould, E. (1998). Stress inhibits the proliferation of granule cell precursors in the developing dentate gyrus. Int J Dev Neurosci *16*, 235-239.

Tanapat, P., Hastings, N. B., Reeves, A. J., and Gould, E. (1999). Estrogen stimulates a transient increase in the number of new neurons in the dentate gyrus of the adult female rat. J Neurosci *19*, 5792-5801.

Taupin, P. (2005). Adult neurogenesis in the mammalian central nervous system: functionality and potential clinical interest. Med Sci Monit *11*, RA247-252.

Teubner, B., Odermatt, B., Guldenagel, M., Sohl, G., Degen, J., Bukauskas, F., Kronengold, J., Verselis, V. K., Jung, Y. T., Kozak, C. A., *et al.* (2001). Functional expression of the new gap junction gene connexin47 transcribed in mouse brain and spinal cord neurons. J Neurosci *21*, 1117-1126.

Theis, M., Sohl, G., Eiberger, J., and Willecke, K. (2005). Emerging complexities in identity and function of glial connexins. Trends Neurosci *28*, 188-195.

Toumane, A., Durkin, T., Marighetto, A., Galey, D., and Jaffard, R. (1988). Differential hippocampal and cortical cholinergic activation during the acquisition, retention, reversal and extinction of a spatial discrimination in an 8-arm radial maze by mice. Behav Brain Res *30*, 225-234.

Toyofuku, T., Yabuki, M., Otsu, K., Kuzuya, T., Hori, M., and Tada, M. (1998). Direct association of the gap junction protein connexin-43 with ZO-1 in cardiac myocytes. J Biol Chem *273*, 12725-12731.

Trexler, E. B., Bennett, M. V. L., Bargiello, T. A., and Verselis, V. K. (1996). Voltage gating and permeation in a gap junction hemichannel. Proc Natl Acad Sci USA *93*, 5836-5841.

Trexler, E. B., Bukauskas, F. F., Bennett, M. V., Bargiello, T. A., and Verselis, V. K. (1999). Rapid and direct effects of pH on connexins revealed by the connexin46 hemichannel preparation. J Gen Physiol *113*, 721-742.

Turin, L., and Warner, A. (1977). Carbon dioxide reversibly abolishes ionic communication between cells of early amphibian embryo. Nature *270*, 56-57.

Unwin, P. N., and Ennis, P. D. (1983). Calcium-mediated changes in gap junction structure: evidence from the low angle X-ray pattern. J Cell Biol *97*, 1459-1466.

Unwin, P. N., and Ennis, P. D. (1984). Two configurations of a channel-forming membrane protein. Nature *307*, 609-613.

Valiunas, V. (2002). Biophysical properties of connexin-45 gap junction hemichannels studies in vertebrate cells. J Gen Physiol *119*, 147-164.

van Praag, H., Kempermann, G., and Gage, F. H. (1999). Running increases cell proliferation and neurogenesis in the adult mouse dentate gyrus. Nat Neurosci *2*, 266-270.

Veenstra, R. D. (1996). Size and selectivity of gap junction channels formed from different connexins. J Bioenerg Biomembr *28*, 327-337.

Venance, L., Cordier, J., Monge, M., Zalc, B., Glowinski, J., and Giaume, C. (1995). Homotypic and heterotypic coupling mediated by gap junctions during glial cell differentiation in vitro. Eur J Neurosci *7*, 451-461.

Venance, L., Glowinski, J., and Giaume, C. (2004). Electrical and chemical transmission between striatal GABAergic output neurones in rat brain slices. J Physiol *559*, 215-230.

Venance, L., Rozov, A., Blatow, M., Burnashev, N., Feldmeyer, D., and Monyer, H. (2000). Connexin expression in electrically coupled postnatal rat brain neurons. Proc Natl Acad Sci USA *97*, 10260-10265.

Waldvogel, H. J., Faull, R. L. M., Williams, M. N., and Dragunow, M. (1991). Differential sensitivity of calbindin and parvalbumin immunoreactive cells in the striatum to excitotoxins. Brain Res *546*, 329-335.

Walsh, J. P., Cepeda, C., Hull, C. D., Fisher, R. S., Levine, M. S., and Buchwald, N. A. (1989). Dye-coupling in the neostriatum of the rat: II. Decreased coupling between neurons during development. Synapse *4*, 238-247.

Wang, J. H., Ko, G. Y., and Kelly, P. T. (1997). Cellular and molecular bases of memory: synaptic and neuronal plasticity. J Clin Neurophysiol *14*, 264-293.

Wang, S., Scott, B. W., and Wojtowicz, J. M. (2000). Heterogenous properties of dentate granule neurons in the adult rat. J Neurobiol *42*, 248-257.

Wang, Y. L., Sun, R. P., Lei, G. F., Wang, J. W., and Guo, S. H. (2004). Neurogenesis of dentate granule cells following kainic acid induced seizures in immature rats. Zhonghua Er Ke Za Ahi *42*, 621-624.

Warner, A. E., Guthrie, S. C., and Gilula, N. B. (1984). Antibodies to gap-junctional protein selectively disrupt junctional communication in the early amphibian embryo. Nature *311*, 127-131.

Wasman, S. G., and Black, J. A. (1984). Freeze-fracture ultrastructure of the perinodal astrocyte and associated glial junctions. Brain Res *308*, 77-87.

Weiss, S., Dunne, C., Hewson, J., Wohl, C., Wheatley, M., Peterson, A. C., and Reynolds, B. A. (1996). Multipotent CNS stem cells are present in the adult mammalian spinal cord and ventricular neuroaxis. J Neurosci *16*, 7599-7609.

Weissman, T. A., Riquelme, P. A., Ivic, L., Flint, A. C., and Kriegstein, A. R. (2004). Calcium waves propagate through radial glial cells and modulate proliferation in the developing neocortex. Neuron *43*, 647-661.

White, T. W., and Bruzzone, R. (1996). Multiple connexin proteins in single intercellular channels: Connexin compatibility and functional consequences. J Bioenerg Biomembr *28*, 339-350.

White, T. W., Bruzzone, R., Wolfram, S., Paul, D. L., and Goodenough, D. A. (1994). Selective interactions among the multiple connexin proteins expressed in the vertebrate lens: the second extracellular domain is a determinant of compatibility between connexins. J Cell Biol *125*, 879-892.

White, T. W., Paul, D. L., Goodenough, D. A., and Bruzzone, R. (1995). Functional analysis of selective interactions among rodent connexins. Mol Biol Cell *6*, 459-470.

Willecke, K., Eiberger, J., Degen, J., Eckardt, D., Romualdi, A., Guldenagel, M., Deutsch, U., and Sohl, G. (2002). Structural and functional diversity of connexin genes in the mouse and human genome. Biol Chem *383*, 725-737.

Williams, B. P., Park, J. P., Alberta, J. A., Muhlebach, S. G., Hwang, G. Y., Roberts, T. M., and Stiles, C. D. (1997). A PDGF-regulated immediate early gene response initiates neuronal differentiation in ventricular zone progenitor cells. Neuron *18*, 553-562.

Wong, W. T., Sanes, J. R., and Wong, R. O. L. (1998). Developmentally regulated spontaneous activity in the embryonic chick retina. J Neurosci *18*, 8839-8852.

Xavier, G. F., Oliveira-Filho, F. J., and Santos, A. M. (1999). Dentate gyrus-selective colchicine lesion and disruption of performance in spatial tasks: difficulties in "place strategy" because of a lack of flexibility in the use of environmental cues? Hippocampus *9*, 668-681.

Yamamoto, T., Ochalski, A., Hertzberg, E. L., and Nagy, J. I. (1990a). LM and EM immunolocalization of the gap junctional protein connexin 43 in rat brain. Brain Res *508*, 313-319.

Yamamoto, T., Ochalski, A., Hertzberg, E. L., and Nagy, J. I. (1990b). On the organization of astrocytic gap junctions in rat brain as suggested by LM immunohistochemistry and Em immunohistochemistry of connexin 43 expression. J Comp Neurol *302*, 853-883.

Yang, Z., Watanabe, M., and Nishiyama, A. (2005). Optimization of oligodendrocyte progenitor cell culture method for enhanced survival. J Neurosci Methods *149*, 50-56.

Ye, Z. C., Wyeth, M. S., Baltan-Tekkok, S., and Ransom, B. R. (2003). Functional hemichannels in astrocytes: a novel mechanism of glutamate release. J Neurosci *23*, 3588-3596.

Yeager, M., and Gilula, N. B. (1992). Membrane topology and quaternary structure of cardiac gap junction ion channels. J Mol Biol *223*, 929-948.

Yoshimura, S., Takagi, Y., Harada, J., Teramoto, T., Thomas, S. S., Waeber, C., Bakowska, J. C., Breakefield, X. O., and Moskowitz, M. A. (2001). FGF-2 regulation of neurogenesis in adult hippocampus after brain injury. Proc Natl Acad Sci USA *98*, 5874-5879.

Yuste, R., Nelson, D. A., Rubin, W. W., and Katz, L. C. (1995). Neuronal domains in developing neocortex: mechanisms of coactivation. Neuron *14*, 7-17.

Yuste, R., Peinado, A., and Katz, L. C. (1992). Neuronal domains in developing neocortex. Science *257*, 665-669.

Zaheer, A., Zhong, W., Uc, E. Y., Moser, D. R., and Lim, R. (1995). Expression of mRNAs of multiple growth factors and receptors by astrocytes and glioma cells: detection with reverse transcription-polymerase chain reaction. Cell Mol Neurobiol *15*, 221-237.

Zahs, K. R. (1998). Heterotypic coupling between glial cells of the mammalian central nervous system. Glia *24*, 85-96.
Zampighi, G. A., Loo, D. D. F., Kreman, M., Eskandari, S., and Wright, E. M. (1999). Functional and morphological correlates of connexin50 expressed in Xenopus laevis oocytes. J Gen Physiol *113*, 507-523.

Zerlin, M., Milosevic, A., and Goldman, J. E. (2004). Glial progenitors of the neonatal subventricular zone differentiate asynchronously, leading to spatial dispersion of glial clones and to the persistence of immature glia in the adult mammalian CNS. Dev Biol *270*, 200-213.

Zheng, W., Nowakowski, R. S., and Vaccarino, F. M. (2004). Fibroblast growth factor 2 is required for maintaining the neural stem cell pool in the mouse brain subventricular zone. Dev Neurosci *26*, 181-196.

Zimmer, D. B., Green, C. R., Evans, W. H., and Gilula, N. B. (1987). Topological analysis of the major protein in isolated intact rat liver gap junctions and gap junction-derived single membrane structures. J Biol Chem *262*, 7751-7763.

Zonta, M., Angulo, M. C., Gobbo, S., Rosengarten, B., Hossmann, K. A., Pozzan, T., and Carmignoto, G. (2003). Neuron-to-astrocyte signaling is central to the dynamic control of brain microcirculation. Nat Neurosci *6*, 43-50.

Appendix 1: List of antibodies

Antibodies against:	Lineage Detected	Final Concentration*	Source
A2B5	Late oligodendrocyte progenitors	1:2	ATCC
BrdU (bromodeoxyuridine)	Cell proliferation	6 µg/mL	Roche
		1:20 (-FITC)	Accurate Chemicals
CaBP (calbindin)	Granule neurons and interneurons	1:200	Chemicon
CNPase (cyclic nucleotide 3'-phosphodiesterase)	Mature oligodendrocytes	1:200	Sigma
Cx32	Cx32+ cells	1:250	Zymed
DCX (doublecortin)	Neuronal progenitors and migrating neuroblasts	1:4000	Chemicon
Enolase (neuron-specific)	Mature neurons	1:10	Calbiochem
F4/80	Microglia	1:100	Abcam
GalC (galactocerebroside C)	Committed oligodendrocytes	1:50	Sigma
		1:200 (Western)	Sigma
GFAP (glial fibrillary acidic protein)	Astrocytes	1:800 (-Cy3)	Sigma
		1:2000 (Western)	Sigma
Nestin	Neural and glial progenitors	1:50	Chemicon
		1:500 (Western)	Chemicon
NeuN	Mature and newly born neurons	1:100	Chemicon
NG2 chondroitin sulfate proteoglycan	Glial and early oligodendrocyte progenitors	1:200	Chemicon
O4	Late oligodendrocyte progenitors	1:50	Chemicon
Parvalbumin	Interneurons	1:1000	Swant
		1:2000	Sigma
PDGFαR (platelet-derived growth factor receptor alpha)	Late oligodendrocyte progenitors	1,5 µg/mL	BD Biosciences
PLP (proteolipid protein)	Committed oligodendrocytes	1:100	Biogenesis
Rip	Mature oligodendrocytes	1:2000	Chemicon
TuJ1 (class III β-tubulin isotype	Immature neurons	1:250	Research Diagnostics Inc
Mouse IgG	Cy3-conjugated	1:800	Jackson
	FITC-conjugated	1:100	Jackson
	Biotin-conjugated	1:10 000	Sigma
	Extravidin peroxidase-conjugated	1:1000	Sigma
	Extravidin alkaline phosphatase-conjugated	1:300 000	Sigma
Mouse IgM	FITC-conjugated	1:600	Jackson
Rabbit IgG	Cy3-conjugated	1:600	Jackson
	FITC-conjugated	1:100	Jackson
	Peroxidase-conjugated	1:5000	Jackson
Rat IgG	Cy3-conjugated secondary	1:400	Jackson

* Final concentrations used for immunofluorescence, unless otherwise indicated.

Appendix 2: Curriculum vitae

Lysanne Melanson-Drapeau
505 Blvd des Hautes-Plaines, Gatineau (Qc), J8Z 2H8
(819) 776-9878 (Home)
lmelansond@hotmail.com

Education

09/2001 – Present: **PhD in biochemistry**
University of Ottawa
Thesis Title: Connexin32-mediated regulation of progenitor specification in uninjured and injured adult rodent brain
(Thesis submitted February 24, 2006)

1998-2001: **B. Sc. with honours, Summa cum laude**
University of Ottawa
Thesis Title: Caractérisation d'un modèle d'enrichissement de cellules souches dépourvues de connexine 32

Employment, Teaching Experience and Volunteer work

October 2005 – April 2006 **Molecular biology technician, Agriculture and Agri-Food Canada**
Duties: Contribute to the development of bioassays and analytical techniques aimed at improving the understanding of plant pathogen detection, identification, biology and control.

April 2003 & 2005 **Volunteer judge at the regional & provincial Expo Sciences finals**
Duties: Judge several exhibits pertaining to various scientific fields

January-April 2003 & 2002 **Teaching Assistant for Biochemistry laboratory**
Duties: Supervise weekly laboratory sessions, mark laboratory reports, conduct private teaching sessions and tutorials

Summer 2001 **NSERC Undergraduate Student Research Award**
Duties: Complete a project pertaining to molecular biology and behavioural studies, learn and master new techniques

1998 - 2001 **Club des petits debrouillards (scientific club for kids)**
Duties (Workshop leader): Develop protocols for scientific workshops, prepare workshop materials and procedures, adapt workshops for different age groups

Awards/Scholarships

- CGS (Canada Graduate Scholarship; 2003-2005) ($70 000)
- University of Ottawa award of excellence (2003-2005) ($13 000)
- OGS (Ontario Graduate Scholarships; 2003) – Declined ($15 000)
- NSERC (National Science and Engineering Research Council, PGS A; 2001-2003) ($34 600)
- SAD Award (Strategic areas of development; 2001-2003) ($6000)
- University of Ottawa award of excellence (2001-2003) ($13 000)
- OGS (2001) – Awarded but Declined ($15 000)
- FCAR (Fonds pour la formation de chercheurs et l'aide à la recherche; 2001) – Declined ($30 000)
- University of Ottawa Admission Scholarship, (1998-2001) ($2500 per year)
- C.P. Leblond Research Presentation Award for best poster presentation at the Annual meeting of the CAANCB (2002) ($400)
- Best presentation prize at the BMI department 2004 & 2002 poster sessions

Publications

Melanson-Drapeau L. and Bennett S.A.L. (2006) Connexin-mediated control of neurogenesis and gliogenesis. In: Jeon, KW (ed) International Review of Cytology. Burlington, Massachusetts, Academic Press. Invited submission. Under editorial review.

Cheung E.C.C., **Melanson-Drapeau L.**, Cregan S.P., Vanderluit J.L., Ferguson K.L., McIntosh W.C., Park D.S., Bennett S.A.L., Slack R.S. (2005) Apoptosis-inducing factor is a key factor in neuronal cell death propagated by BAX-dependent and BAX-independent mechanisms, *J Neurosci* **25(6)**: 1324-1334.

Melanson-Drapeau L., Beyko S., Davé S., Hebb A.L.O, Franks D.J., Sellitto C., Paul D.L., Bennett S.A.L. (2003) Oligodendrocyte progenitor enrichment in the connexin32 null-mutant mouse, *J Neurosci* **23(5)**: 1759-1768.

Bennett S.A.L. and **Melanson-Drapeau L.** (2003) Primary culture of adult neural progenitors. In: Wang JQ (ed) Methods in Molecular Medicine: Drugs of Abuse: Analysis of Neurological Effects. Human Press, Totowa, New Jersey, volume 79, p.397-404.

Oral Communications

Melanson-Drapeau L., Morin M. and Bennett S.A.L. (2005) Augmentation of brain repair by connexin modulation, Oral presentation given at the Winter Conference on Neural Plasticity, Guadeloupe (February 2005)

Melanson-Drapeau L., Morin M. and Bennett S.A.L. (2004) Connexin32-mediated regulation of progenitor specification following brain injury, Oral presentation given at the Merck Frosst Pharmacology Research Day, Montreal, Canada (October 2004)

Abstract presentations (*Presented by Lysanne Melanson-Drapeau)

Melanson-Drapeau L.*, Morin M.Y. and Bennett S.A.L. (2005) Connexin32-mediated regulation of progenitor specification following brain injury, Molecular regulation of stem cells, Banff, Alberta, Canada (February 2005)

Melanson-Drapeau L., Morin M.Y. and Bennett S.A.L. (2004) Connexin32-mediated regulation of progenitor specification following brain injury, Society for Neuroscience 2004 Conference, San Diego, United States (October 2004)

Bennett S.A.L, **Melanson-Drapeau L.** and Morin M.Y. (2004) Kinetics of neurodegeneration and neuroregeneration in the Cx32 null mutant mouse following kainic acid induced seizure, San Diego, United States (October 2004)

Cheung E.C., **Melanson-Drapeau L.**, Ferguson K.L., Maclaurin J.G., McIntosh W.C., Callaghan S.M., Park D.S., Bennett S.A.L. and Slack R.S. (2004) AIF is a key factor in neuronal cell death propagated by BAX-dependent and BAX-independent mechanisms, San Diego, United States (October 2004)

Melanson-Drapeau L.*, Davé S., Hebb A.L.O. and Bennett S.A.L. (2003) Oligodendrocyte progenitor enrichment in the connexin32-null mutant mouse, Society for Neuroscience 2003 Conference, New Orleans, United States (November 2003)

Bennett S.A., **Melanson-Drapeau L.**, Davé S., Ryan S.D. and Hebb A.L.O. (2003) Cyclic fluctuations in progenitor proliferation across the estrous cycle are mediated by connexin32, Society for Neuroscience 2003 Conference, New Orleans, United States (November 2003)

Melanson-Drapeau L.*, Hebb A.L.O. and Bennett S.A.L. (2002) Characterization of an *in vivo* model of neural progenitor enrichment, Society for Neuroscience 2002 Conference, Orlando, United States (November 2002)

Hebb A.L.O., **Melanson-Drapeau L.** and Bennett S.A.L. (2002) Increased habituation to repeated exposure to a novel environment in female Cx32 KO C57Bl/6J mice: neural progenitor correlates associated with behavior, Society for Neuroscience 2002 Conference, Orlando, United states (November 2002)

Melanson-Drapeau L.* and S.A.L. Bennett (2002) Functional characterization of an *in vivo* model of neural progenitor enrichment, CFBS 2002 Conference (Canadian Federation of Biological Sciences), Montreal, Canada (June 2002)

Melanson-Drapeau L.*, Sellito C., Paul D.L., Bennett S.A.L. (2001), Western Analysis of Central Nervous System Lineage Markers in the Adult Cx32 Knockout Mouse, Society for Neuroscience 2001 Conference (November 2001; San Diego, USA), Life Sciences 2001 Conference (Ottawa, Canada) and CFBS 2001 Conference (Ottawa, Canada).

Laboratory techniques

Mammalian tissue culture and primary culture, extraction and isolation of DNA, RNA and proteins from cells and rodent tissue, PCR and RT-PCR analysis, cloning, DNA electrophoresis, SDS-Page, Western analysis, histology, immunohistochemistry, TUNEL assays, epifluorescent microscopy, densitometry analysis, mouse handling: maintenance and breeding, cytological smear (estrous cycle), genotyping, behavioural studies, intraperitoneal injections, seizure induction, transcardial perfusion and decapitation, tissue cutting (cryostat, vibratome), neurosphere assays; Computer skills: Microsoft Word, WordPerfect, Excel, Powerpoint, Openlab, Adobe Photoshop, DeltaGraph, Systat, Acrobat, EndNote, Lasergene